

INVERSE OPTIMAL CONTROL FOR NONLINEAR SYSTEMS



Ph.D. THESIS

Moayed ALMOBAIED

Department of Control and Automation Engineering

Control and Automation Engineering Programme

MAY 2017

INVERSE OPTIMAL CONTROL FOR NONLINEAR SYSTEMS



Ph.D. THESIS

Moayed ALMOBAIED
(504112007)

Department of Control and Automation Engineering

Control and Automation Engineering Programme

Thesis Advisor: Prof. Dr. İbrahim EKSİN
Co-advisor: Prof. Dr. Müjde GÜZELKAYA

MAY 2017

DOĞRUSAL OLMAYAN SİSTEMLER İÇİN TERS OPTİMAL KONTROL

DOKTORA TEZİ

**Moayed ALMOBAIED
(504112007)**

Kontrol ve Otomasyon Mühendisliği Anabilim Dalı

Kontrol ve Otomasyon Mühendisliği Programı

**Tez Danışmanı: Prof. Dr. İbrahim EKSİN
Eş Danışman: Prof. Dr. Müjde GÜZELKAYA**

MAYIS 2017

Moayed ALMOBAIED, a Ph.D. student of ITU Graduate School of Science Engineering and Technology 504112007 successfully defended the thesis entitled “INVERSE OPTIMAL CONTROL FOR NONLINEAR SYSTEMS”, which he/she prepared after fulfilling the requirements specified in the associated legislations, before the jury whose signatures are below.

Thesis Advisor : **Prof. Dr. İbrahim EKSİN**
Istanbul Technical University

Co-advisor : **Prof. Dr. Müjde GÜZELKAYA**
Istanbul Technical University

Jury Members : **Prof. Dr. M. Turan SÖYLEMEZ**
Istanbul Technical University

Assoc. Prof. Dr. Ahmet ONAT
Sabanci University

Asst. Prof. Dr. İlker ÜSTOĞLU
Yıldız Technical University

Asst. Prof. Dr. Dilek Bilgin TÜKEL
Doğuş University

Asst. Prof. Dr. Tufan KUMBASAR
Istanbul Technical University

Date of Submission : **21 April 2017**

Date of Defense : **22 May 2017**



*To the memory of my beloved brother, Ashraf. To my parents and family in Palestine.
To my dear wife Lamyaa, and lovely kids: Wafiq, Ashraf, Mohammed, and Meral.*



FOREWORD

This work would have never been possible without the continued support and the excellent research environment provided by many people.

First and foremost, I would like to express my deepest and sincere gratitude to my academic supervisors, Prof. Dr. İbrahim EKSİN and Prof. Dr. Müjde GÜZELKAYA for their enthusiasm, enlightening and inspiring guidance, constructive comments, and unrelenting support throughout my doctoral program. Each meeting with them added invaluable aspects to the implementation and broadened my perspective.

I would like to thank my reading committee members: Prof. Dr. M. Turan SÖYLEMEZ, Assoc. Prof. Dr. Ahmet ONAT, and Asst. Prof. Dr. İlker ÜSTOĞLU for their time, support, helpful comments, and encouragement throughout this work. I would also like to thank the other two members of my oral defense committee, Asst. Prof. Dr. Dilek Bilgin TÜKEL and Asst. Prof. Dr. Tufan KUMBASAR, for their time and insightful questions.

I gratefully acknowledge the financial assistance provided by Türkiye scholarships " YTB - Yurt Dışı Türkler ve Akraba Topluluklar Başkanlığı" during my PhD studies.

I would like to extend my special thank to my boss in ISBAK, Mr. Yusuf DURSUN, who gave me encouragement during my PhD research.

I would like to thank my mother, father, brother, sisters, and all my family in Palestine for their unconditional support and for encouraging me to do this work even when that meant traveling thousands of miles and staying away during this period.

Last but not least, I would like to express my deepest gratitude and thanks to my dear wife Lamyaa for her understanding, unfailing encouragement and support as well as her patience. She has been my inspiration and motivation for continuing to improve my knowledge and move my career forward. I also would like to extend my special thank to my wonderful children: Wafıqa, Ashraf, Mohammed, and Meral who knew only to encourage and never did complain about anything even when they had to suffer a lot in my absence.

May 2017

Moayed ALMOBAIED

TABLE OF CONTENTS

	<u>Page</u>
FOREWORD	ix
TABLE OF CONTENTS	xi
ABBREVIATIONS	xiii
LIST OF TABLES	xv
LIST OF FIGURES	xvii
SUMMARY	xix
ÖZET	xxi
1. INTRODUCTION	1
2. OPTIMAL CONTROL PROBLEM	7
2.1 Basic Concepts of Optimal Control.....	7
2.2 Hamilton-Jacobi-Belman Equation for Discrete-Time Nonlinear Systems ...	8
2.3 Hamilton-Jacobi-Bellman Equation for Linear Systems (LQR Equation).....	10
2.4 Big Bang-Big Crunch Optimization for LQR Controller.....	12
2.4.1 Big Bang-Big Crunch Optimization Algorithm	13
2.4.2 Simulation results for inverted pendulum on cart.....	15
2.4.3 Experimental results for the DC-DC boost converter.....	19
3. INVERSE OPTIMAL CONTROL PROBLEM	25
3.1 Lyapunov Stability Theory	25
3.2 Inverse Optimal Control Based on CLF For Discrete-Time Nonlinear System	27
4. AN OFF-LINE INVERSE OPTIMAL CONTROL APPROACH FOR DISCRETE-TIME NONLINEAR SYSTEMS	33
4.1 PSO algorithm for inverse optimal control.....	33
4.2 Particle Swarm Optimization (PSO)	33
4.3 Multi-objective Big Bang-Big Crunch Optimization algorithm for inverse optimal control.....	37
4.3.1 Multi-objective Optimization Criteria	37
4.4 Simulation Examples.....	39
4.4.1 A nonlinear system case	39
4.4.2 An inverted pendulum on cart case	43
5. AN ON-LINE INVERSE OPTIMAL CONTROL BASED ON EXTENDED KALMAN FILTER APPROACH FOR DISCRETE-TIME NONLINEAR SYSTEMS	47
5.1 EKF Algorithm for Inverse Optimal Control	47
5.1.1 General Information on Extended Kalman Filter.....	47
5.1.2 Extended Kalman Filter equations as parameter optimizer in inverse optimal control.....	49

5.2 Simulation Examples.....	52
5.2.1 A nonlinear system_1	52
5.2.2 A nonlinear system_2	53
5.3 Experimental Results of the DC-DC Boost Converter	57
5.3.1 Mathematical model of the DC-DC boost converter	57
5.3.2 EKF-based Inverse Optimal Control for DC-DC Boost Converter as a Real Time Application	60
6. CONCLUSIONS AND RECOMMENDATIONS.....	71
REFERENCES.....	73
APPENDICES.....	79
APPENDIX A.1	81
CURRICULUM VITAE.....	86



ABBREVIATIONS

HJB	: Hamilton Jacobi Bellman
SG	: Speed Gradient
CLF	: Control Lyapunov Function
PSO	: Particle Swarm Optimization
BB-BC	: Big Bang-Big Crunch
RMSE	: Root Mean Square Error
EMF	: Electromotive Force
LQR	: Linear quadratic regulator
GA	: Genetic Algorithm
PID	: Proportional Integral Derivative
KF	: Kalman Filter
EKF	: Extended Kalman Filter
LTI	: Linear Time Invariant
ARE	: Algebraic Riccati Equation



LIST OF TABLES

	<u>Page</u>
Table 2.1 : Physical quantities for the inverted pendulum on cart for LQR based BB-BC.	16
Table 2.2 : Comparison between the response of LQR based BB-BC and experiential-LQR for the cart of the pendulum.....	17
Table 2.3 : DC-DC boost converter model parameters.	20
Table 4.1 : Difference between off-line inverse optimal controller scenarios.	42
Table 4.2 : Physical quantities for the inverted pendulum on cart.	44
Table 5.1 : Comparison results between the proposed EKF-based approach and other approaches for nonlinear system_1.....	52
Table 5.2 : Comparison results between the proposed EKF-based approach and other approaches for nonlinear system_2.....	54
Table 5.3 : Parameters values of the DC-DC boost converter.	61
Table 5.4 : Step response analysis of the DC-DC boost converter for EKF-based controller, LQR state feedback controller and Ziegler-Nichols PID controller.....	66



LIST OF FIGURES

	<u>Page</u>
Figure 2.1 : LQR controller for state space model.....	12
Figure 2.2 : Nonlinear optimal control problem solving approaches.....	13
Figure 2.3 : Flowchart of the BB-BC optimization algorithm for LQR controller.	15
Figure 2.4 : The structure of inverted pendulum on cart system.....	16
Figure 2.5 : Oscillation of the pendulum's angle for proposed controller and the experiential-LQR one.	18
Figure 2.6 : Step response of the cart's position for proposed controller and the experiential-LQR one.....	18
Figure 2.7 : DC-DC boost converter circuit.	19
Figure 2.8 : DC-DC converter board and ARDUINO Mega 2560 controller kit..	21
Figure 2.9 : The proposed controller algorithm within Simulink interface.	22
Figure 2.10 : Transient response for the proposed controller under sudden changes in reference voltage.	22
Figure 2.11 : Transient response of the proposed controller with load variation....	23
Figure 2.12 : Transient response of the proposed controller with input voltage variation.	23
Figure 3.1 : The platform of Trial and Error method for inverse optimal control.	29
Figure 3.2 : The platform of speed gradient algorithm method for inverse optimal control.	30
Figure 3.3 : Inverse optimal control approach and traditional solution for optimal control problem.....	31
Figure 4.1 : Swarm flocks.	34
Figure 4.2 : Swarm algorithm flowchart.	36
Figure 4.3 : The proposed PSO optimization based inverse optimal controller for discrete-time nonlinear system.....	36
Figure 4.4 : The proposed multi-objective Big Bang-Big Crunch optimization based inverse optimal controller for discrete-time nonlinear system..	39
Figure 4.5 : The platform of PSO algorithm for inverse optimal control.	40
Figure 4.6 : Swarm platform result.	40
Figure 4.7 : MATLAB GUI for the proposed multi-objective Big Bang-Big Crunch Optimization controller for inverse optimal control.....	41
Figure 4.9 : The structure of inverted pendulum on cart system.....	44
Figure 4.10 : MATLAB GUI for the proposed multi-objective Big Bang-Big Crunch Optimization controller for inverted pendulum on cart.....	46
Figure 5.1 : Extended Kalman filter equations.....	49
Figure 5.2 : The proposed EKF-based inverse optimal control for discrete-time nonlinear system.	51
Figure 5.3 : The flowchart of the proposed EKF-based inverse optimal control. .	51

Figure 5.6 : MATLAB GUI of the proposed EKF-based inverse optimal control for system_1.	55
Figure 5.9 : MATLAB GUI of the proposed EKF-based inverse optimal control for system_2.	56
Figure 5.10 : MATLAB GUI for the proposed EKF-based inverse optimal control for DC-DC boost converter.....	59
Figure 5.11 : Schematic diagram of DC-DC boost converter circuit.	60
Figure 5.12 : DC-DC converter board and ARDUINO Mega 2560 controller kit..	61
Figure 5.14 : Internal blocks of the EKF-based inverse optimal controller for boost converter.	64
Figure 5.15 : Step response analysis of the DC-DC boost converter for EKF-based controller, LQR state feedback controller and Ziegler-Nichols PID controller.....	65
Figure 5.16 : Output response for EKF-based inverse optimal controller, LQR state feedback controller and Ziegler-Nichols PID controller with load variation.	67
Figure 5.17 : Output response for EKF-based inverse optimal controller, LQR state feedback controller and Ziegler-Nichols PID controller with input voltage variation.	68
Figure 5.18 : Output response for EKF-based inverse optimal controller, LQR state feedback controller and Ziegler-Nichols PID controller with reference voltage variation.....	69

INVERSE OPTIMAL CONTROL FOR NONLINEAR SYSTEMS

SUMMARY

The design of optimal controllers for nonlinear systems has been an area of intense research interest in control theory. Optimal nonlinear control deals with the problem of finding a stabilizing control law for a given nonlinear system while achieving a certain optimality criterion. The traditional approach to solve the nonlinear optimal control problem leads to a Hamilton-Jacobi-Bellman (HJB) equation that has no exact analytical solution for general nonlinear systems. In this study, the inverse optimal controller methodology based on defining an appropriate quadratic control Lyapunov function (CLF) has been chosen as the basis for the proposed methods. The inverse optimal control problem, which was initially presented by Kalman for linear systems, deals with the question of whether a given state feedback can be the optimal control with respect to some useful performance index.

This thesis proposes two different approaches to implement the inverse optimal controller design for affine-in-input discrete-time nonlinear systems. In the first approach, the parameters of the candidate CLF were optimized in an off-line manner by using Particle Swarm Optimization (PSO) and Big Bang-Big Crunch (BB-BC) algorithms. Then, the inverse optimal controller that relied on a multi-objective optimization criterion in off-line manner is also proposed; where the root-mean-square-error (RMSE) of system states with respect to a reference trajectory and the sum-of-squares of control effort are utilized as the multi-objective optimization criterion in the Big Bang-Big Crunch optimizing algorithm. In order to test the performance of the proposed off-line approach, a nonlinear example from the literature of inverse optimal control is firstly taken into consideration. Next, the proposed controller is used to stabilize an inverted pendulum on cart. Simulation results within the MATLAB show that the proposed method can effectively solve the nonlinear optimal control problem for affine-in-input discrete-time nonlinear systems.

Secondly, an inverse optimal control approach based on extended Kalman filter (EKF) algorithm to solve the optimal control problem for affine-in-input discrete-time nonlinear systems is presented. In this on-line approach, the parameters of the candidate quadratic CLF were estimated by adopting the EKF equations. The RMSE of system states is used as the observed error in the equations of EKF algorithm; whereas, here, the EKF tries to eliminate the same RMSE error defined over the parameters by generating a CLF matrix with appropriate elements. The performance and the applicability of the proposed scheme is illustrated through both simulations performed on two different nonlinear system models and a real time laboratory experiment. Simulation study demonstrate the effectiveness of the proposed method in comparison with two other inverse control approaches from the literature. Finally, the proposed controller is implemented on a professional control board to stabilize a DC-DC boost converter and minimize a meaningful cost function. The experimental results show the applicability and effectiveness of the proposed EKF-based inverse optimal control

even in real time control systems with a very short time constant.

In order to compare the results of the proposed EKF-based inverse optimal control approach with classical linearization based technique, this thesis proposes an effective solution to the HJB equation for linear system cases. Indeed, this solution leads to the traditional linear quadratic regulator (LQR) controller which is the most popular technique that provides an optimal control law for linear systems among the state space feedback control strategies. However, the conventional LQR controller synthesis is unfortunately an iterative process due to the trial and error approach involved in determining the parameters values of the weighing matrices Q and R . In the proposed method, the BB-BC optimization algorithm is used to find an appropriate value for these weighing matrices Q and R ; thus avoiding the repeated adjustment process of LQR parameters in constructing the state feedback optimal control law. Here, a special performance fitness function that is inversely proportional to the certain time domain step response criteria of a dynamical system is proposed for the optimization procedure. In order to test the performance of the proposed method, firstly a simulation study is done within the MATLAB to stabilize an inverted pendulum on cart. Then, the proposed controller is used in a real time implementation to stabilize a DC-DC boost converter benchmark in the lab. Both MATLAB simulations and laboratory experiments demonstrate the effectiveness of the proposed BB-BC based LQR controller.

DOĞRUSAL OLMAYAN SİSTEMLER İÇİN TERS OPTİMAL KONTROL

ÖZET

Doğrusal olmayan sistemler için optimal kontrolör tasarımı her zaman yoğun bir araştırma alanı olmuş ve bu alanda çok sayıda yayınlar yapılmış ve de araştırmalar devam etmektedir.

Doğrusal olmayan kontrolör tasarım problemi verilen bir doğrusal olmayan sistem için belirli bir optimal olma ölçütünü sağlayarak söz konusu sistemi dengeleyecek kontrol yasasını oluşturmaya çalışır. Doğrusal olmayan optimal kontrol problemine geleneksel yaklaşım bizi Hamilton-Jacobi-Bellman (HJB) denklemine götürür ki bu denklemlerin genel doğrusal olmayan sistemler için tam analitik bir çözümü yoktur. Burada, farklı ters optimal kontrolör tasarım yöntemlerine temel yaklaşımın, uygun bir kuadratik kontrol Lyapunov fonksiyonu (Quadratic Liapunov Function - CLF) tanımlanması veya bir şekilde oluşturulması olarak belirtilebilir.

Ters optimal kontrol problemi ilk olarak Kalman tarafından lineer sistemleri için önerilmiştir. Bu problem de verilen bir durum geri beslemesinin belirli bir amaç ölçütüne göre optimal olup olmadığı sorusuna yanıt arar. Sonuç olarak ters optimal kontrol kuramının arkasındaki temel düşünce bir kararlı kılıcı geri besleme kontrol kuralı oluşturup daha sonra bu kontrol kuralını giriş değişkenlerine ve durumlara bağlı bir anlamlı amaç ölçütünün optimizasyonunda kullanmaktır.

Bu yaklaşım klasik optimal kontrol problemi ile karşılaştırıldığında bir kafa karıştırıcı bulunabilir. Çünkü klasik optimal kontrol problemine çözüm yaklaşımında öncelikle amaç ölçütünün bilinmesi zorunluluğu vardır. Son yıllarda özellikle havacılık alanındaki problemler ters optimal kontrol yaklaşımı sıkça kullanılmaya başlamıştır. Böylece, lineer olmayan sistemlerde karşımıza çıkan ve çözümü bazen imkânsız veya çok zor olan Hamilton- Jacobi- Bellman denklemini çözmek durumunda kalınmamaktadır. Ancak, ters optimal kontrol problemlerinde de temel sorun, bu güne kadar, en genel şekilde tüm lineer olmayan sistemler için bir kontrol Liapunov fonksiyonun (Control Liapunov Function – CLF) bulabilmek için sistematik bir yaklaşım önerilememiş olmasıdır.

Bu tezde, zamanda ayırık affine doğrusal olmayan sistemlerde uygulanmak üzere ters optimal kontrol problemi çözümüne iki farklı yaklaşım önerilmektedir. Birinci yaklaşımda, aday CLF'nin parametreleri çevrim-dışı bir şekilde Parçacık Sürü Optimizasyon (Particle Swarm Optimization-PSO) ve Büyük Patlama - Büyük Çöküş (Big Bang - Big Crunch BB-BC) optimizasyon yöntemleri kullanarak optimum değerleri belirlenmeye çalışılmıştır.

Ayrıca, bu yaklaşımda, yine çevrim dışı olarak çok ölçütlü optimizasyon problemine dayalı bir ters optimal kontrolör tasarım yöntemi geliştirilmiştir. Bu yöntemde, birbirleriyle çatışan ölçütler olan hataların karelerinin karekökü (RMSE) ve kontrol aksiyonun karelerinin toplamı ifadelerini birlikte eniyileyecek biçimde ve global bir optimizasyon yöntemi olan BB-BC kullanılarak, bir ters optimal kontrolör tasarlanmıştır.

Bilindiği üzere çok ölçütlü optimizasyon yönteminde birden çok optimal nokta olacağı açıktır. Bu nedenle, çok ölçütlü optimizasyon problemi bir ağırlık katsayıları aracılığıyla tek boyuta indirgenmiştir. Ancak, bu ağırlık katsayılarına değişik değerler atanarak irdemeler de yapılmıştır. Sonuç olarak bu değişik katsayılar verilerek elde edilen sonuçları tasarımcının irdeleyerek kendisi için en uygun çözümü seçmesi beklenmektedir. Bu yöntemlerin başarımını test etmek için de literatürden bir doğrusal olmayan sistem örneği üzerinde denemeler yapılmış ve sonuçlar karşılaştırma bir biçimde irdelenmiştir.

Benzetim sonuçları tasarımcıya klasik ters optimal kontrol çözümü ile çoklu-optimizasyon fonksiyonu üzerinden sunulan çözümler arasında seçim yapması açısından bir farkındalık yaratmaktadır. Daha sonra, Bu önerilen yaklaşımlar araba üzerindeki ters sarkaç problemine de uygulanmıştır. Benzetim sonuçları, önerilen yöntemin, zamanda ayırık affine ve doğrusal olmayan sistemlerin, doğrusal olmayan kontrolünde etkin sonuçlar verdiğini göstermiştir.

İkinci yaklaşım olarak, yine zamanda ayırık affine doğrusal olmayan sistemlerin optimal kontrol çözümü için Extended Kalman Filter (EKF) algoritmasına dayalı bir ters optimal kontrol tasarım yöntemi önerilmiştir. Burada, sistem durumlarının RMSE değeri gözlenen hata olarak kullanılmış ve EKF, en uygun CLF matris eleman değerlerini yaratarak RMSE hatasını en aza indirecek şekilde tasarlanmıştır. Yöntemin başarımı ve etkinliği iki farklı doğrusal olmayan sistem modeli üzerinde benzetimler yapılarak gösterilmiştir.

Ayrıca, yöntem bir gerçek zaman laboratuvar deney düzeneği üzerinde de çalıştırılarak başarımı ve etkinliği gözlenmiştir. Benzetim çalışmaları önerilen yöntemin literatürde söz edilen diğer iki ters optimal kontrol yöntemlerine kıyaslandığında daha verimli ve etkin çözümler sunduğu görülmüştür. Son olarak, önerilen yöntemle, anlamlı bir maliyet fonksiyonunu en aza indirecek bir biçimde, profesyonel bir kontrol kartı üzerinden, Doğru Akım- Doğru Akım (DA-DA) dönüştürücünün (DC-DC boost converter) kontrol edilmesi sağlanmıştır. Gerçek zamandaki deneysel sonuçları, bize önerilen EKF tabanlı ters optimal kontrol yöntemin, çok kısa zaman sabiti olan sistemler üzerinde bile rahatlıkla ve de etkin bir şekilde uygulanabilirliğini göstermiştir.

Bu tez, ayrıca, doğrusal sistemler için HJB denkleminde etkin bir çözüm de sunmaktadır. Doğrusal sistemler ve kuadratik başarımlı ölçütü durumunda geleneksel çözüm olarak doğrusal kuadratik düzenleyici (Linear Quadratic Regulator - LQR) problemine varıldığı bilinir. Bu problemin çözümü de doğrusal sistemler için durum uzayında durum geri beslemeli kontrolör tasarımı için en bilinen ve etkin kullanışlı yöntemdir. Ancak, burada bulunan Q ve R matrislerini elemanlarının seçimi daha çok deneme yanılmaya dayalı olarak belirlenmektedir. Burada, yenin bir yaklaşım önerilmiştir.

Bu yaklaşımda, Q ve R matrislerinin elemanları zaman tanım bölgesinde tanımlı bir başarımlı ölçütünü en iyi yapacak bir biçimde ve global bir arama algoritması olan Big Bang Big Crunch (BB-BC) kullanılarak belirlenmiştir. Bu yaklaşımda önerilen özel uygunluk başarımlı fonksiyonu bazı zaman tanım bölgesi ölçütlerinin (yüzde aşım, yerleşme zamanı, yükselme zamanı ve sürekli hal hatası) ters fonksiyonu olarak tanımlanmıştır. Bu yöntemin başarımını ölçmek üzere önce araba üzerindeki ters sarkaç probleminin dengelenmesi için bir benzetim çalışması yapılmıştır. Daha sonra, önerilen yöntem, Doğru Akım- Doğru Akım (DA-DA) dönüştürücü (DC-DC boost converter) laboratuvar deney setinin kontrol edilmesinde gerçek zamanda denenmiştir. Bu iki çalışma da, yani MATLAB üzerinde yapılan benzetim çalışmaları ve gerçek

zamanda laboratuvar deneyleri, yöntemin işlerliğini ve başarımını teyit etmiştir. Bu tez üzerine olası gelecek geliştirme çalışması olarak sistemdeki belirsizliklere karşı dayanıklılık analizleri yapmak ilk akla gelen çalışma olmaktadır. Ayrıca, yüksek mertebeden gerçek sistemler üzerinde bu geliştirilen EKF tabanlı ve gerçek zamanlı ters optimal kontrol yöntemin uygulamalarını yapabilmek de önemli bir aşama olacaktır kanısındayız.





1. INTRODUCTION

The main challenge in modern control theory is to develop efficient controllers for nonlinear systems that achieve the desired system performance as well as have the simplest design procedures. In nature, most dynamical systems such as inverted pendulum, power converters, robotic systems, and industrial processes etc., are inherently nonlinear and the equations of such kind of models are difficult to solve. Designing optimal controllers for such kind of nonlinear systems has been an area of intense research interest in control theory. "The main objective of optimal control is to determine control signals that will cause a given nonlinear process (plant) to satisfy some physical constraints and at the same time extremize (maximize or minimize) a chosen performance criterion (performance index or cost function)" [1]. Indeed, the classical solution of the nonlinear optimal control problem leads to a mathematical Hamilton-Jacobi-Bellman (HJB) equation which is extremely difficult to solve and has no exact analytical solution for general nonlinear systems [2–4]. For linear systems, it is also a well-known fact that HJB equation reduces to the Riccati equation [4, 5].

The inverse optimal control problem, which was initially presented by Kalman for linear systems, deals with the question of whether a given state feedback can be the optimal control with respect to some useful performance index [5]. The main idea behind the theory of inverse optimal control is to construct a stabilizing feedback control law as a first step, and then subsequently, to use this control law in the optimization of a meaningful cost functional which depends on the state variables and the control inputs [3, 6]. This definition can be a bit confusing when it is compared to the definition of optimal control problem where the cost functional should be known a priori in forming a stabilizing control law. The inverse optimal control for linear discrete-time systems is presented in [7]. Whereas for nonlinear systems, the inverse optimal control is an alternative method for solving the nonlinear optimal control problem while avoiding the tedious task of solving the HJB equation. In recent years, the inverse optimality approach has been increasingly used for solving the nonlinear optimal control problem in many real time applications, especially in aerospace

industry [8, 9]. The inverse optimality method is used for nonlinear deterministic system and nonlinear stochastic system with multiplicative and additive noises, and it is applied on a stochastic model of a human arm in [10]. In [11], it has been proven that it is possible to construct a controller which is optimal with respect to a meaningful cost functional for every system with a stochastic control Lyapunov function. In the above mentioned researches, the inverse optimality approach based on defining a control Lyapunov function (CLF) is used to construct the control law. In various studies on this approach, it has been proven that the Lyapunov function can be considered as a solution to the HJB equation in optimal control problems corresponding to a meaningful cost functional [3,6,12]. Up to this date, there does not exist any systematic procedures for defining a CLF for general nonlinear control systems. However, several researchers have proposed some systematic approaches to find the CLF for certain class of nonlinear systems such as feed-forward systems, feedback linearizable and strict feedback [13–15]. A continuous-time version of an inverse optimal control based on CLF has been proposed for a helicopter flight system in [16]. A main theorem related to the inverse optimal control problem for affine-in-input discrete-time nonlinear systems has been given in [17], where the necessary conditions needed to construct a discrete quadratic CLF has been illustrated in establishing the control law. A speed-gradient (SG) algorithm was used in [18] to adjust a single time-variant parameter which defines the discrete quadratic Lyapunov function. Moreover, the authors in [19] discussed the inverse optimal control for discrete-time nonlinear systems via passivity approach.

In this study, the inverse optimal control based on CLF theory is considered that is mainly motivated by the work presented in [17]. This thesis proposes two different approaches to implement the inverse optimal controller design for affine-in-input discrete-time nonlinear systems.

In the first approach, the parameters of the candidate CLF were optimized in an off-line manner by using Particle Swarm Optimization (PSO) and Big Bang-Big Crunch (BB-BC) algorithms. The BB-BC algorithm which proposed in [20] is derived from one of the evolution of the universe theories in physics and astronomy which called BB-BC theory. It has been demonstrated in [20] the effectiveness and superiority of BB-BC algorithm in comparison to genetic algorithm for many benchmark test functions. BB-BC algorithm has already been applied to different areas with encouraging results such as fuzzy model inversion [21] and power system stabilizer

[22]. Real world control problems in engineering are usually multi objectives or multi criteria. Hence, the multi-objective optimization problems have been intensively studied for several decades [23–26].

The novel contribution of this approach is that the multi-objective BB-BC optimization algorithm is proposed as an off-line parameters optimizer to construct the CLF of the inverse optimal control for affine-in-input discrete-time nonlinear systems; where the root-mean-square-error (RMSE) of system states with respect to a reference trajectory and the sum-of-squares of control effort are utilized as the multi-objective optimization criterion in the BB-BC optimizing algorithm. In order to test the performance of the proposed approach, a nonlinear example from the literature of inverse optimal control is firstly taken into consideration. The simulation results enlighten the designer in making a choice between the single objective inverse optimal control solution and the multi-objective function included case. Next, the proposed controller is used to stabilize an inverted pendulum on cart. The inverted pendulum is one of the most well-publicized problems in control system and many novel control techniques (such as linear quadratic regulator, genetic algorithms, fuzzy logic control, PID controllers, neural networks, etc.) have been tested on it [27], [28–30]. Simulation results within the MATLAB show that the proposed method can effectively solve the nonlinear optimal control problem for affine-in-input discrete-time nonlinear systems.

In the second approach, an inverse optimal control approach based on extended Kalman filter (EKF) algorithm to solve the optimal control problem of affine-in-input discrete-time nonlinear systems is presented. Researchers in the field of nonlinear estimation problems have utilized the EKF algorithm in estimation of a nonlinear dynamic system states and parameter estimation. Hence, the estimation process has been used for many applications, such as in a fuzzy modeling control problem [31] where EKF has been used in formation of fuzzy membership functions in an on-line manner. Another application is illustrated in [32], where the EKF algorithm was employed to estimate the back electromotive force (EMF) in an induction machine control problem.

The novel contribution of this study is that EKF algorithm is used as a parameter identifier in the formation of the CLF within the inverse optimal control loop for affine-in-input discrete-time nonlinear systems in an on-line manner for the first time in literature. The initial background and motivations of this work are laid out and

presented in [33]. Then, the proposed method is implemented in a DC-DC boost converter prototype, which is an inherently nonlinear system with a non-minimum phase characteristics and highly sensitive to load variations. In fact, the problem of stabilizing and regulating the output voltage of the DC-DC boost converter has been a research interest area and is widely used as a benchmark for testing various control forms such as Proportional-Integral-Derivative (PID), Fuzzy etc., [34–36]. The proposed EKF-based inverse optimal control method is fully developed and adopted for a real time application in [37].

In order to compare the results of the proposed EKF-based inverse optimal control approach with classical linearization based technique, this thesis also proposes an effective solution to the HJB equation for linear systems. Indeed, this solution leads to the traditional linear quadratic regulator (LQR) controller which is the most popular technique in the field of industry that provides an optimal control law for linear systems among the state space feedback control strategies. In despite of the good results of the LQR technique, the selection process of the weight matrices (Q and R) in the conventional LQR controller is given by trial and error that based on the experience of the designer. For that, the optimizing process of these matrices, which are straight affect the control performance, is still an active research topic [38]. Michael Athans in [39] derives a linear quadratic regulator which is robust to real parametric uncertainty. Genetic optimization algorithm (GA) was used in [27] to find the initial values of the connection weights of the neural network and initial values of PID in order to stabilize the inverted pendulum on cart system. Another application for using the GA and LQR is the aircraft pitch control has been demonstrated in [40]. Using BB-BC optimization algorithm to determine the weighing matrices (Q and R) of the LQR controller is the main contribution of this part. The proposed controller is then used to stabilize both an inverted pendulum on cart and a DC-DC boost converter. Both MATLAB simulations and laboratory experiments demonstrate the effectiveness of the proposed controller [41].

The remainder of this thesis is organized as follows: Chapter 2 describes the classical solution of discrete time optimal control problem for both linear and nonlinear cases. Chapter 3 introduces the inverse optimal control based on CLF approach. Chapter 4 presents the proposed off-line inverse optimal control approach for discrete-time nonlinear systems. An in-depth explanation on the proposed on-line EKF-based

inverse optimal control is given in Chapter 5. Finally, some conclusions are drawn in Chapter 6.





2. OPTIMAL CONTROL PROBLEM

This chapter presents the conventional solution of nonlinear optimal control problem and describes the resultant HJB equation which is extremely difficult to solve and has no exact analytical solution for general nonlinear systems.

In the second part of this chapter, the solution of the HJB equation for linear systems is presented where this solution reduces to the Riccati equation. Here, the BB-BC optimization algorithm is proposed to determine the weighing matrices (Q and R) of the LQR controller. In order to test the performance of the proposed method, firstly a simulation study is done within the MATLAB to stabilize an inverted pendulum on cart. Then, the proposed controller is used in a real time implementation to stabilize a DC-DC boost converter benchmark in the lab. Both MATLAB simulations and laboratory experiments demonstrate the effectiveness of the proposed controller [41].

2.1 Basic Concepts of Optimal Control

Optimal control theory, which related in its origins to the theory of calculus of variations, is a mathematical optimization method that deals with the problem of finding a stabilizing control law for a given dynamical system such that a certain performance criterion is minimized. This criterion is usually formulated as a cost functional, which is a function of state and control variables. There are various types of optimal control problems, depending on the nature of the system (linear, nonlinear), the type of time domain (continuous, discrete), the performance index and the different types of constraints, etc.

In the design process, there is no guarantee for stability margins and adequate performance in case of implementing a continuous-time control scheme on real-time application due to the well known fact that the continuous time schemes could become unstable after sampling process. Moreover, the discrete-time framework is technically more appropriate for implementing digital controllers and can be directly implemented in a digital processor. For that, the optimal control problem of affine discrete-time

nonlinear systems is considered in this study.

The major drawback for the conventional solution of optimal nonlinear control is the need to solve the associated HJB equation, which introduces a significant computational bottleneck and there is no analytical solution for general nonlinear systems at present. It has only been solved for the linear regulator problem [3–5].

2.2 Hamilton-Jacobi-Belman Equation for Discrete-Time Nonlinear Systems

In this research, the affine-in-input discrete-time nonlinear systems are considered. Affine simply means "linear", whereas non-affine means "nonlinear". Hence, if the input appears linearly in the system then it is affine-in-input system.

Considering the affine-in-input discrete-time nonlinear system of the form:

$$x_{k+1} = f(x_k) + g(x_k)u_k \quad (2.1)$$

where $x \in \mathbb{R}^n$ is the state of the system, $u \in \mathbb{R}^m$ is the control input. $f(x_k) : \mathbb{R}^n \rightarrow \mathbb{R}^n$ and $g(x_k) : \mathbb{R}^n \rightarrow \mathbb{R}^{n \times m}$ are smooth matrices. Without loss of generality, by shifting the origin of the system, it can be assumed that the origin ($x = 0$) is the equilibrium point of the system (2.1), $f(0) = 0$ and $g(x_k) \neq 0$ for all $x_k \neq 0$. System (2.1) is assumed to be stabilizable on a predefined compact set $\Omega \in \mathbb{R}^n$.

- **Definition 2.1:** Stabilizable system; a nonlinear dynamical system is said to be a stabilizable system on a compact set $\Omega \in \mathbb{R}^n$ if there exists a control input $U \in \mathbb{R}^m$ such that, for all initial conditions $x_0 \in \Omega$, the state $x \rightarrow 0$ as $k \rightarrow \infty$ [42].

For a nonlinear optimal control problem, it is desirable to determine a control law u_k , which minimizes the following cost functional:

$$V(x_k) = \sum_{n=k}^{\infty} (L(x_n) + u_n^T E u_n) \quad (2.2)$$

where $V : \mathbb{R}^n \rightarrow \mathbb{R}^+$ is the cost functional, $L : \mathbb{R}^n \rightarrow \mathbb{R}^+$ is positive semi-definite function to weight the performance of the state vector x_k , and $E : \mathbb{R}^n \rightarrow \mathbb{R}^{m \times m}$ is a real symmetric positive definite weighing matrix to weight the control effort and could be a function of the system state in order to vary the control efforts according to the state value [2, 3, 42].

Equation (2.2) can be written as:

$$\begin{aligned} V(x_k) &= L(x_k) + u_k^T E u_k + \sum_{n=k+1}^{\infty} (L(x_n) + u_n^T E u_n) \\ &= L(x_k) + u_k^T E u_k + V(x_{k+1}) \end{aligned} \quad (2.3)$$

From Bellman's optimality principle, which is solved backwards in time, it is known that the value function $V^*(x_k)$ is time invariant and satisfies the discrete time Bellman equation for an infinite horizon optimization case [43–45]:

$$V^*(x_k) = \min_{u_k} \{L(x_k) + u_k^T E u_k + V^*(x_{k+1})\} \quad (2.4)$$

The discrete-time Hamiltonian equation $\mathcal{H}(x_k, u_k)$ which is used to obtain the control law is defined as:

$$\mathcal{H}(x_k, u_k) = L(x_k) + u_k^T E u_k + V^*(x_{k+1}) - V^*(x_k) \quad (2.5)$$

Hence, the control law u_k should minimize this Hamiltonian equation as following:

$$\min_{u_k} \mathcal{H}(x_k, u_k) = \mathcal{H}(x_k, u_k^*) \quad (2.6)$$

The necessary condition for the feedback optimal control law in order to achieve this minimization is:

$$\mathcal{H}(x_k, u_k^*) = 0 \quad (2.7)$$

The formula of the optimal control u_k^* can be calculated by taking the gradient of the right-hand side of Equation (2.4) with respect to u_k :

$$\frac{\partial \{L(x_k) + u_k^T E u_k + V^*(x_{k+1})\}}{\partial u_k} = 0 \quad (2.8)$$

where:

$$\begin{aligned} \frac{\partial L(x_k)}{\partial u_k} &= 0, & \frac{\partial \{u_k^T E u_k\}}{\partial u_k} &= 2E u_k, \\ \frac{\partial \{V^*(x_{k+1})\}}{\partial u_k} &= \frac{\partial x_{k+1}}{\partial u_k} * \frac{\partial \{V^*(x_{k+1})\}}{\partial x_{k+1}}, & \frac{\partial x_{k+1}}{\partial u_k} &= g(x_k) \end{aligned}$$

The optimal control u_k^* will be:

$$u_k^* = \bar{u}(x_k) = -\frac{1}{2} E^{-1} g^T(x_k) \frac{\partial V^*(x_{k+1})}{\partial x_{k+1}} \quad (2.9)$$

which is a state feedback control law $\bar{u}(x_k)$ with $\bar{u}(0) = 0$. Hence, the boundary condition $V(0) = 0$ in Equation (2.2) is satisfied for $V(x_k)$, and V becomes a Lyapunov

function [2, 3, 45]. Moreover, if $\mathcal{H}(x_k, u_k)$ has a quadratic form in u_k and $E > 0$, then the following sufficient condition for the optimality will be satisfied:

$$\frac{\partial^2 \mathcal{H}(x_k, u_k)}{\partial u_k^2} > 0 \quad (2.10)$$

and the optimal control law in Equation (2.9) will globally minimize $\mathcal{H}(x_k, u_k)$ and performance index at Equation (2.3) [2, 3, 45].

By substituting the optimal control formula u_k^* in $V^*(x_k)$ at Equation (2.4), the discrete-time HJB equation will be:

$$V^*(x_k) = L(x_k) + V^*(x_{k+1}) + \frac{1}{4} \frac{\partial V^{*T}(x_{k+1})}{\partial x_{k+1}} g(x_k) E^{-1} g^T(x_k) \frac{\partial V(x_{k+1})}{\partial x_{k+1}} \quad (2.11)$$

Unfortunately, the HJB is extremely difficult to solve for a general nonlinear system. Hence, it precludes any hope of an exact global solution to the general nonlinear optimal control problem [3, 43–45].

2.3 Hamilton-Jacobi-Bellman Equation for Linear Systems (LQR Equation)

For linear regulator problem case with no constraints, the HJB equation can be reduced to the Riccati equation, which has been efficiently solved in the literature to derive a linear state feedback control [3, 5]. The linear quadratic regulator is an optimal controller for linear systems and is clearly the most important and influential result in optimal control theory that is widely used in all field of industry control. Actually, the LQR is popular used technique for state space feedback control design that takes into account the states of the dynamical system and control input to make the optimal control decisions [46].

Considering the system governed by the following linear time invariant (LTI) state-space equations:

$$\begin{aligned} \dot{x} &= Ax + Bu \\ Y &= Cx + Du \end{aligned} \quad (2.12)$$

The pair (A, B) must be controllable. The state feedback control $u = -kx$ leads to the following closed-loop state-space equations:

$$\dot{x} = (A - Bk)x \quad (2.13)$$

Where k is derived from minimization the following infinite horizon quadratic cost function:

$$J = \int_0^{\infty} (x^T Q x + u^T R u) dt \quad (2.14)$$

The weighing matrix Q is a symmetric positive semi-definite matrix, while R is defined as a symmetric positive definite symmetric matrix. Actually, The LQR problem is the weighted minimization of a linear combination of the states x and the control input u . The weighing matrix Q demonstrates which states are to be controlled more tightly than others. Increasing the values of the R matrix leads to applying a larger penalty to the aggressiveness of the control action.

By writing the well known HJB equation for linear system in Equation (2.12), we have:

$$0 = \min_u \left[x^T Q x + u^T R u + \frac{\partial J^*}{\partial x} (Ax + Bu) + \frac{\partial J^*}{\partial t} \right] \quad (2.15)$$

For infinite-horizon case, all dependence of J on t will drop out. Hence, the HJB equation reduces to:

$$0 = \min_u \left[x^T Q x + u^T R u + \frac{\partial J^*}{\partial x} (Ax + Bu) \right] \quad (2.16)$$

The formula of the optimal control u^* can be calculated by taking the gradient with respect to u and setting it to zero:

$$2u^T R + \frac{\partial J^*}{\partial x} B = 0 \Rightarrow u^* = -\frac{1}{2} R^{-1} B^T \frac{\partial J^*}{\partial x} \quad (2.17)$$

In order to find the solution, we can try a particular form for the cost-to-go function J^* :

$$\partial J^* = x^T P x \quad P^T = P > 0 \quad (2.18)$$

Then the LQR optimal control u^* is given by:

$$u^* = -R^{-1} B^T P x \quad (2.19)$$

Therefore, at minimum u :

$$0 = x^T \left[Q + 2PA - PBR^{-1}B^T P \right] x \quad (2.20)$$

Since $x^T P A x = x^T A^T P x$, we can equivalently write the symmetric form:

$$0 = x^T \left[Q + PA + A^T P - PBR^{-1}B^T P \right] x \quad (2.21)$$

Therefore, P must satisfy the condition (known as the continuous time Algebraic Riccati Equation (ARE)):

$$Q + PA + A^T P - PBR^{-1}B^T P = 0 \quad (2.22)$$

The LQR controller construction is shown in Figure 2.1. In order to reduce the steady state error of the system output, a value of feed forward gain (N_{bar}) may be added after the reference $r(t)$ as a scaling factor.

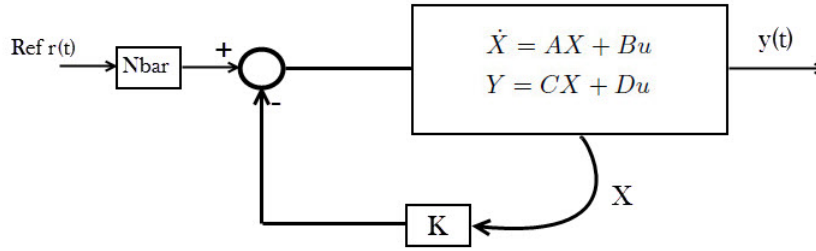


Figure 2.1 : LQR controller for state space model.

In spite of the good results of the LQR technique, the selection process of the weighing matrices (Q and R) in the conventional LQR controller is given by trial and error that based on the experience of the designer. For that, the optimizing process of these matrices, which are straight affect the control performance, is still an active research topic [47].

Here, Figure 2.2 illustrates the difference between the two main available approaches in solving the nonlinear optimal control problem.

2.4 Big Bang-Big Crunch Optimization for LQR Controller

In this section, the BB-BC optimization algorithm is used to find an appropriate value for the weighing matrices Q and R ; thus avoiding the repeated adjustment process of LQR parameters in constructing the state feedback optimal control law. Here, a special performance fitness function that is inversely proportional to the certain time domain step response criteria of a dynamical system is proposed for the optimization procedure.

In the proposed method, the BB-BC algorithm will optimize the weighing matrices (Q and R) in off-line mode, then these optimal matrices will be used by the LQR controller to stabilize the system.

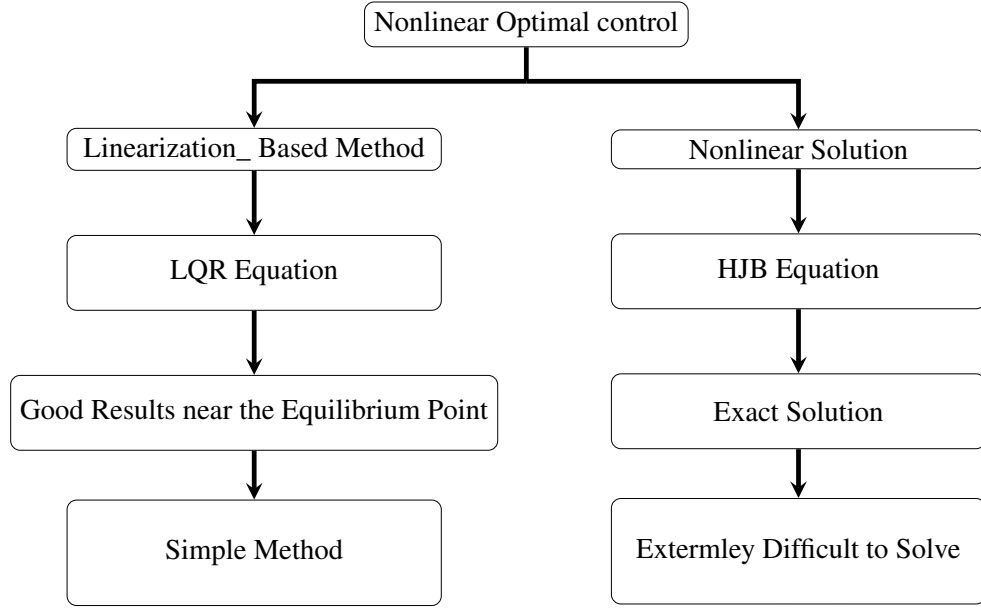


Figure 2.2 : Nonlinear optimal control problem solving approaches.

2.4.1 Big Bang-Big Crunch Optimization Algorithm

The authors in [20] introduced a new evolutionary optimizing algorithm named Big Bang-Big Crunch (BB-BC); the BB-BC algorithm is derived from one of the evolution of the universe theories in physics and astronomy which called BB-BC theory. The BB-BC optimization method is formed by two phases: a Big Bang phase where candidate solutions are randomly distributed over the search space in a uniform manner and a Big Crunch phase where candidate solutions are drawn into a single representative point via a center of mass for the population [20]. The initial Big Bang population is randomly generated over the entire search space just like the other evolutionary search algorithms. All subsequent Big Bang phases are randomly distributed about the center of mass in a similar fashion. The Big Bang phase is followed by the Big Crunch phase which is a convergence operator. This operator takes the current positions of each candidate solution in the population and its associated cost function value to calculate the center of mass. The point representing the center of mass that is denoted by x^c is calculated according to the formula:

$$\bar{x}^c = \frac{\sum_{i=1}^N \frac{1}{f^i} \bar{x}^i}{\sum_{i=1}^N \frac{1}{f^i}} \quad (2.23)$$

where x^i is a point within an n-dimensional search space generated, f^i is a fitness function value of this point, N is the population size in Big Bang phase. After the Big Crunch phase, new points are produced to be used in the Big Bang of the next iteration step. The new generation is normally distributed around the center of mass x^c in every direction as follows:

$$x^{new} = x^c + \sigma \quad (2.24)$$

The standard deviation of this normal distribution is given as

$$\sigma = \frac{r\alpha(x_{max} - x_{min})}{k} \quad (2.25)$$

where r is a normal random number; α is a parameter limiting the size of the search space and k is the iteration step. Therefore, the new point is generated as follows:

$$x^{new} = x^c + \frac{r\alpha(x_{max} - x_{min})}{k} \quad (2.26)$$

These consecutive explosion and contraction are carried repetitively until a stopping criterion has been met. High convergence speed, low computation time and few parameters to be selected are the leading advantages of BB-BC optimization method [20]. BB-BC algorithm has already been applied to different areas with encouraging results such as fuzzy model inversion [21], and power system stabilizer [22].

The BB-BC optimization algorithm can be used to extremize (minimize or maximize) the fitness function. Actually, selecting the fitness function is the most important part in any type of optimization algorithms. A fitness function based on time domain is proposed to satisfy the smallest overshoot, faster rise time, very small steady state error and quickest settling time. In order to combine all of these objectives together, the following fitness function is used [21]:

$$J = \frac{100}{2 * O.S + 6 * T_s + 12 * T_r + 44 * SSE} \quad (2.27)$$

The constants of this fitness function have been adjusted in such way that normalize the time domain step response criteria to be in same scale. Highest constant 44 is attached to steady state error to emphasis on this criterion in the optimization process. This fitness function is inversely proportional to the step response parameters of the dynamic system. Hence, the center of mass equation in BB-BC optimization algorithm

can be adopted for maximization case as following:

$$\bar{x}^c = \frac{\sum_{i=1}^N f^i \bar{x}^i}{\sum_{i=1}^N f^i} \quad (2.28)$$

For simplicity, the Q matrix is reduced to diagonal form i.e. $Q = \text{Diag}[q_1, \dots, q_n]$; hence, the parameters of Q and R matrices are combined into one vector in order to be used within the BB-BC optimization algorithm: $V = [q_1, \dots, q_n, r_1, \dots, r_k]$.

Figure 2.3 demonstrates the flowchart of BB-BC optimization algorithm. Once the stopping criterion is satisfied in BB-BC algorithm, the optimized Q and R matrices will be ready to construct the feedback state control law for LQR controller which will stabilize the control system and minimize the cost function.

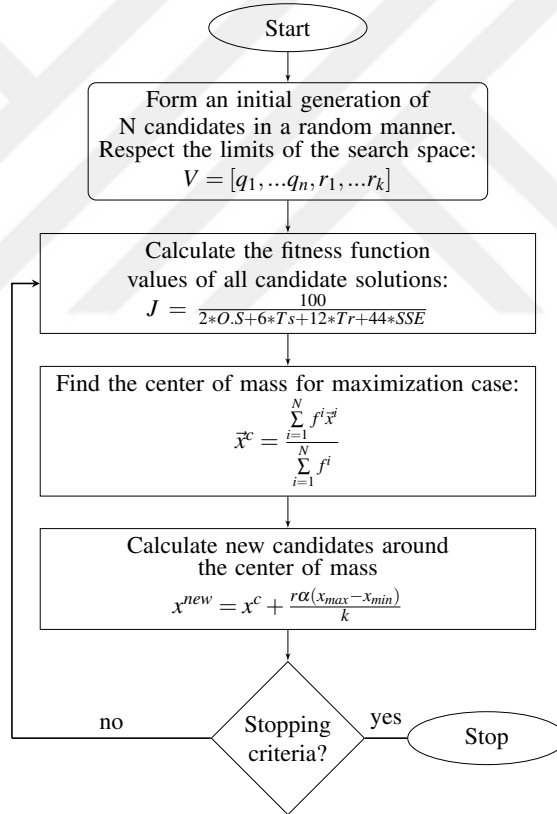


Figure 2.3 : Flowchart of the BB-BC optimization algorithm for LQR controller.

2.4.2 Simulation results for inverted pendulum on cart

The inverted pendulum on cart is a classic control problem in dynamics and control theory that is a suitable benchmark for testing prototype controllers due to its high nonlinearities and lack of stability [27, 29, 30]. The physical model of the system is

shown in Figure 2.4. The studied system consists of an inverted pole attached on a cart which is free to move in the x -direction. It is assumed that the pendulum rod is massless, and the joint is frictionless. The cart mass and the ball mass at the upper end of the inverted pendulum are denoted as M and m , respectively. F is an externally x -directed force on the cart which driven by a DC motor. x represents the cart position and θ is the angle of the rod from the vertically upward direction.

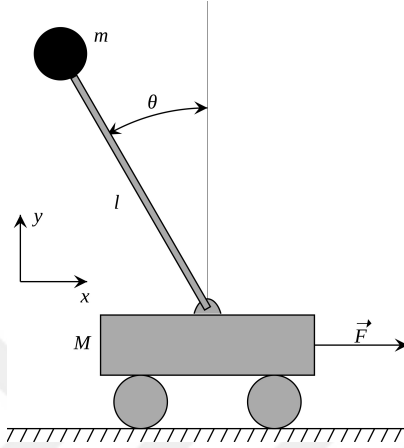


Figure 2.4 : The structure of inverted pendulum on cart system.

Table 2.1 contains the physical quantities for the inverted pendulum on cart.

Table 2.1 : Physical quantities for the inverted pendulum on cart for LQR based BB-BC.

Symbol	Parameter	Value	Unit
M	Mass of the cart	0.5	Kg
m	Mass of the pendulum	0.2	Kg
L	Length of the pendulum	0.3	m
b	Coefficient of friction for cart	0.1	$N/m/sec$
I	Pendulum moment of inertia	0.006	$kg.m^2$
g	Gravity	9.8	m/s^2

By summing the forces in the free body diagram of the inverted pendulum system in horizontal and vertical direction, we get the following equations of motion:

$$(M + m)\ddot{x} + b\dot{x} + mL\ddot{\theta}\cos\theta - mL\dot{\theta}^2\sin\theta = F \quad (2.29)$$

$$(I + mL^2)\ddot{\theta} + mgL\sin\theta = -mL\ddot{x}\cos\theta \quad (2.30)$$

The dynamic equations in (2.29) and (2.30) are linearized about $\theta = \pi$ at the upright (unstable) equilibrium position. Assume that $\theta = \pi + \phi$ where (ϕ represents a small

angle from the vertical upward direction). The state-space form of the linearized equations for the inverted pendulum on cart system will be:

$$\begin{bmatrix} \dot{x}(t) \\ \ddot{x}(t) \\ \dot{\phi}(t) \\ \ddot{\phi}(t) \end{bmatrix} = \begin{bmatrix} 0 & 1 & 0 & 0 \\ 0 & -\frac{(I+mL^2)b}{I(M+m)+MmL^2} & \frac{m^2gL^2}{I(M+m)+MmL^2} & 0 \\ 0 & 0 & 0 & 1 \\ 0 & -\frac{mLb}{I(M+m)+MmL^2} & \frac{mgL(M+m)}{I(M+m)+MmL^2} & 0 \end{bmatrix} \begin{bmatrix} x(t) \\ \dot{x}(t) \\ \phi(t) \\ \dot{\phi}(t) \end{bmatrix} + \begin{bmatrix} 0 \\ \frac{I+mL^2}{I(M+m)+MmL^2} \\ 0 \\ \frac{mL}{I(M+m)+MmL^2} \end{bmatrix} u(t) \quad (2.31)$$

$$y(t) = \begin{bmatrix} 1 & 0 & 0 & 0 \\ 0 & 0 & 1 & 0 \end{bmatrix} \begin{bmatrix} x(t) \\ \dot{x}(t) \\ \phi(t) \\ \dot{\phi}(t) \end{bmatrix} + \begin{bmatrix} 0 \\ 0 \end{bmatrix} u(t) \quad (2.32)$$

A constant gain factor can be added in order to reduce the steady state error of the system output. The value of constant gain N_{bar} is selected to be: $N_{bar} = -70.7107$. The search domains for q_1, q_2, q_3, q_4 are selected to be $[1, 10^7]$ and $[1, 10^3]$ for r . After 25 iterations in BB-BC algorithm, the optimal weighing matrices are obtained as: $Q = [4.070 * 10^6 \quad 2.632 \quad 2249.7 \quad 23514.1], R = [821.72]$. Hence, the feedback gain matrix will be : $K = [-70.3786 \quad -44.4010 \quad 143.4788 \quad 30.6465]$.

The experiential-LQR method for the same inverted pendulum on cart has been used in [48, 49] where the LQR matrices are selected as $Q = C' * C$ and $R = [I]$. Here, the output responses of the pendulum's angle and cart's position stabilized by the proposed controller compared with the experiential-LQR results in [49] are shown in Figure 2.5 and Figure 2.6, respectively.

Table 2.2 demonstrates the comparison between the step responses of the proposed method and the experiential-LQR technique for the cart of the pendulum.

Table 2.2 : Comparison between the response of LQR based BB-BC and experiential-LQR for the cart of the pendulum.

Time Response of Cart	LQR Based BB-BC	Experiential-LQR
Settling time	0.95 s	0.99 s
SSE	0	0
Rising Time Tr	0.44	0.41
Percentage Overshoot	0 %	0 %

From Table 2.2, the experiential-LQR has faster rising time of 0.41 seconds while the

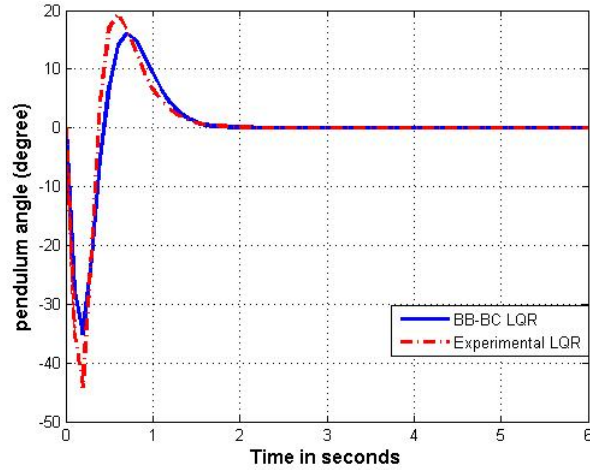


Figure 2.5 : Oscillation of the pendulum’s angle for proposed controller and the experiential-LQR one.

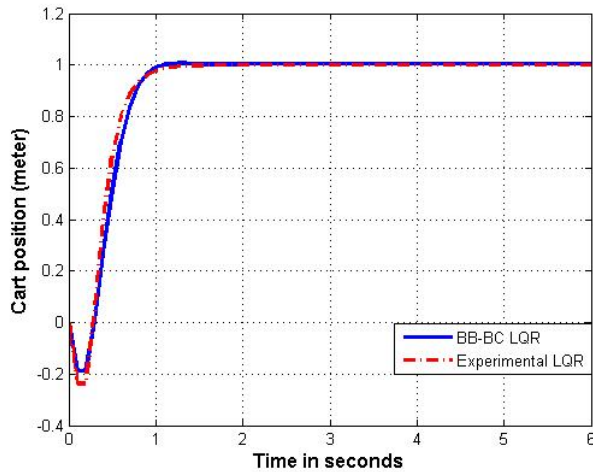


Figure 2.6 : Step response of the cart’s position for proposed controller and the experiential-LQR one.

proposed one has the rising time of 0.44 seconds. However, the proposed controller has smaller settling time of 0.95 seconds. In addition, from Figure 2.6 it is worth to remark that the pendulum’s angle has a 35° maximum overshoot range in the oscillation while in experiential-LQR method it is exceeded the 44° . Both the proposed controller and experiential-LQR method have percent overshoot and steady state error for the cart almost equal to 0. Finally, the effectiveness and superiority of the proposed method is due to the fact that it is automatically calculated the parameters of the weighing matrices and there is no need for trial and error time conservative approach.

2.4.3 Experimental results for the DC-DC boost converter

The DC-DC boost converters are widely used in power conversion applications where the required output voltage is higher than the source voltage. The DC-DC boost converter dynamics are nonlinear in nature due to switching action and saturation of the duty-cycle. The control law obtained for these converters is usually based on linear techniques which is simpler and of lower cost than other nonlinear approaches [35]. Hence, the small signal model of this converter is derived by linearization around a specific equilibrium point where the stability is basically achieved around the small vicinity of this point.

Considering the DC-DC boost converter circuit shown in Figure 2.7.

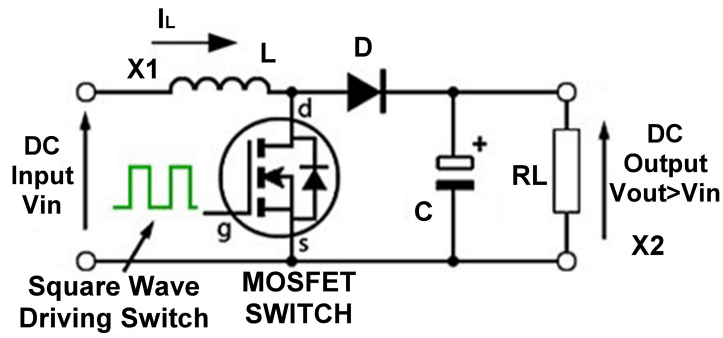


Figure 2.7 : DC-DC boost converter circuit.

To derive the state equations of this converter, states x_1 and x_2 are allocated to the current of inductor L and the voltage of capacitor C , respectively. The commutated model for the DC-DC boost converter can be presented as:

$$\frac{di_L}{dt} = \dot{x}_1 = \frac{V_{in}}{L} - \mu \cdot \frac{x_2}{L} \quad (2.33)$$

$$\frac{dv_c}{dt} = \dot{x}_2 = \mu \cdot \frac{x_1}{C} - \frac{x_2}{R_L C} \quad (2.34)$$

Where $\mu = \{0, 1\}$ is the switch position, D_d is the duty-cycle of the control signal μ and D'_d is the complementary operating point duty-cycle (i.e. $D'_d = 1 - D_d$). If the switching frequency is significantly higher than the converter's natural frequencies, then this discontinuous model can be approximated around an appropriate equilibrium point and reformed in a continuous averaged model.

Hence, the equilibrium point is selected as in [35]:

$$X = \begin{bmatrix} \frac{V_g}{D_d^2 R} \\ \frac{V_g}{D_d} \end{bmatrix}, \quad U = Dd \quad (2.35)$$

Since we consider the control of the boost converter around the equilibrium point, we can neglect the nonlinear term of the converter average model and obtain a linearized model. Hence, the state space model of the boost converter is obtained as:

$$\begin{bmatrix} \dot{x}_1 \\ \dot{x}_2 \end{bmatrix} = \begin{bmatrix} 0 & -\frac{D'_d}{L} \\ \frac{D'_d}{C} & -\frac{1}{R_L C} \end{bmatrix} \begin{bmatrix} x_1 \\ x_2 \end{bmatrix} + \begin{bmatrix} \frac{V_{in}}{LD'_d} \\ -\frac{V_{in}}{(D'_d R_L)C} \end{bmatrix} u(t) \quad (2.36)$$

$$y = [0 \quad 1] \begin{bmatrix} x_1 \\ x_2 \end{bmatrix} \quad (2.37)$$

The DC-DC converter parameters are given in Table 2.3.

Table 2.3 : DC-DC boost converter model parameters.

Element	Value
Diode	1n4007
Power Mosfet	IRF 620
Inductor	4.9 mH
Capacitor	470 uF
Load resistor	470 Ω \rightarrow 570 Ω
Input voltage	9V

Hence, the optimal control problem for DC-DC boost converter is to determine a control signal μ that achieves stability for the converter and minimizes a certain cost function. The controlled DC-DC boost converter should be robust in the presence of disturbances, such as step changes in load or changes in source voltage and converter parameters. In a boost converter, the output voltage response of the DC-DC boost converter is controlled by changing the duty cycle of the pulse width modulation (PWM) signal. The structure of the converter with the proposed controller is shown in Figure 2.8. The circuit has a current sensor and differential amplifier in order to measure the inductor current. The load change experiments have been carried out by means of a multi-steps switch at the load side. A variable power supply is used in order to test the transient waveform of output voltage with respect to changes in input voltage.

The feed forward gain scaling factor $N_{bar} = 6.44$ is used. The search domains for $q1, q2$ and r are selected to be $[1, 10^4]$. After 32 iterations within the proposed algorithm, the

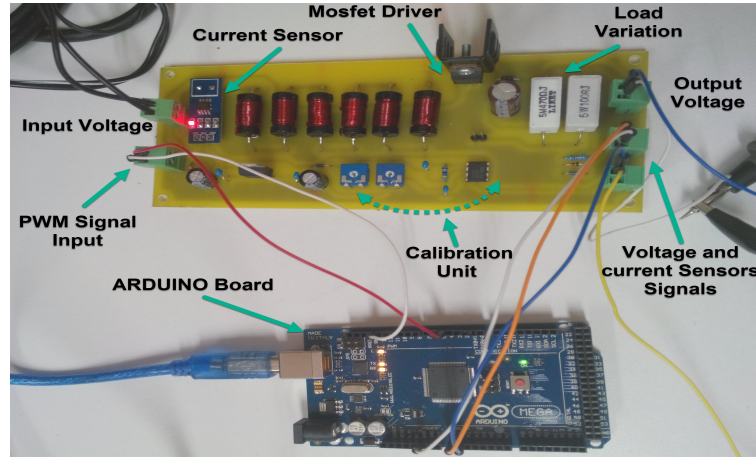


Figure 2.8 : DC-DC converter board and ARDUINO Mega 2560 controller kit

optimal weight matrices are obtained as: $Q = \text{diag}[403.159 \quad 749.712]$, $r = [732.293]$. Hence, the feedback gain matrix will be: $K = [1.1016 \quad 0.9751]$.

The proposed controller is implemented on an ARDUINO MEGA 2560 starter kit. One output pin is connected to the gate of the Mosfet driver in order to control the duty cycle by the mean of a PWM technique. The switching frequency of the converter was selected as 20 KHz. Two analog input pins were used to read the current flow in the inductor and the output voltage level on the capacitor. Figure 2.9 illustrates the algorithm block diagram for the proposed controller in a Simulink/MATLAB interface to be implemented on an ARDUINO controller.

The transient responses of the stabilized boost converter under sudden changes in desired reference voltage from 18V to 25V and then from 25V to 18V are shown in Figure 2.10. The overshoot is equal to 11.1% and undershoot equal to 28.4%. The settling and rising time were equal to .9s and 0.15s, respectively. However, there exist no remarkable steady state error value. The upper waveform of each figure shows the output voltage signal on the capacitor V_C , while the lower waveform depicts the inductor's current I_L .

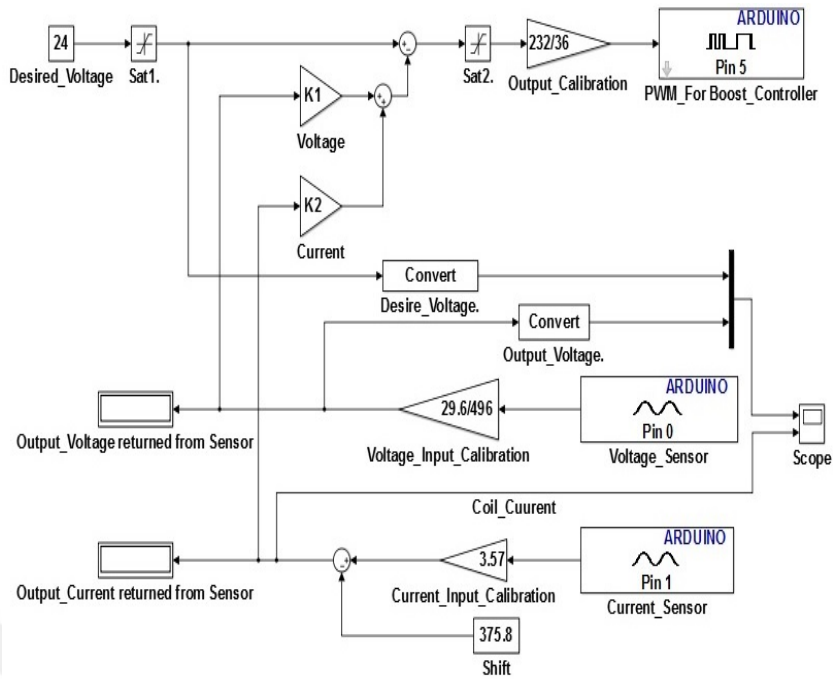


Figure 2.9 : The proposed controller algorithm within Simulink interface.

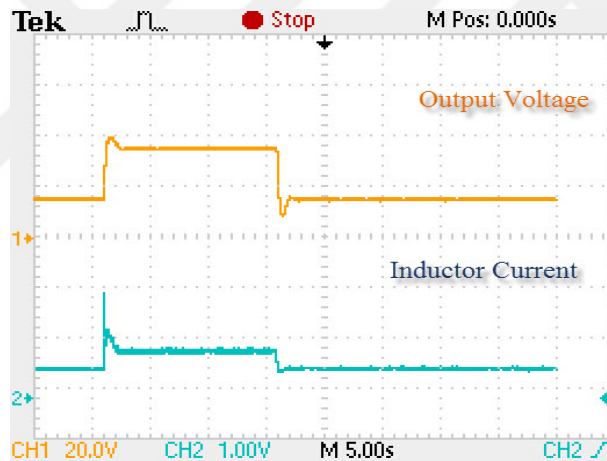


Figure 2.10 : Transient response for the proposed controller under sudden changes in reference voltage.

In order to check the robustness of the proposed controller, we have obtained the transient response under a set of load changes ($470\Omega \rightarrow 570\Omega \rightarrow 510\Omega \rightarrow 470\Omega \rightarrow 570\Omega$). The corresponding responses for the output voltage and inductor's current under the load perturbations have been grouped and shown in Figure 2.11. Hence, the output waveform illustrates the performance of the proposed controller in presence of the load perturbations. Furthermore, we have verified the response of the proposed controller to supply voltage changes where the experimental result, shown in Figure 2.12, illustrates the positive behavior of the proposed controller in stabilizing the output

voltage within the range of desired value 25V under input voltage variations from 9V, 7V, 10V and then to 12V.

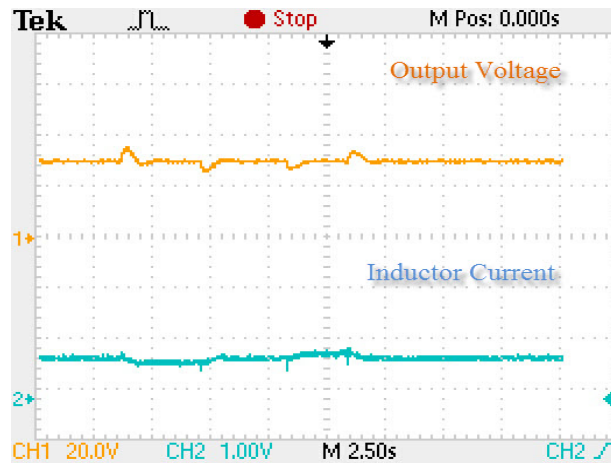


Figure 2.11 : Transient response of the proposed controller with load variation.

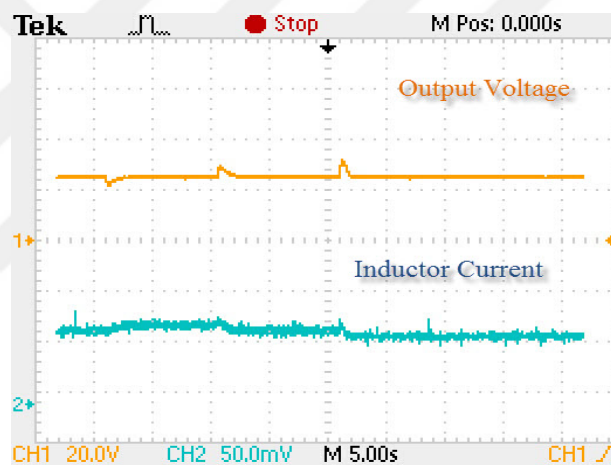


Figure 2.12 : Transient response of the proposed controller with input voltage variation.

From the previous results, it is obvious that the proposed method has been successfully stabilized the DC-DC boost converter prototype while optimizing a fitness function based on time domain. The correctness of this approach is verified in presence of step changes of load and line voltage.



3. INVERSE OPTIMAL CONTROL PROBLEM

This chapter describes some useful formulas required in the Lyapunov stability analysis where this analysis is important for the inverse optimal control based on CLF approach. Section (3.2) illustrates the inverse optimal control theorem for affine-in-input discrete-time nonlinear systems proposed in [3, 17]. This theorem will be used as basis for the proposed methods in the following chapters. Finally, the differences between the inverse optimal control problem and the optimal control problem is briefly discussed.

3.1 Lyapunov Stability Theory

In this section, the tools of Lyapunov stability are reviewed in order to analyze the stability properties of inverse optimal control theory based on CLF which is the basis of the proposed approaches in the following chapters. Here, only definitions and theorems are presented, with no proofs. For further information, the reader could find more details in standard texts of nonlinear systems, such as Khalil [50] or Vidyasagar [51]. Considering the affine-in-input discrete-time nonlinear system of the form:

$$x_{k+1} = f(x_k) + g(x_k)u_k \quad (3.1)$$

where $x \in \mathbb{R}^n$ is the state of the system, $u \in \mathbb{R}^m$ is the control input. $f(x_k) : \mathbb{R}^n \rightarrow \mathbb{R}^n$ and $g(x_k) : \mathbb{R}^n \rightarrow \mathbb{R}^{n \times m}$ are smooth matrices.

Definition 3.1: Equilibrium State [52]

An equilibrium point $x_k = E$ is such that:

$$\text{if } x_0 = E \Rightarrow x_k = E, \text{ for all } k$$

Without loss of generality, by shifting the origin of the system, it can be assumed that the origin ($x_0 = 0$) is the equilibrium point of the system (3.1).

Definition 3.2: Positive Definite Function [52]

A function $V(x_k)$ is said to be a positive definite function if

$$V(x_k) > 0 \quad \forall x_k \neq 0, \text{ and } V(0) = 0$$

Definition 3.3: Radially Unbounded Function [50]

A positive definite function $V(x_k)$ is said to be radially unbounded function if

$$V(x_k) \rightarrow \infty \text{ as } \|x_k\| \rightarrow \infty$$

Definition 3.2: Decrescent Function [50]

A function $V : \mathbb{R}^n \rightarrow \mathbb{R}$ is said to be decrescent if there is a positive definite function β such that the following inequality holds:

$$V(x_k) \leq \beta(\|x_k\|) \quad \forall k \geq 0$$

Theorem 3.1: Global Asymptotic Stability [52]

The equilibrium point $x_k = 0$ of (3.1) is globally asymptotically stable if there exists a function $V : \mathbb{R}^n \rightarrow \mathbb{R}$ such that:

- (i) V is a positive definite function, decrescent and radially unbounded.
- (ii) $-\Delta V(x_k, u_k)$ is a positive definite function, where

$$\Delta V(x_k, u_k) = V(x_k + 1) - V(x_k)$$

■

Theorem 3.2: Exponential Stability [3, 51]

Suppose that there exists a positive definite function $V : \mathbb{R}^n \rightarrow \mathbb{R}$ and constants $c_1, c_2, c_3 > 0$ and $p > 1$ such that

$$c_1 \|x\|^p \leq V(x_k) \leq c_2 \|x\|^p$$

$$\Delta V(x_k) \leq -c_3 \|x\|^p, \quad \forall k \geq 0, \quad \forall x \in \mathbb{R}^n$$

Then the equilibrium point $x_k = 0$ is an exponentially stable for system (3.1). ■

Definition 3.3: Control Lyapunov Function [53, 54]

Let $V(x_k)$ be a radially unbounded function, with $V(x_k) > 0, \forall x_k \neq 0$ and $V(0) = 0$. If for any $x_k \in \mathbb{R}^n$ there exist real values u_k such that

$$\Delta V(x_k, u_k) < 0$$

where the Lyapunov difference is defined as

$$\Delta V(x_k, u_k) = V(f(x_k) + g(x_k)u_k) - V(x_k)$$

then $V(\cdot)$ is said to be a discrete-time control Lyapunov function (CLF) for system (3.1).

Assumption 3.1: [3]

Let us assume that $x_k = 0$ is an equilibrium point for system (3.1), and that there exists a control Lyapunov function $V(x_k)$ such that

$$\alpha_1(\|x\|) \leq V(x_k) \leq \alpha_2(\|x\|)$$

$$\Delta V(x_k, u_k) \leq -\alpha_3(\|x\|)$$

where $\alpha_1, \alpha_2, \alpha_3$ are class \mathbb{H}_∞ functions and $\|\cdot\|$ denotes the usual Euclidean norm. Then, the origin of the system is an asymptotically stable equilibrium point by means of u_k as input.

The existence of this CLF is guaranteed by a converse theorem of the Lyapunov stability theory. As a special case, the calculus of class \mathbb{H}_∞ functions in (Assumption 3.1) simplifies when they take the special form $\alpha_i(r) = k_i r^c, k_i > 0, c = 2$, and $i = 1, 2$. In particular, for a quadratic positive definite function $V(x_k) = \frac{1}{2}x_k^T P x_k$, with P a positive definite and symmetric matrix, inequality in (Assumption 3.1) results in

$$\lambda_{\min}(P)\|x\|^2 \leq x_k^T P x_k \leq \lambda_{\max}(P)\|x\|^2$$

where $\lambda_{\min}(P)$ is the minimum eigenvalue of matrix P and $\lambda_{\max}(P)$ is the maximum eigenvalue of matrix P .

3.2 Inverse Optimal Control Based on CLF For Discrete-Time Nonlinear System

Considering the affine-in-input discrete-time nonlinear system (3.1) where this system is assumed to be stabilizable on a predefined compact set $\Omega \in \mathbb{R}^n$. For a nonlinear optimal control problem, it is desirable to determine a control law u_k , which minimizes the following cost functional:

$$V(x_k) = \sum_{n=k}^{\infty} (L(x_n) + u_n^T E u_n) \quad (3.2)$$

The optimal control u_k^* has been driven in Chapter (2) Equation (2.9) as:

$$u_k^* = \bar{u}(x_k) = -\frac{1}{2}E^{-1}g^T(x_k) \frac{\partial V^*(x_{k+1})}{\partial x_{k+1}} \quad (3.3)$$

Definition 3.4: The control law u_k^* at Equation (3.3) can be assumed to be inverse optimal control if:

- a) It achieves a global exponential stability of the equilibrium point $x_k = 0$ for the system (3.1).
- b) It minimizes the cost functional in Equation (3.2), for which $L(x_k) := -\bar{V}$, with $\bar{V} := V(x_{k+1}) - V(x_k) + u_k^{*T} E u_k^* \leq 0$, where $V(x_k)$ is radially unbounded positive definite function.

In this approach, inverse optimal control is based on knowledge of $V(x_k)$. Hence, a CLF $V(x_k)$ is proposed such that (a) and (b) are guaranteed. In [6], the authors proved that the Lyapunov function can be considered as a solution to the HJB equation in optimal control problems corresponding to a meaningful cost functional. That is, instead of solving HJB in Equation (2.11) for $V(x_k)$, a candidate quadratic control Lyapunov function $V(x_k)$ is proposed with the form:

$$V(x_k) = \frac{1}{2}x_k^T P x_k \quad (3.4)$$

where $P \in \mathbb{R}^{n \times n}$ is assumed to be positive definite and symmetric, i.e. $P = P^T > 0$. However, an appropriate matrix P must be selected in order to achieve stability and to minimize a meaningful cost functional.

The state feedback control law can be rewritten as:

$$u_k^* = -\frac{1}{2}(E + \frac{1}{2}g^T(x_k)Pg(x_k))^{-1}g(x_k)^T P f(x_k). \quad (3.5)$$

The following theorem gives the necessary condition for matrix P to satisfy the requirements of Definition (3.4).

Theorem 3.3: [3, 17]

Considering the affine discrete-time nonlinear system (3.1). If there exists a matrix $P = P^T > 0$ such that the following inequality holds

$$V_f(x_k) - \frac{1}{4}P_1^T(x_k)(E + P_2(x_k))^{-1}P_1(x_k) \leq -\zeta_Q \|x_k\|^2 \quad (3.6)$$

where:

$V_f(x_k) = V(f(x_k)) - V(x_k)$, with $V(f(x_k)) = \frac{1}{2}f^T(x_k)P f(x_k)$; $\zeta_Q > 0$
 $P_1(x_k) = g^T(x_k)P f(x_k)$; $P_2(x_k) = \frac{1}{2}g^T(x_k)P g(x_k)$ then the equilibrium point ($x_k = 0$) of the system (3.1) is globally exponential stabilized by the control law in Equation (3.5) with the CLF in Equation (3.4). Moreover, this control law will minimize the cost functional given in Equation (3.2), with $L(x_k) := -\bar{V}|_{u_k^*}$. Hence, the optimal value function will be equal to $V^*(x_0) = V(x_0)$. ■

This theorem was proved in [17] and presented in Appendix A.

The process of finding an appropriate P matrix is still an active research topic [3, 17, 18].

In [17], the authors used the form $V(x_k) = \frac{1}{2}x_k^T P x_k$ as a CLF and they proposed the

Trial and Error method to select an appropriate value for P matrix. Moreover in [18] the same authors proposed a time-variant parameter P_k to be adjusted where $P = P_k * P'$ and P' is a predefined matrix.

In this research, two different methods to find P matrix are proposed; the first is the off-line method using different search algorithm which presented in Chapter (4), and then in Chapter (5), the EKF approach to estimate the overall elements of the P matrix in on-line manner within the loop of inverse optimal control is presented.

Here, the simulation results which appeared in [17,18] are re-done and presented to be used in the comparison process at following chapters.

Considering the following affine-in-input nonlinear dynamical system [17,18]:

$$x_{k+1} = f(x_k) + g(x_k)u_k \quad (3.7)$$

where:
$$f(x_k) = \begin{bmatrix} x_{1,k}x_{2,k} - 0.8x_{2,k} \\ x_{1,k}^2 + 1.8x_{2,k} \end{bmatrix}, \quad g(x_k) = \begin{bmatrix} 0 \\ -2 + \cos(x_{2,k}) \end{bmatrix}$$

The stabilizing optimal control law can be calculated according to Equation (3.5). Matrix P is selected as : $P = \begin{bmatrix} 10 & 0 \\ 0 & 10 \end{bmatrix}$. The MATLAB platform of the Trial and Error method for inverse optimal control is shown in Figure 3.1.

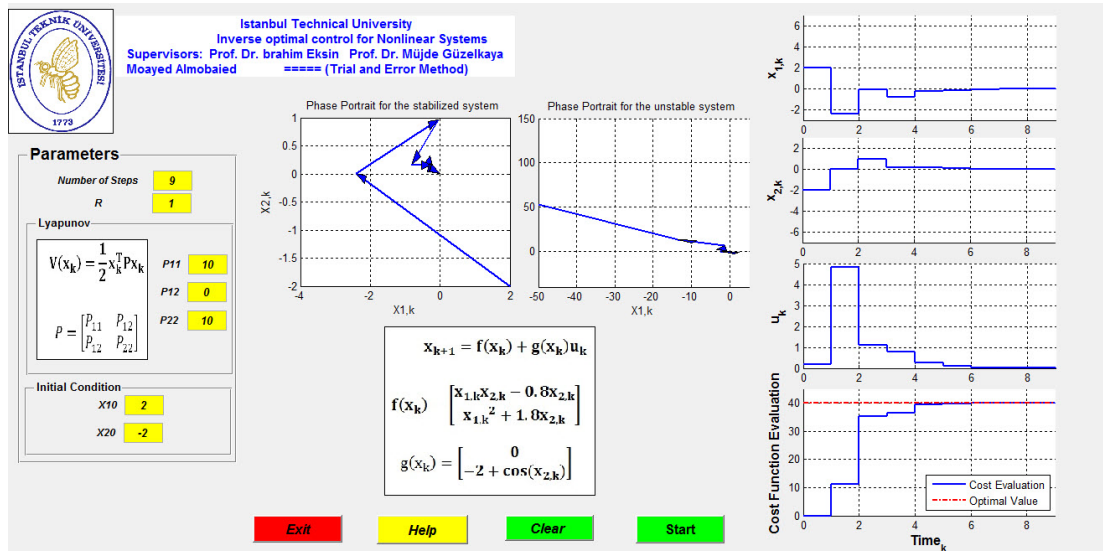


Figure 3.1 : The platform of Trial and Error method for inverse optimal control.

The MATLAB platform of the speed gradient algorithm method for inverse optimal control is shown in Figure 3.2.

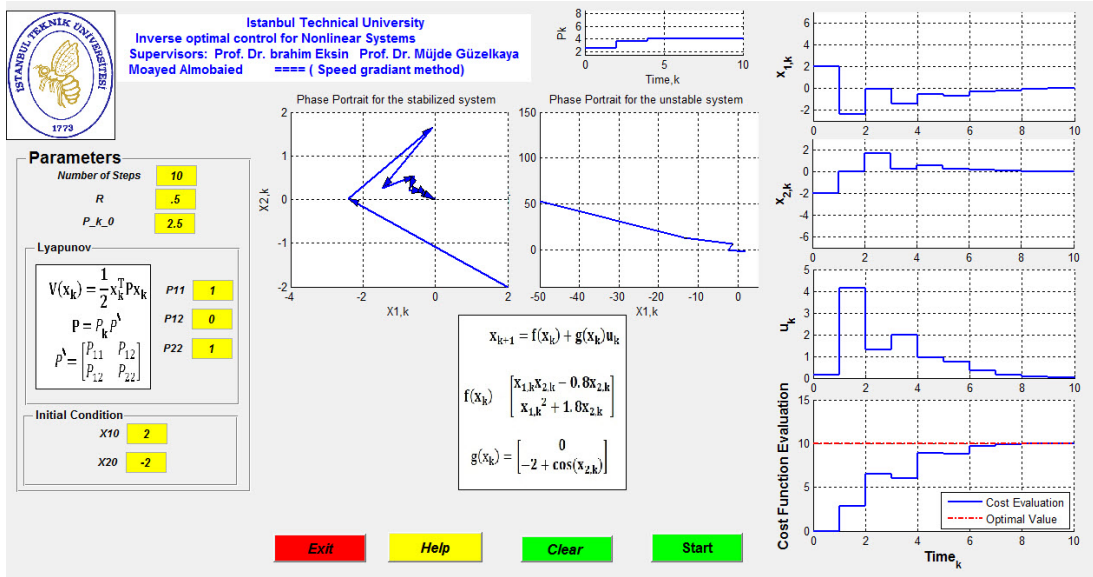


Figure 3.2 : The platform of speed gradient algorithm method for inverse optimal control.

Figures (3.1 , 3.2) illustrate the effectiveness of the speed gradient algorithm [18] over the Trial and Error method [17] for inverse optimal control problem in minimizing the cost functional.

Shortly, the distinction between the traditional solution for the nonlinear optimal control problem and the inverse optimal control approach based on control Lyapunov function is illustrated in Figure 3.3.

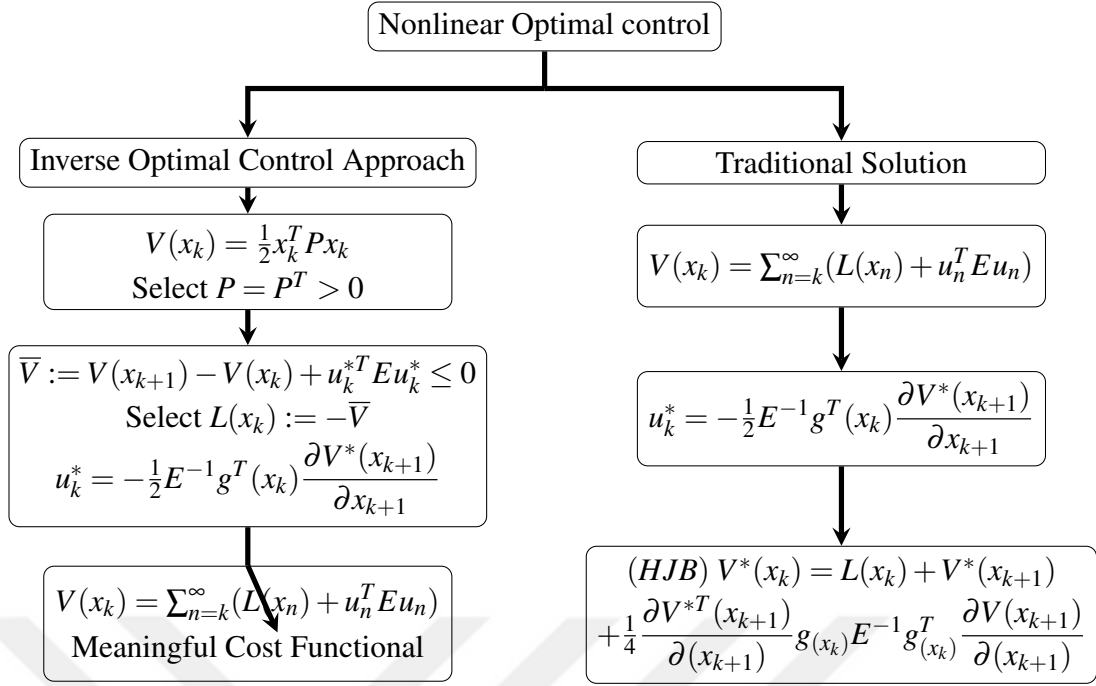


Figure 3.3 : Inverse optimal control approach and traditional solution for optimal control problem.

- "For optimal control, the state cost function $L(x_k) > 0$ and the input weighing term $E > 0$ are given a priori. Then, they are used to determine $u(x_k)$ and $V(x_k)$ by the means of the discrete-time HJB equation solution" [3].
- "For inverse optimal control, the control Lyapunov function $V(x_k) > 0$ and the input weighing term $E > 0$ are given a priori. Then, these functions are used to compute $u(x_k)$ and the penalty term $L(x_k)$ which used in constructing a meaningful cost function" [3].



4. AN OFF-LINE INVERSE OPTIMAL CONTROL APPROACH FOR DISCRETE-TIME NONLINEAR SYSTEMS

This chapter presents an inverse optimal control design method for affine-in-input discrete-time nonlinear systems where the parameters of the candidate CLF were optimized in an off-line manner by using Particle Swarm Optimization (PSO). The Big Bang-Big Crunch multi-objective algorithm is also proposed where the root-mean-square-error (RMSE) of system states with respect to a reference trajectory and the sum-of-squares of control effort are utilized as the multi-objective optimization criterion. In order to test the performance of the proposed method, a nonlinear example from the literature of inverse optimal control is firstly taken into consideration. The simulation results enlighten the designer in making a choice between the single objective inverse optimal control solution and the multi-objective function included case. Next, the proposed controller is used to stabilize an inverted pendulum on cart.

4.1 PSO algorithm for inverse optimal control

In this section, the P matrix of the candidate quadratic control Lyapunov function $V(x_k)$, which illustrated in Chapter (3), will be optimized in an off-line manner in order to construct the control law of the inverse optimal control by using PSO algorithm.

4.2 Particle Swarm Optimization (PSO)

PSO algorithm which proposed by Kennedy and Eberhart [55], is a population-based search algorithm simulates social behavior of insect swarms or bird flocks shown in Figure 4.1 [56]. The optimization process of PSO depends on a population of candidate solutions, called particles. These candidate solutions are iteratively improved by the the particles' movements around in the search space according to a mathematical equation over the particle's position and velocity. The particle's movement is influenced by its local best known position and is also guided toward the best known positions in the search-space which are better positions found by other

particles. Therefore, the swarm is expected to move toward the best solutions [55].

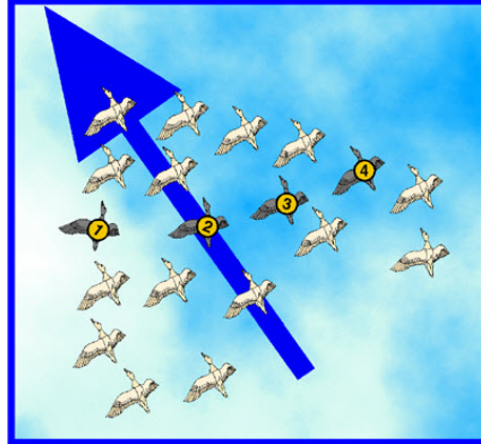


Figure 4.1 : Swarm flocks.

Each particle moves through a n -dimensional search space, with an associated position vector:

$$x_i(t) = \{x_{i1}, x_{i2}, \dots, x_{in(t)}\} \quad (4.1)$$

and velocity vector:

$$v_i(t) = \{v_{i1}, v_{i2}, \dots, v_{in(t)}\} \quad (4.2)$$

For the current evolutionary iteration t . The individual particle in PSO flies in the search space with velocity which is dynamically adjusted according to its own flying experience and its companions' flying experience. The former was termed cognition-only model and the latter was termed social-only model. By integrating these two types of knowledge, the particle behavior in a PSO can be modeled by using the following equations:

$$v_i(t+1) = w * v_i(t) + c_1 * rand * (Pbest_i - x_i(t)) + c_2 * rand * (Gbest_i - x_i(t)) \quad (4.3)$$

$$x_i(t+1) = x_i(t) + v_i(t+1) \quad (4.4)$$

where

c_1, c_2 : acceleration constants;

$rand$: random number between 0 and 1;

$x_i(t)$: the position of particle i at iteration t ;

$v_i(t)$: the velocity of particle i at iteration t ;

w : inertia weight factor;

$Gbest$: the best previous position among all the particles;

$Pbest_i$: the best previous position of particle i .

Equation 4.3 represents the velocity-updating rule which consist of:

- The first term $w * v_i(t)$ represents the previous velocity as the necessary momentum for particles to fly across the search space.
- The second term $c_1 * rand * (Pbest_i - x_i(t))$ represents the personal thinking of each particle, which encourages the particles to move toward their own best positions found so far.
- The third term $c_2 * rand * (Gbest_i - x_i(t))$ represents the collaborative effect of the particles in finding the global optima.

A typical PSO algorithm consists a population of particles initialized with random position x_i and velocity v_i . Fitness of particles is evaluated by calculating the objective function $f(x_i)$. The current position of each particle is set as $Pbest_i$. The $Pbest_i$ with best value in the swarm is set as $Gbest$. As evolution continues, next position for each particle is evaluated by using the previous equations. If a better position is achieved by an agent, the $Pbest_i$ value is replaced by the current value. If a new $Gbest$ value is better than the previous $Gbest$ value, the $Gbest$ value is replaced by the current $Gbest$ value. Iterations repeat until a predetermined iteration number is reached. The flow chart of PSO algorithm is shown in Figure 4.2.

Here, the root mean square error of the system states is selected as the fitness function F to be minimized using PSO while searching the appropriate value for P matrix.

The formula of RMSE is given by:

$$RMSE = \sqrt{\frac{(x_1 - x_{1ref})^2 + (x_2 - x_{2ref})^2 + \dots + (x_n - x_{nref})^2}{n}} \quad (4.5)$$

Figure 4.3 illustrates the block diagram of the proposed PSO inverse optimal control approach.

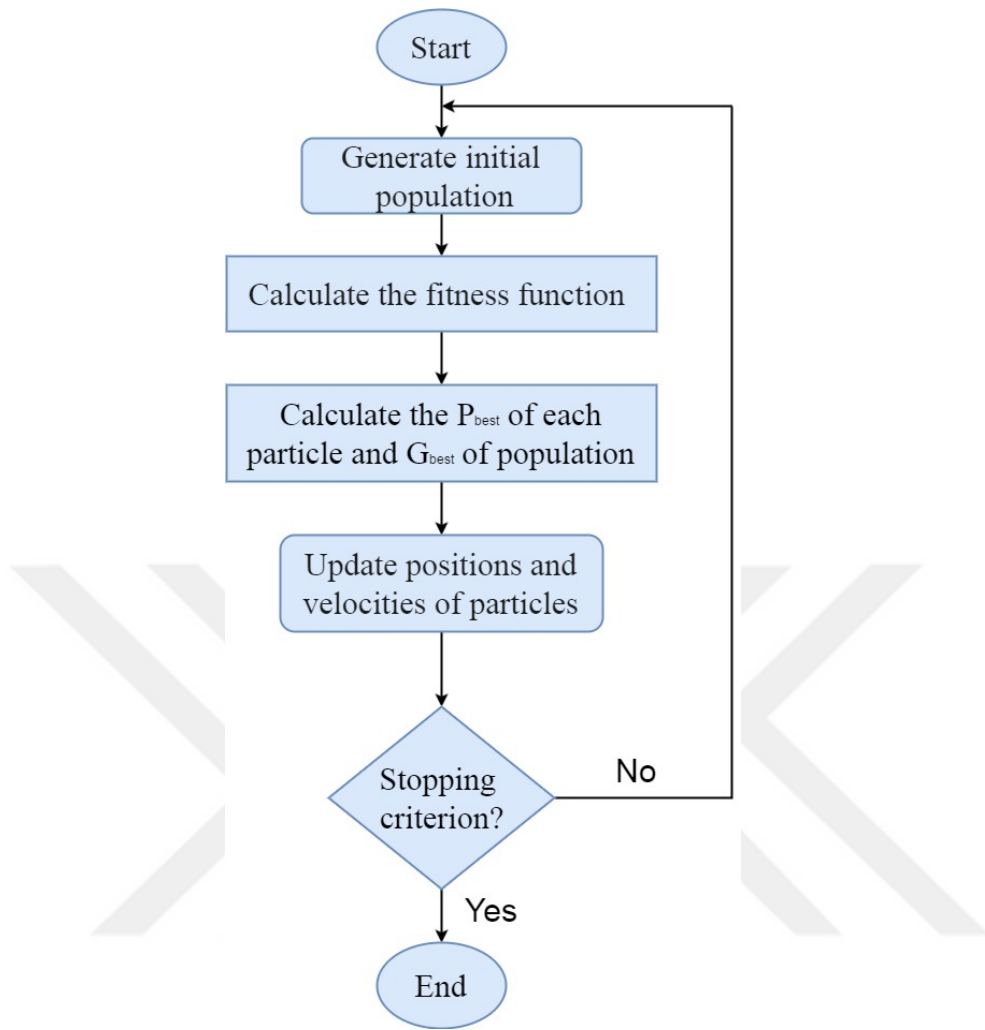


Figure 4.2 : Swarm algorithm flowchart.

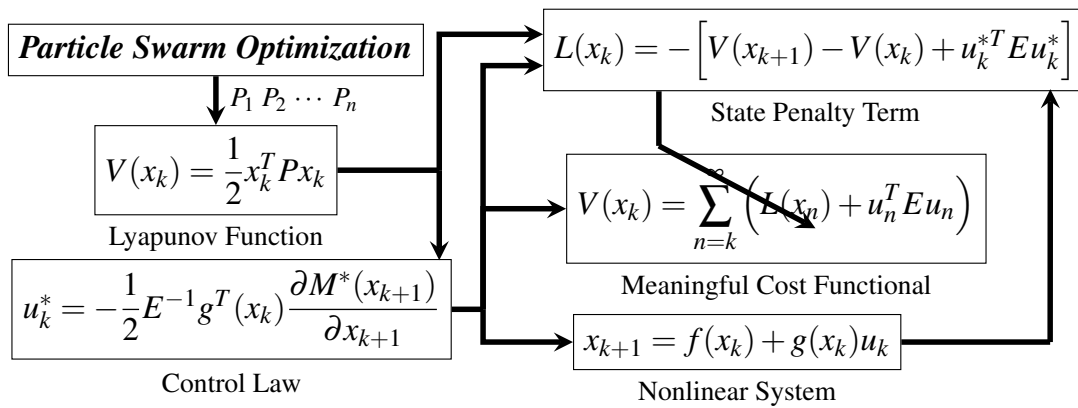


Figure 4.3 : The proposed PSO optimization based inverse optimal controller for discrete-time nonlinear system.

4.3 Multi-objective Big Bang-Big Crunch Optimization algorithm for inverse optimal control

In this section, the parameters of the candidate control Lyapunov matrix are optimized by using multi-objective Big Bang-Big Crunch algorithm.

The BB-BC algorithm is already presented in details at section 2.4.1.

4.3.1 Multi-objective Optimization Criteria

Most of optimization problems in the real-world appears to be in a multi-objective nature where these multiple objectives are often in conflict with each other. In a single objective optimization problem, the best design solution is the unique optimal point and value. However, for multi-objective optimization problems, there exist more than one optimal solution points. Therefore, the decision maker is required to select a solution from a finite set of solution points by making compromises [57]. A multi-objective optimization problem with m objectives can be written in general as:

$$\begin{aligned} & \text{Minimize } f_1(x), f_2(x), \dots, f_m(x) \\ & \text{Subject to } x \in \mathbb{S} \end{aligned} \tag{4.6}$$

In many multi-objective optimization approaches it is possible to transform the multi-objective problem into a single composite objective optimization problem. One of the simplest methods that is commonly used for this purpose is the weighting sum method [57]. Therefore, the single objective can be considered as:

$$f = \sum_{i=1}^m w_i f_i \tag{4.7}$$

with

$$\sum_{i=1}^m w_i = 1, w_i > 0 \tag{4.8}$$

where m is the number of objectives and $w_i (i = 1, \dots, m)$ are non-negative weights. Hence, the optimization process will produce a single point for each given set of w_i . The fundamental idea of the weighted sum approach is that the weighted coefficients act as the preferences for these objectives [57]. These weights are randomly generated; therefore, different weights are used to generate different optimal solutions and then the decision maker is asked to select the most appropriate one.

Considering the CLF used in inverse optimal control law which explained at Theorem (3.3).

$$V(x_k) = \frac{1}{2}x_k^T P x_k \quad P = P^T > 0 \quad (4.9)$$

where P_1, P_2, \dots, P_m are the elements of matrix P to be optimized by the proposed method. Figure 4.4 illustrates the block diagram of the proposed method.

The steps of the proposed method are illustrated as following:

1. Find the optimal value of P matrix using Big Bang-Big Crunch optimization method by:

- a. Form an initial generation of N candidates; each candidate is a vector of parameters equal to the number of the optimized elements in P matrix.
- b. Calculate the fitness function values of all the candidate solutions. Both the RMSE of system states and the sum-of-squares of control law values are used as the fitness functions:

- Fitness function (1):

$$RMSE = \sqrt{\frac{(x_1 - x_{1ref})^2 + (x_2 - x_{2ref})^2 + \dots + (x_n - x_{nref})^2}{n}}$$

- Fitness function (2):

$$\text{Sum-of-squares of control law values} = \sum_{k=1}^n |u(k)|^2$$

- c. A constraint for maximum value of $u(k)$ can be added as a physical constraint.
- d. Combine the multi-objective problem into a composite single objective optimization problem as described in Section 4.3.1.
- e. Calculate new candidate vectors around the center of

$$x^{new} = x^c + \frac{r\alpha(x_{max} - x_{min})}{k}$$

- f. Return to step b if the stopping criteria is not satisfied.

2. Construct the control Lyapunov function (CLF), and then establish the control law of the inverse optimal control.

3. Calculate the penalty term $L(x_k)$ for the meaningful cost functional.

4. Calculate the new states of the nonlinear discrete system.

In summary, the Big Bang-Big Crunch algorithm is carried out off-line and minimized the RMSE of system states and Sum-of-squares of control law values by generating a CLF matrix with appropriate elements. Hence, guaranteeing system stability by the meaning of eliminating the RMSE. The best value for this CLF matrix which is determined by the Big Bang-Big Crunch optimization algorithm is then used for establishing the inverse optimal controller for discrete-time affine nonlinear systems

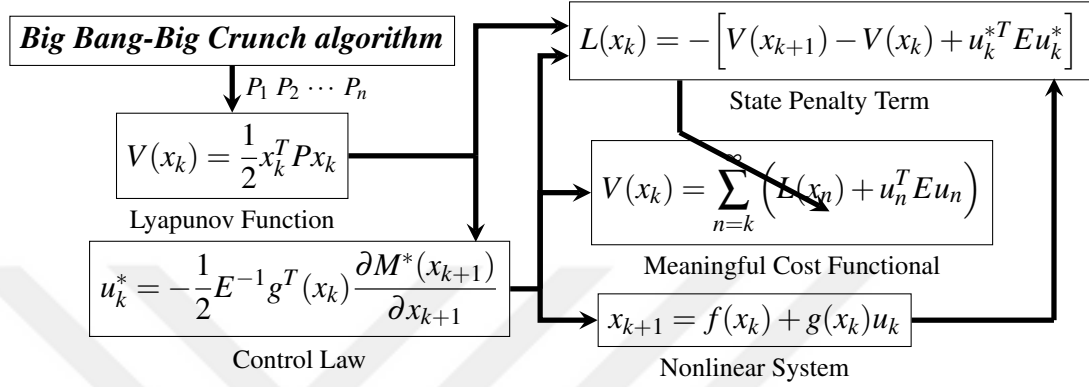


Figure 4.4 : The proposed multi-objective Big Bang-Big Crunch optimization based inverse optimal controller for discrete-time nonlinear system.

4.4 Simulation Examples

The performance of both PSO algorithm and the multi-objective Big Bang-Big Crunch optimization is examined through a comparison study over a nonlinear example for inverse optimal control presented at [17] where the authors proposed the trial and error method to select an appropriate value for matrix P . Finally, the proposed multi-objective Big Bang-Big Crunch optimization algorithm for inverse optimal control is used to stabilize an inverted pendulum on cart by MATLAB simulation.

4.4.1 A nonlinear system case

Considering the following affine-in-input nonlinear dynamical system:

$$x_{k+1} = f(x_k) + g(x_k)u_k \quad (4.10)$$

where:
$$f(x_k) = \begin{bmatrix} x_{1,k}x_{2,k} - 0.8x_{2,k} \\ x_{1,k}^2 + 1.8x_{2,k} \end{bmatrix}, \quad g(x_k) = \begin{bmatrix} 0 \\ -2 + \cos(x_{2,k}) \end{bmatrix}$$

The stabilizing optimal control law can be calculated according to Equation (3.5). Matrix P is estimated by the proposed method, where $E = 1$ is the constant in the cost

functional equation. The initial condition for the states is selected as $x_0 = [2 \quad -2]$. The MATLAB platform of the proposed PSO algorithm for inverse optimal control is shown in Figure 4.5.

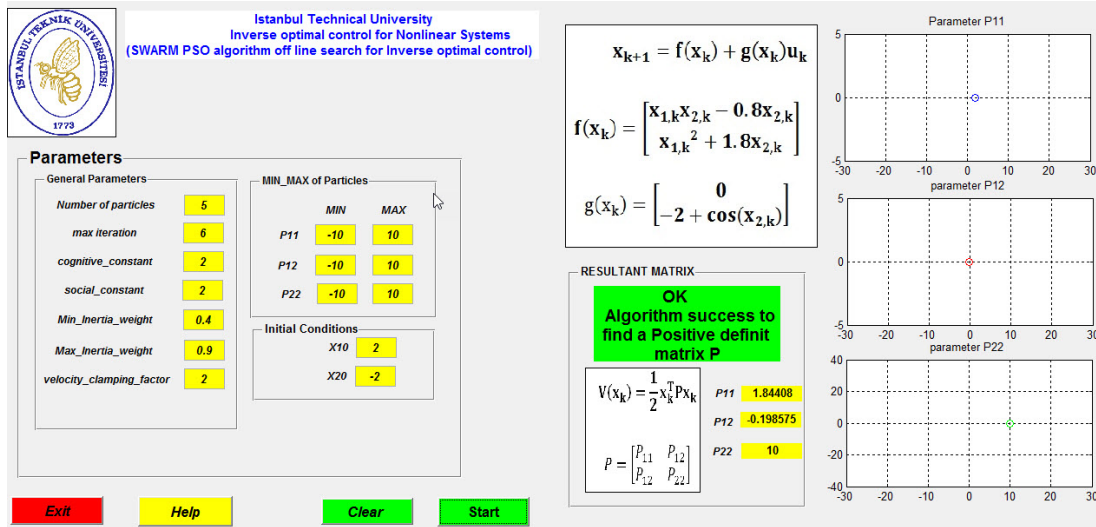


Figure 4.5 : The platform of PSO algorithm for inverse optimal control.

Figure 4.6 illustrates the response of the closed loop system with the resultant P matrix from the proposed PSO algorithm.

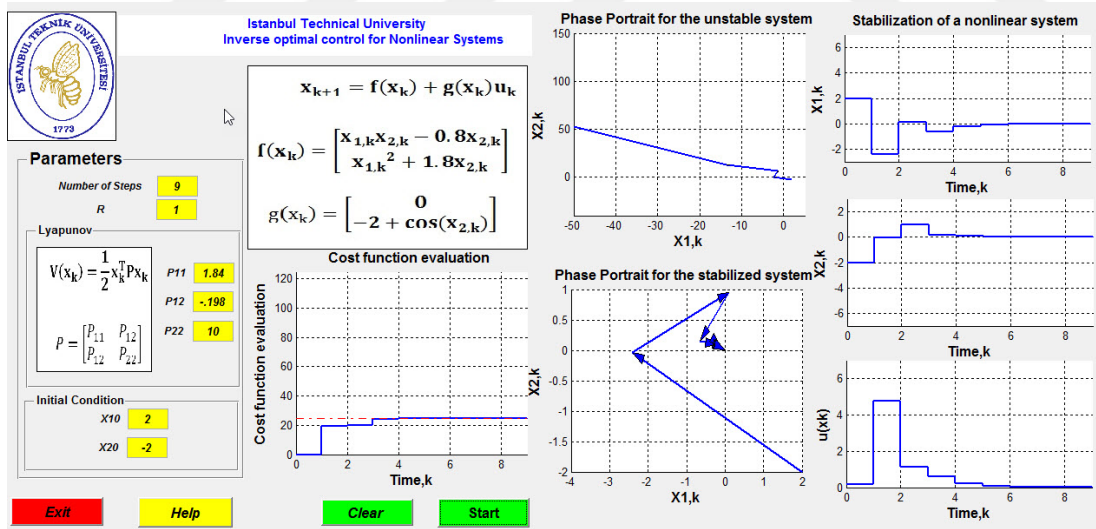


Figure 4.6 : Swarm platform result.

Figure 4.7 demonstrates the MATLAB GUI simulation platform that used in order to adapt the parameters of the proposed multi-objective BB-BC algorithm and to analysis the output states of the nonlinear example.

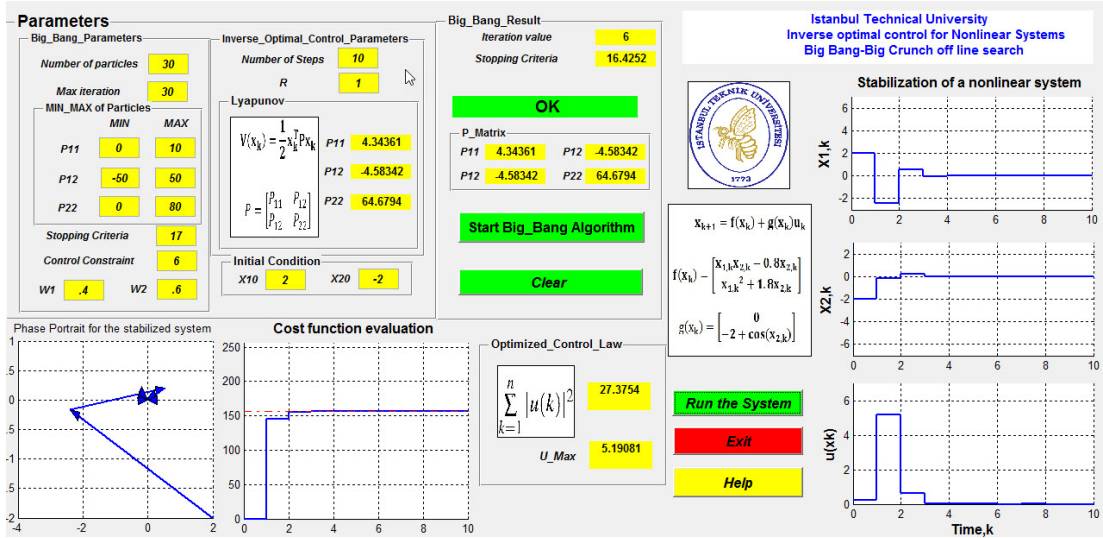


Figure 4.7 : MATLAB GUI for the proposed multi-objective Big Bang-Big Crunch Optimization controller for inverse optimal control.

The following parameters can be configured by using the platform of the multi-objective Big Bang-Big Crunch Optimization controller for inverse optimal control :

- Boundaries of the elements in P matrix.
- The weighting parameters of the objectives.
- The stopping criterion.
- The max value of the control law $u(k)$.
- The initial conditions of the system's states.

Four scenarios are presented here for the Big Bang-Big Crunch inverse optimal controller:

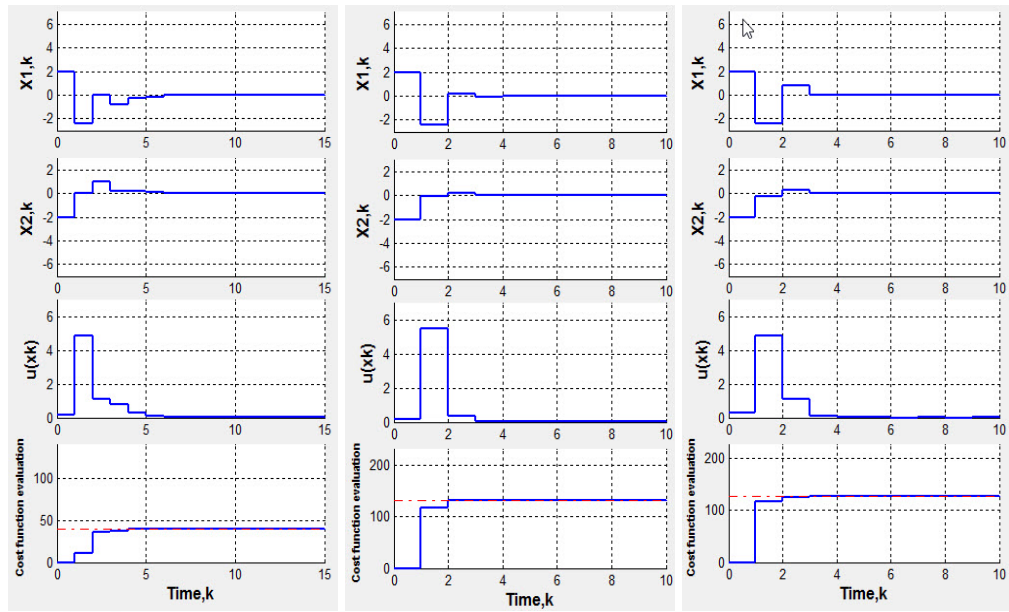
1. Only considering the minimization part of RMSE for the system states ($W_1 = 1, W_2 = 0$) as shown in Figure 4.8 (b).
2. Highly consideration of the minimization part of RMSE for the system states ($W_1 = .8, W_2 = 0.2$) as shown in Figure 4.8 (c).
3. Equally considering the minimization of RMSE for the system states and the Sum-of-squares for the control effort ($W_1 = .5, W_2 = 0.5$) as shown in Figure 4.8 (d).

4. Highly consideration of the minimization part of Sum-of-squares for the control effort ($W_1 = .2, W_2 = 0.8$) as shown in Figure 4.8 (e).

Here, a comparison study for the previous example is done between the proposed PSO based inverse optimal controller, multi-objective Big Bang-Big Crunch inverse optimal controller with different cases and the trial and error method used in [17]. MATLAB simulation results in Figure 4.8 show the superior performance of multi-objective Big Bang-Big Crunch inverse optimal controller and demonstrate its potential in minimizing the cost functional. Table 4.1 shows the difference between off-line inverse optimal controller scenarios.

Table 4.1 : Difference between off-line inverse optimal controller scenarios.

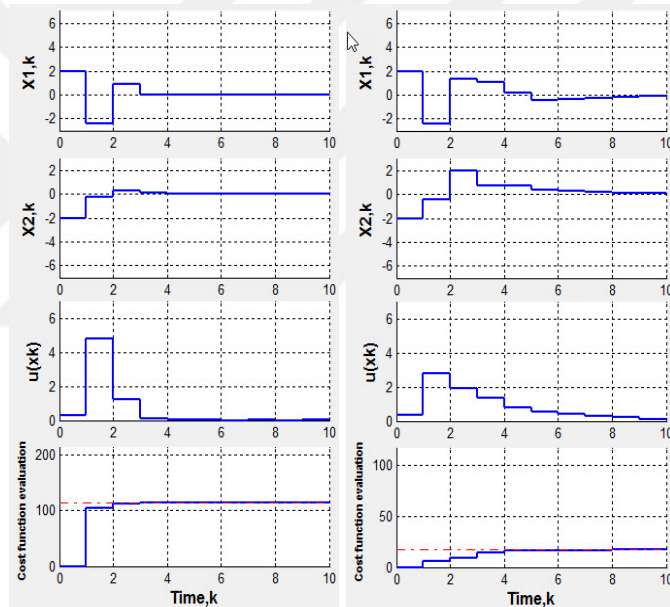
Cases	W_1	W_2	U-Constraint	U-Max	$\sum_{k=1}^n u_k^2$	Cost	State1	State2	P-Matrix		
									P_{11}	$P_{12} = P_{21}$	P_{22}
Case1	1	0	7	5.48	30.26	131	4	3	4.81	-1.11	58.52
Case2	.8	.2	6	4.86	24.89	126	5	4	3.88	-5.3	48.9
Case3	.5	.5	6	4.76	24.33	114	5	4	4.24	-5	42.85
Case4	.2	.8	4	2.8	14.58	16.71	9	8	4.05	-.65	3.08
PSO	-	-	-	3.65	19.788	32	5	6	1.84	-.198	10
Trial & Error	-	-	-	4.819	25.169	40	5	5	10	0	10



(a) Trial and Error

(b) Case1

(c) Case2



(d) Case3

(e) Case4

Figure 4.8 : Stabilized nonlinear system with different cases.

4.4.2 An inverted pendulum on cart case

The inverted pendulum on cart is a classic control problem in dynamics and control theory that is a suitable benchmark for testing prototype controllers due to its high nonlinearities and lack of stability [27, 29, 30]. The physical model of the system is shown in Figure 4.9. The studied system consists of an inverted pole attached on a cart which is free to move in the x -direction. It is assumed that the pendulum rod is massless, and the joint is frictionless. The cart mass and the ball mass at the upper

end of the inverted pendulum are denoted as M and m , respectively. F is an externally x -directed force on the cart which driven by a DC motor. x represents the cart position and θ is the angle of the rod from the vertically upward direction.

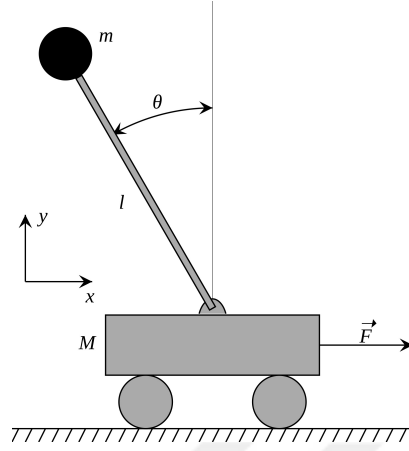


Figure 4.9 : The structure of inverted pendulum on cart system.

Table 4.2 contains the physical quantities for the inverted pendulum on cart.

Table 4.2 : Physical quantities for the inverted pendulum on cart.

Symbol	Parameter	Value	Unit
M	Mass of the cart	0.5	Kg
m	Mass of the pendulum	0.2	Kg
L	Length of the pendulum	0.3	m
I	Pendulum moment of inertia	0.006	$kg.m^2$
g	Gravity	9.8	m/s^2

By summing the forces in the free body diagram of the inverted pendulum system in horizontal and vertical direction, we get the following equations of motion:

$$(M + m)\ddot{x} + mL\ddot{\theta}\cos\theta - mL\dot{\theta}^2\sin\theta = \vec{F} \quad (4.11)$$

$$(I + mL^2)\ddot{\theta} + mgL\sin\theta = -mL\ddot{x}\cos\theta \quad (4.12)$$

Hence, the dynamics of the inverted pendulum on cart are given as in [58]:

$$\begin{aligned} \dot{x} &= v_x \\ \dot{v}_x &= \frac{ml\omega^2\sin\theta - mg\sin\theta\cos\theta + \vec{F}}{M + m\sin^2\theta} \\ \dot{\theta} &= \omega \\ \dot{\omega} &= \frac{-ml\omega^2\sin\theta\cos\theta + (M + m)g\sin\theta - \vec{F}\cos\theta}{M + m\sin^2\theta} \end{aligned} \quad (4.13)$$

Euler approximation method $\left(\dot{x} = \frac{x_{k+1} - x_k}{\Delta T}\right)$ is used in order to discretize the boost converter equations. Hence, the discrete-time model for the inverted pendulum on cart is obtained as:

$$\begin{aligned}
x_{k+1} &= x_k + \Delta T v_{x,k} \\
v_{x,k+1} &= v_{x,k} + \Delta T \left(\frac{ml\omega_k^2 \sin\theta_k - mg\sin\theta_k \cos\theta_k}{M + m\sin^2\theta_k} \right) + \frac{\Delta T}{M + m\sin^2\theta_k} \vec{F}_k \\
\theta_{k+1} &= \theta_k + \Delta T \omega_k \\
\omega_{k+1} &= \omega_k + \Delta T \left(\frac{-ml\omega_k^2 \sin\theta_k \cos\theta_k + (M + m)mg\sin\theta_k}{Ml + m\sin^2\theta_k} \right) - \frac{\Delta T \cos\theta_k}{Ml + m\sin^2\theta_k} \vec{F}_k
\end{aligned} \tag{4.14}$$

where ΔT is the sampling time. In order to apply the proposed inverse optimal controller method, the dynamics of the inverted pendulum on cart should be rewrite in affine-in-input discrete-time form as following:

$$\begin{aligned}
x_{k+1} &= f(x_k) + g(x_k) \vec{F}_k \\
f(x_k) &= \begin{bmatrix} x_k + \Delta T v_{x,k} \\ v_{x,k} + \Delta T \left(\frac{ml\omega_k^2 \sin\theta_k - mg\sin\theta_k \cos\theta_k}{M + m\sin^2\theta_k} \right) \\ \theta_k + \Delta T \omega_k \\ \omega_k - \Delta T \left(\frac{(ml\omega_k^2 \sin\theta_k \cos\theta_k) + (M + m)g\sin\theta_k}{Ml + m\sin^2\theta_k} \right) \end{bmatrix} \\
g(x_k) &= \begin{bmatrix} 0 \\ \frac{\Delta T}{M + m\sin^2\theta_k} \\ 0 \\ -\frac{\Delta T \cos\theta_k}{Ml + m\sin^2\theta_k} \end{bmatrix}
\end{aligned} \tag{4.15}$$

Figure 4.10 demonstrates the MATLAB GUI simulation platform that used in order to adapt the parameters of the proposed multi-objective BB-BC algorithm and to analysis the output states for inverted pendulum on cart.

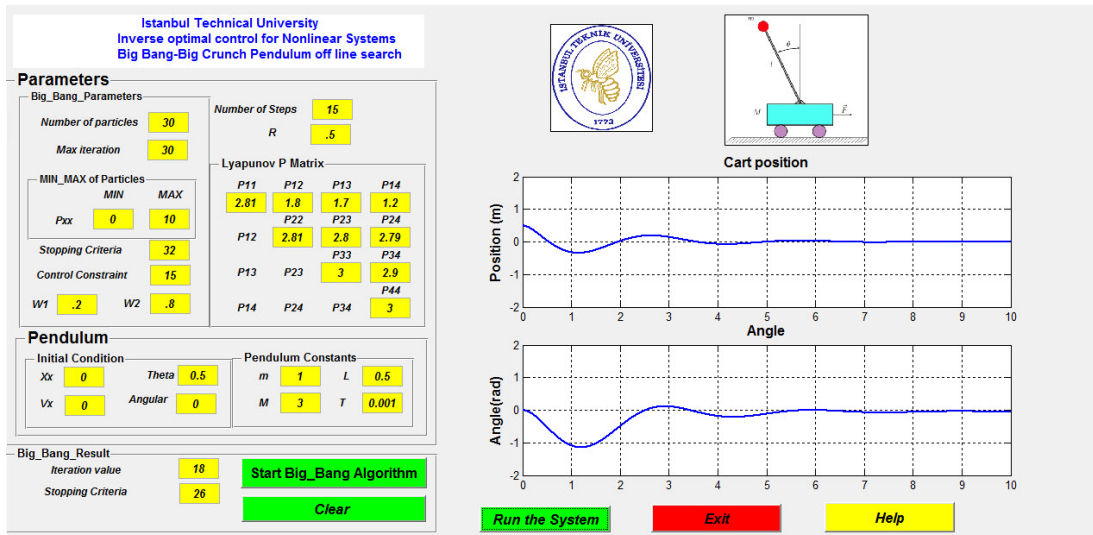


Figure 4.10 : MATLAB GUI for the proposed multi-objective Big Bang-Big Crunch Optimization controller for inverted pendulum on cart.

By means of MATLAB simulations, the proposed multi-objective BB-BC algorithm for inverse optimal control as an off-line approach is successfully stabilized the inverted pendulum on cart nonlinear dynamics.

5. AN ON-LINE INVERSE OPTIMAL CONTROL BASED ON EXTENDED KALMAN FILTER APPROACH FOR DISCRETE-TIME NONLINEAR SYSTEMS

In this chapter, the extended Kalman filter (EKF) equations are adopted to be used as an on-line parameter identifier for optimizing the elements of the control Lyapunov function (CLF). This CLF will be used to construct the inverse optimal control law as it has been defined in Chapter (3). The performance and the applicability of the proposed scheme is illustrated through several reliability nonlinear examples using MATLAB and a real time laboratory experiments. For the real time, the proposed controller is implemented on a professional control board to stabilize a DC-DC boost converter and minimize a meaningful cost function [33, 37].

5.1 EKF Algorithm for Inverse Optimal Control

In this study, a novel method for inverse optimal control is proposed; where the parameters of the candidate control Lyapunov matrix in the control law are estimated using EKF after certain adaptations.

5.1.1 General Information on Extended Kalman Filter

The Kalman filter (KF), a set of mathematical equations, has become a standard technique as an optimal estimator and is quite an easy method to estimate the unmeasurable states in linear systems, in a way that minimizes the mean of the squared error [59]. For nonlinear systems, the Kalman filter cannot be applied directly. However, if the nonlinearity of the system is sufficiently smooth, then it can be linearized about the current mean and covariance of the state estimation. Kalman filter that linearizes about the current mean and covariance is referred to as an extended Kalman filter (EKF). This filter has diverse applications in the areas of radar target tracking, aerospace, marine navigation and control systems [31, 60].

EKF algorithms are usually used to estimate the state variables which are normally represented by $\{x_1, x_2, \dots, x_n\}$ symbols. In this research, the EKF is used as a parameter

identifier. Hence, to avoid the confusion with symbols in the proposed inverse optimal control method, the symbols $\{a_1, a_2, \dots, a_n\}$ are used instead of $\{x_1, x_2, \dots, x_n\}$ to represent the states to be estimated (or parameters to be identified) inside EKF equations.

The state of the system at time $t_k (k = 1, 2, \dots)$ is modelled as a stochastic variable a_k . The evolution of the state in time is given by a stochastic difference equation

$$a_k = w(a_{k-1}, u_k) + \varepsilon_k \quad (5.1)$$

The measurements z_k are related to the state by

$$z_k = h(a_k) + \delta_k \quad (5.2)$$

State transition probability and measurement probability are governed by nonlinear functions w and h , respectively. ε_k represents the system process noise and is assumed to be Gaussian white noise with zero mean and covariance matrix Q_k . δ_k represents the measurement noise and is assumed to be Gaussian white noise with zero mean and covariance matrix R_k . Finally, u_k is the input control vector. The equations of an EKF are illustrated in Figure 5.1. Where the matrix W_k is the Jacobian of the state function and is defined as the derivatives of each component of w with respect to each component of a_{k-1} . Moreover, matrix H_k is the Jacobian of the measurement function and it is defined as the derivatives of each component of h with respect to each component of a_k . The EKF notations from [61] are: \hat{a}_k Posterior mean estimate at time step t_k , \hat{a}_k^- Prior mean estimate at time step t_k , Σ_k Posterior covariance at time step t_k , Σ_k^- Prior covariance at time step t_k , K_k Kalman gain, z_k Actual measurement, and \hat{z}_k^- Predicted measurement.

Since the covariance matrices that are used in EKF are approximations and the estimation is based on the linearization of nonlinear functions w and h , there is no guarantee of stability and performance for the system prior to experimental data analysis. Indeed, the approach seems to work well if the linearization is sufficiently smooth and a proper tuning for filter parameters is achieved [62]. The next section illustrates how to modify EKF equations to estimate the parameters in the proposed inverse optimal control law.

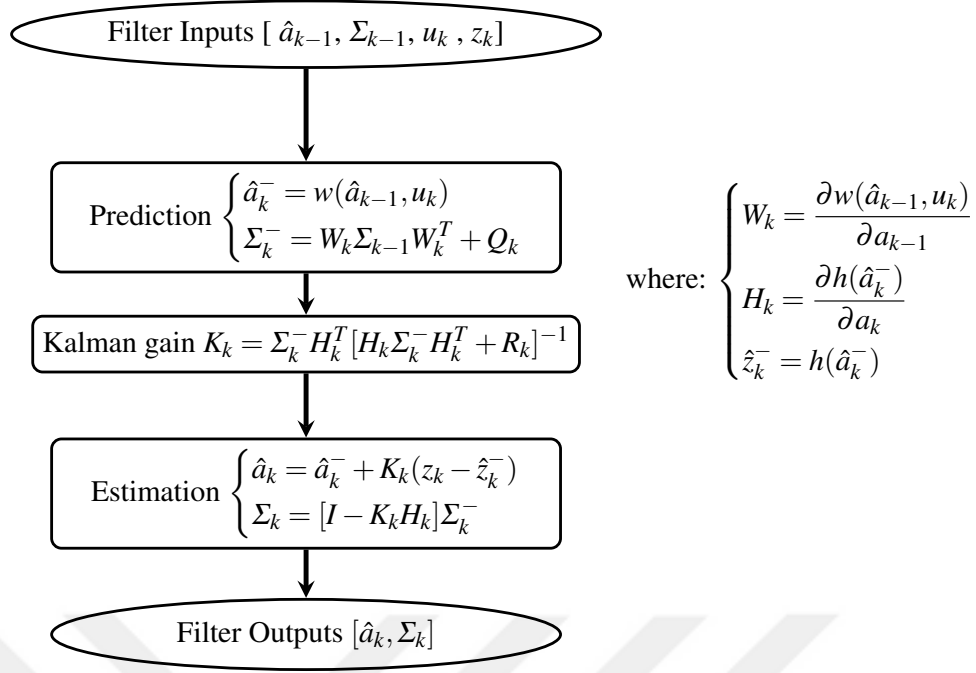


Figure 5.1 : Extended Kalman filter equations.

5.1.2 Extended Kalman Filter equations as parameter optimizer in inverse optimal control

Here, we consider the following quadratic CLF which explained in Chapter 3.

$$V(x_k) = \frac{1}{2} x_k^T P x_k \quad P = P^T > 0 \quad (5.3)$$

where P_1, P_2, \dots, P_m are the elements of matrix P to be estimated by the adopted EKF equations. Due to symmetric property of matrix P , $m = \frac{n(n+1)}{2}$ where n is the number of states. In order to adopt the EKF equations as a parameter identifier, the matrix P elements are accepted as the state variables of the classical EKF procedure. The on-line estimating process requires the initial values for these parameters and their corresponding covariance values.

$$\hat{a}_{k-1} = \hat{a}_k^- = w(\hat{a}_{k-1}, u_k) = \begin{bmatrix} P_1 \\ P_2 \\ \cdot \\ \cdot \\ P_m \end{bmatrix} \quad (5.4)$$

The state Jacobian matrix W_k will be equal to the identity matrix.

$$W_k = \begin{bmatrix} \frac{\partial P_1}{\partial P_1} & \frac{\partial P_1}{\partial P_2} & \cdots & \frac{\partial P_1}{\partial P_m} \\ \frac{\partial P_2}{\partial P_1} & \frac{\partial P_2}{\partial P_2} & \cdots & \frac{\partial P_2}{\partial P_m} \\ \vdots & \vdots & \ddots & \vdots \\ \frac{\partial P_m}{\partial P_1} & \frac{\partial P_m}{\partial P_2} & \cdots & \frac{\partial P_m}{\partial P_m} \end{bmatrix} = I \quad (5.5)$$

For simplicity, it can be assumed that covariance matrices Q_k and R_k are constant.

$$Q_k = q_0 \times I \quad , \quad \Sigma_0 = s_0 \times I \quad , \quad R_k = r_0 \quad (5.6)$$

where q_0 , s_0 , and r_0 are constants to be specified by the designer.

In this research, the main adopting in the EKF algorithm is done at the estimating equation

$$\hat{a}_k = \hat{a}_k^- + K_k(z_k - \hat{z}_k^-) \quad (5.7)$$

where the term $(z_k - \hat{z}_k^-)$ is used to calculate the difference between the actual measurement and the predicted measurement. This term is adopted as following:

\hat{z}_k^- in the EKF equations can be used as an error indicator and z_k can be set to be equal to zero to minimize the total error $(z_k - \hat{z}_k^-)$. The root mean square error (RMSE) of the state variables are used as the observed error instead of measurement error \hat{z}_k^- . (i.e., $\hat{z}_k^- = \text{RMSE}$), which equal to $h(\hat{a}_k^-)$ as shown in Figure 5.1.

$$\hat{z}_k^- = h(\hat{a}_k^-) = \text{RMSE} = \sqrt{\frac{(x_1 - x_{1ref})^2 + (x_2 - x_{2ref})^2 + \dots + (x_n - x_{nref})^2}{n}} \quad (5.8)$$

To calculate the Jacobian H_k , it is necessary to define $h(\hat{a}_k^-)$ as a function of the parameters to be optimized $[P_1, P_2, \dots, P_m]$. Then the Jacobian matrix can be found as following:

$$H_k = \begin{bmatrix} \frac{\partial h(\hat{a}_k^-)}{\partial P_1} & \frac{\partial h(\hat{a}_k^-)}{\partial P_2} & \cdots & \frac{\partial h(\hat{a}_k^-)}{\partial P_m} \end{bmatrix} \quad (5.9)$$

Figure 5.2 shows the block diagram of the proposed method, and Figure 5.3 illustrates the flowchart of the proposed EKF-based inverse optimal control algorithm.

In summary, the EKF tries to eliminate the RMSE of all system states by generating a CLF matrix with appropriate elements. This new P matrix should minimize the RMSE value if the filter parameters are well adjusted. Hence, guaranteeing system stability.

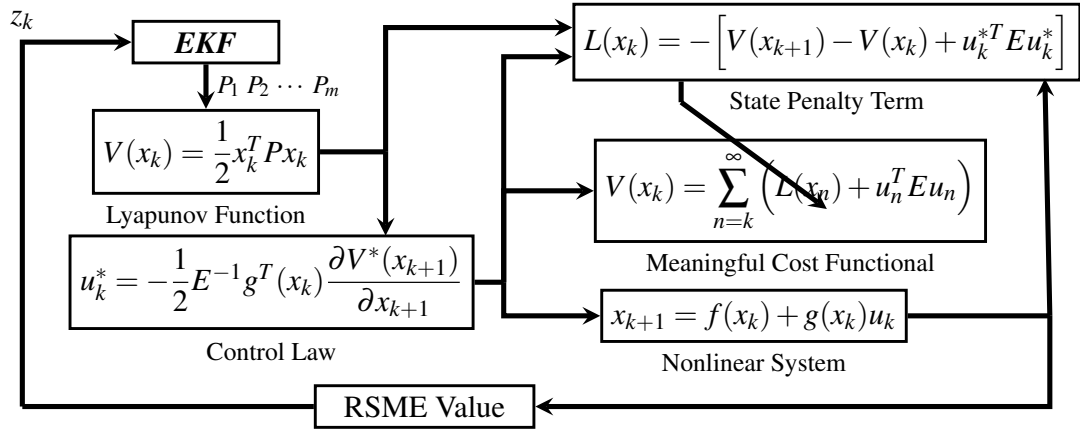


Figure 5.2 : The proposed EKF-based inverse optimal control for discrete-time nonlinear system.

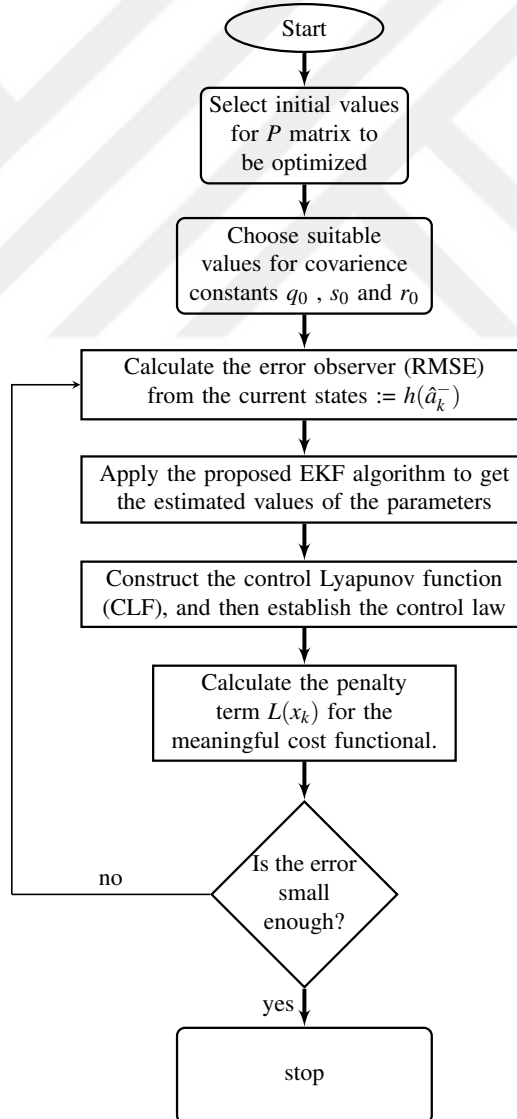


Figure 5.3 : The flowchart of the proposed EKF-based inverse optimal control.

5.2 Simulation Examples

The performance of the proposed EKF-based inverse optimal controller method has been tested via a comparison study between speed-gradient inverse optimal controller presented in [18] and the trial and error method used in [17] over two different nonlinear system models. In trial and error method, the authors try to select an appropriate value for matrix P . While in a speed gradient algorithm (SG), the authors proposed a quadratic function of the form $V(x_k) = \frac{1}{2}x_k^T P x_k$ with a time-variant parameter P_k to be optimized by speed gradient algorithm where $P = P_k * P'$ and P' is a predefined matrix.

5.2.1 A nonlinear system_1

Considering the following affine-in-input nonlinear dynamical system used in Chapter (4):

$$x_{k+1} = f(x_k) + g(x_k)u_k \quad (5.10)$$

where: $f(x_k) = \begin{bmatrix} x_{1,k}x_{2,k} - 0.8x_{2,k} \\ x_{1,k}^2 + 1.8x_{2,k} \end{bmatrix}$, $g(x_k) = \begin{bmatrix} 0 \\ -2 + \cos(x_{2,k}) \end{bmatrix}$

The stabilizing optimal control law can be calculated according to Equation (3.5). Matrix P is estimated by the proposed method, where $E = 1$ is the constant in the cost functional equation. The initial condition for the states is selected as $x_0 = [2 \quad -2]$. The constants of the EKF algorithm are selected as: $q_0 = 100$; $r_0 = 0.001$; $s_0 = 0.001$. The phase portraits for the unstable system and for the stabilized one by the mean of the proposed EKF-based inverse optimal control are illustrated in Figure 5.4. The MATLAB simulation results in Figure 5.5 show the noticeable amelioration in performance of the proposed technique and demonstrate its high potential in minimizing the cost functional when compared to the other methods.

Table 5.1 illustrates the comparison results between the three methods.

Table 5.1 : Comparison results between the proposed EKF-based approach and other approaches for nonlinear system_1.

Methods	$x_1 \rightarrow 0$ (within 5 % error)	$x_2 \rightarrow 0$ (within 5 % error)	Cost Functional
Trial and Error	5 Steps	5 Steps	40
Speed Gradient	7 Steps	6 Steps	10
EKF-based	3 Steps	2 Steps	4

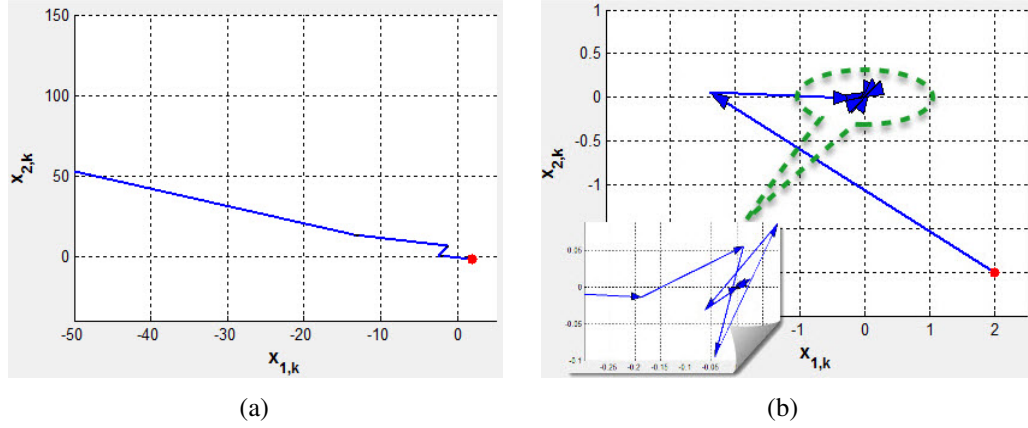


Figure 5.4 : The phase portrait of: (a) the unstable system_1, (b) the stabilized system_1 by the proposed method.

Figure 5.6 demonstrates the MATLAB GUI simulation platform that used to adapt the parameters of the proposed EKF-based inverse optimal control and to analysis the output states of the nonlinear example in Equation (5.10).

The following parameters can be configured by this platform:

- The constants of EKF algorithms (q_0 , s_0 , and r_0).
- The number of steps to be simulated.
- The initial value of matrix P .
- The E value in the cost functional equation.
- The initial conditions of the system's states.

5.2.2 A nonlinear system_2

Considering the following affine-in-input nonlinear dynamical system:

$$x_{k+1} = f(x_k) + g(x_k)u_k \quad (5.11)$$

$$f(x_k) = \begin{bmatrix} 2x_{1,k}\sin(0.5x_{1,k}) + 0.1x_{2,k}^2 \\ 0.1x_{1,k}^2 + 1.8x_{2,k} \end{bmatrix}, \quad g(x_k) = \begin{bmatrix} 0 \\ 2 + 0.1\cos(x_{2,k}) \end{bmatrix}.$$

The stabilizing optimal control law can be calculated according to Equation (3.5). Matrix P is estimated by the proposed method, where $E = 1$ is the constant in the cost functional equation. The initial condition for the states is selected as $x_0 = [2.5 \quad -1]$. The constants of the EKF algorithm are selected as: $q_0 = .01$; $r_0 = 0.01$; $s_0 = .05$.

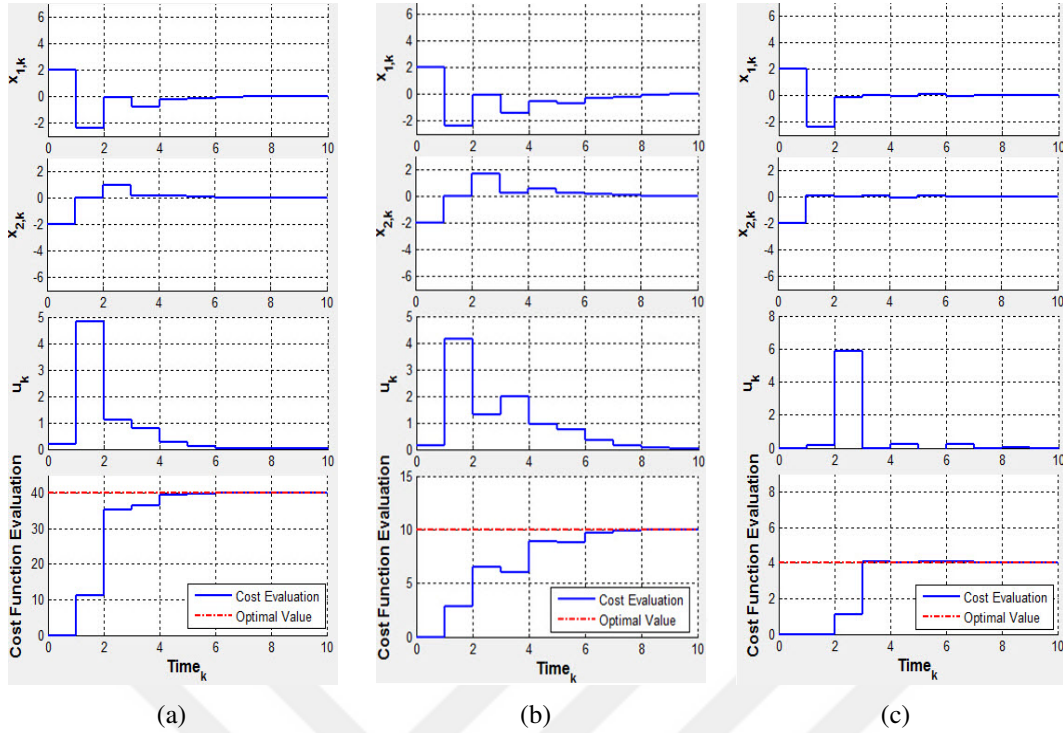


Figure 5.5 : Stabilized nonlinear system_1 using: (a) Trial and error method, (b) Speed-gradient based method, (c) Proposed EKF-based method.

The phase portraits for the unstable system and for the stabilized one by the mean of the proposed EKF-based inverse optimal control are illustrated in Figure 5.7.

The MATLAB simulation results in Figure 5.8 show the noticeable amelioration in performance of the proposed technique and demonstrate its high potential in minimizing the cost functional when compared to the other methods. The negative values of the cost functional evaluation appeared at the simulation is due to the penalty value $L(x_k)$ which can be positive or negative at the cost evaluation in Equation (3.2). However, the total cost function should be positive for the physical meaning as shown in the main theorem at section 3. Table 5.2 illustrates the comparison results between the three methods.

Table 5.2 : Comparison results between the proposed EKF-based approach and other approaches for nonlinear system_2.

Methods	$x_1 \rightarrow 0$ (within 5 % error)	$x_2 \rightarrow 0$ (within 5 % error)	Cost Functional Value
Trial and Error	10 Steps	10 Steps	59.5
Speed Gradient-based	8 Steps	6 Steps	22.725
EKF-based	6 Steps	2 Steps	10.625

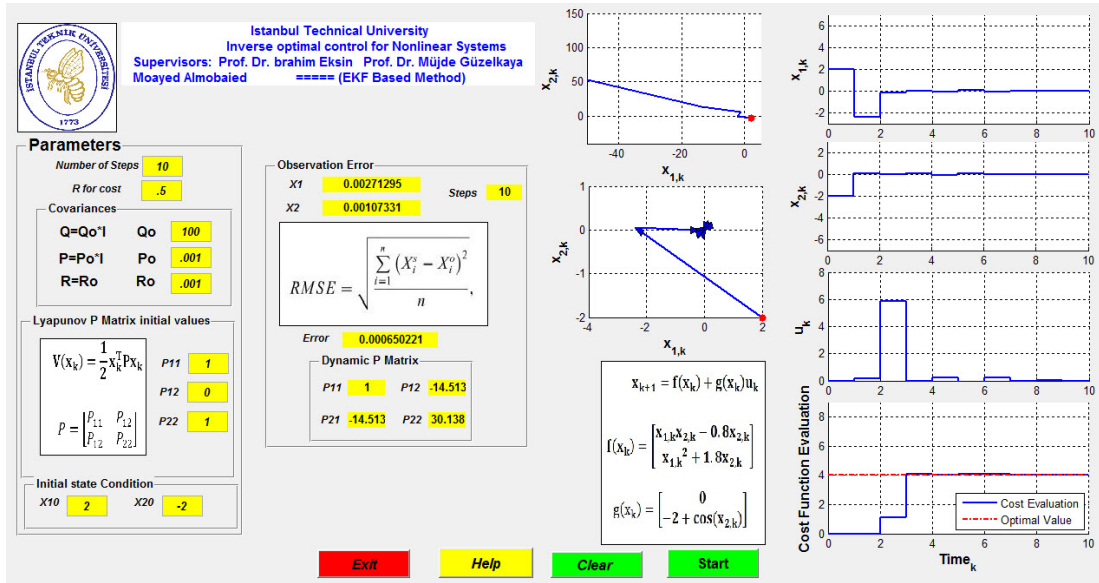


Figure 5.6 : MATLAB GUI of the proposed EKF-based inverse optimal control for system_1.

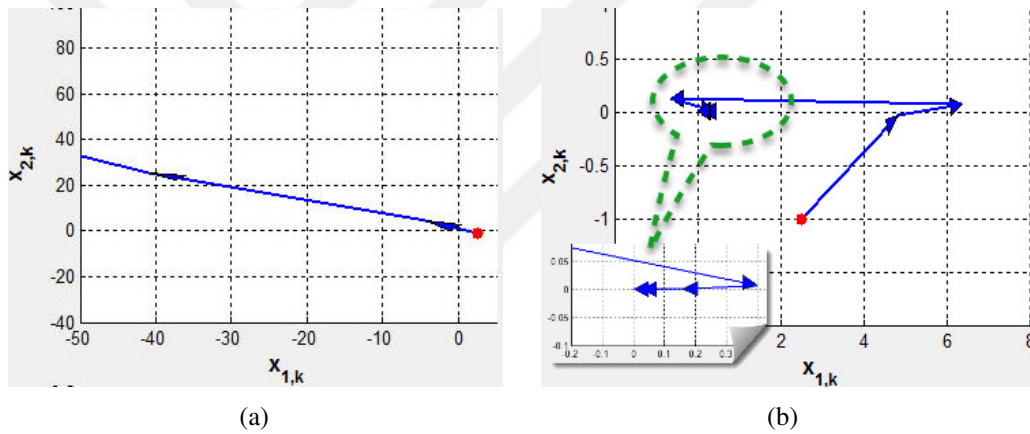


Figure 5.7 : The phase portrait of: (a) the unstable system_2, (b) the stabilized system_2 by the proposed method.

As the previous example, Figure 5.9 demonstrates the MATLAB GUI simulation platform that used to adapt the parameters of the proposed EKF-based inverse optimal control and to analysis the output states of the nonlinear example.

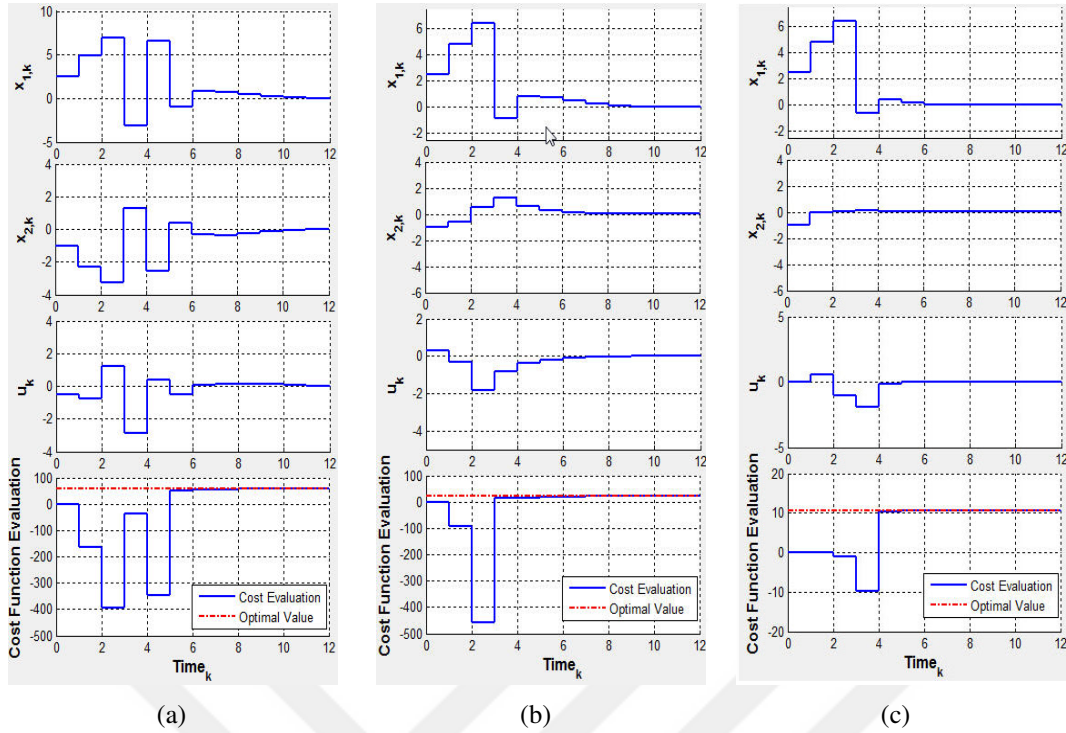


Figure 5.8 : Stabilized nonlinear system_2 using: (a) Trial and error method, (b) Speed-gradient based method, (c) Proposed EKF-based method.

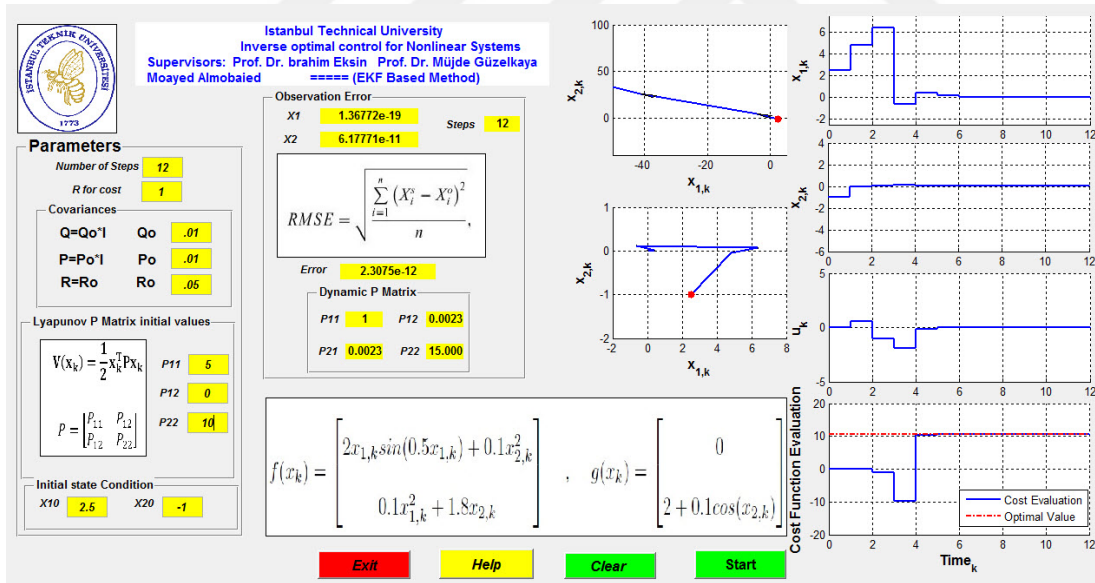


Figure 5.9 : MATLAB GUI of the proposed EKF-based inverse optimal control for system_2.

5.3 Experimental Results of the DC-DC Boost Converter

The DC-DC boost converters are widely used in power conversion applications where the required output voltage is higher than the source voltage. The DC-DC boost converter dynamics are nonlinear in nature due to switching action and saturation of the duty-cycle. The control law obtained for these converters is usually based on linear techniques which is simpler and of lower cost than other nonlinear approaches [35]. Hence, the small signal model of this converter is derived by linearization around a specific equilibrium point where the stability is basically achieved around the small vicinity of this point. Therefore, the problem of stabilizing these converters in nonlinear form has been a research interest area and is widely used as a benchmark for testing new control strategies. The optimal control problem for DC-DC boost converter is to determine a control signal that achieves stability for the converter and minimizes a certain cost functional [34, 35]. Moreover, the controlled DC-DC boost converter must be robust in the presence of disturbances, such as step changes in load and source voltage. The difficulty in the control of DC-DC boost converters is due to its nonminimum phase characteristics where the control input appears in both the voltage and current equations.

5.3.1 Mathematical model of the DC-DC boost converter

The principal components of the DC-DC boost converter are illustrated in Figure 2.7.

The equations that describe the operation of the converter can be written as:

$$L \cdot \frac{dI_L}{dt} = V_{in} - \mu \cdot V_{out} \quad (5.12)$$

$$C \cdot \frac{dV_{out}}{dt} = \mu \cdot I_L - \frac{V_{out}}{R_L}, \quad (5.13)$$

where $\mu = \{0, 1\}$ define the switch position; the parameters R_L, L, C , and V_{in} for the circuit are the resistance, inductance, capacitance, and source voltage, respectively.

These equations can be represented by the mean of the state variables as follows:

$$\dot{x}_1 = \frac{V_{in}}{L} - \frac{x_2}{L} \mu, \quad (5.14)$$

$$\dot{x}_2 = \frac{x_1}{C} \mu - \frac{x_2}{R_L C}, \quad (5.15)$$

where the state variable x_1 represents the average current in the coil and the state x_2 represents the average voltage at the output. Euler approximation method is used to discretize the boost converter equations. Hence, the discrete-time model for the boost converter is obtained as:

$$x_{1,k+1} = x_{1,k} + \Delta T \left(\frac{V_{in}}{L} - \frac{x_{2,k}}{L} \mu_k \right), \quad (5.16)$$

$$x_{2,k+1} = x_{2,k} + \Delta T \left(\frac{x_{1,k}}{C} \mu_k - \frac{x_{2,k}}{R_L C} \right), \quad (5.17)$$

where ΔT is the sampling time. In order to use these equations within the framework of the proposed EKF-based inverse optimal controller method, the system should be written in the general affine-in-input form as follows:

$$x_{k+1} = f(x_k) + g(x_k)u_k \quad (5.18)$$

where:

$$x_k = [x_{1,k+1} \quad x_{2,k+1}]^T,$$

$$f(x_k) = \begin{bmatrix} x_{1,k} + \Delta T \left(\frac{V_{in}}{L} \right) \\ x_{2,k} - \Delta T \left(\frac{x_{2,k}}{R_L C} \right) \end{bmatrix}, \quad g(x_k) = \begin{bmatrix} -\Delta T \left(\frac{x_{2,k}}{L} \right) \\ \Delta T \left(\frac{x_{1,k}}{C} \right) \end{bmatrix}.$$

The basic operation of a boost converter consists of two stages:

1. When the switch is closed, the diode will be in reverse bias mode. Hence, the inductor will store some energy by generating a magnetic field. During this stage, the reverse diode prevents the capacitor from discharging through the switch. The switch should be opened again fast enough to avoid having the capacitor discharge a large amount through the load resistor.
2. When the switch is open, the diode will be in a forward bias mode and the inductor current is forced to flow through diode D, capacitor C and with load RL. In this mode, both the stored energy of the inductor and input voltage source supply power to the load. Finally, a higher voltage level than the input voltage is produced.

Figure 5.10 demonstrates the MATLAB GUI simulation platform that used to adapt the parameters of the proposed EKF-based inverse optimal control and to analysis the

output of the DC-DC boost converter. The following parameters can be configured and observed by this platform:

- The constants of EKF algorithms (q_0 , s_0 , and r_0).
- The number of steps to be simulated.
- The initial value of matrix P .
- The E value in the cost functional equation.
- The initial conditions of the system's states.
- Parameters of the DC-DC boost converter.
- The variations at matrix P .
- The output voltage value of the DC-DC boost converter.

The simulation results at Figure 5.10 demonstrates the superiority of the proposed EKF-based inverse optimal control when compared to the fixed matrix P approach during the stabilization process of the DC-DC boost converter.

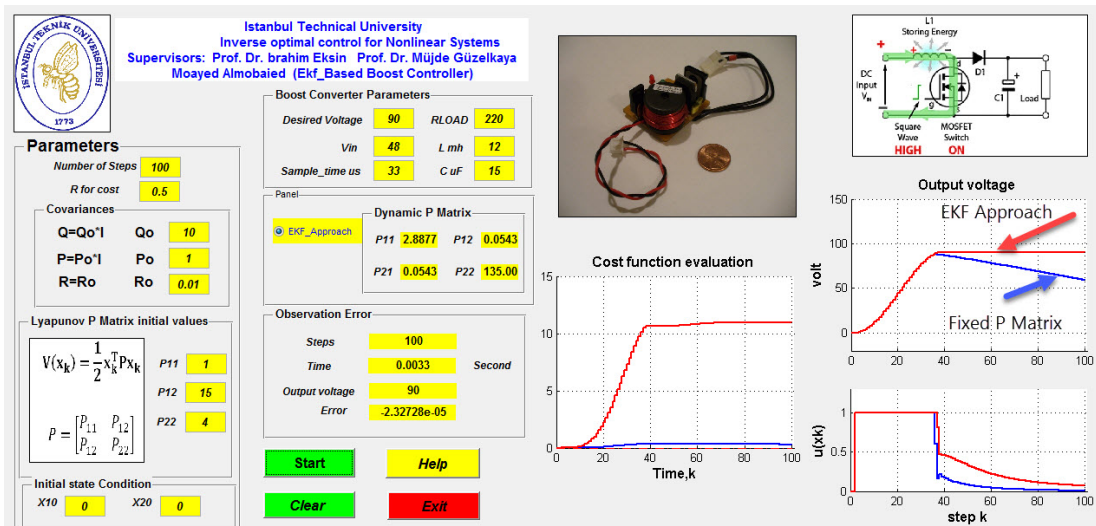


Figure 5.10 : MATLAB GUI for the proposed EKF-based inverse optimal control for DC-DC boost converter.

5.3.2 EKF-based Inverse Optimal Control for DC-DC Boost Converter as a Real Time Application

Here, the DC-DC boost converter is used as a real time application for the proposed EKF-based inverse optimal control. Figure 5.11 shows a complete schematic diagram for the DC-DC boost converter that used in this section where the values of the converter parameters are given in Table 5.3. The circuit contains a current sensor to measure the value of inductor’s current, and it also contains a small switch at the load side to change the load resistance as a disturbance model. Moreover, a variable power supply is used to test the output voltage response with respect to variations in input voltage.

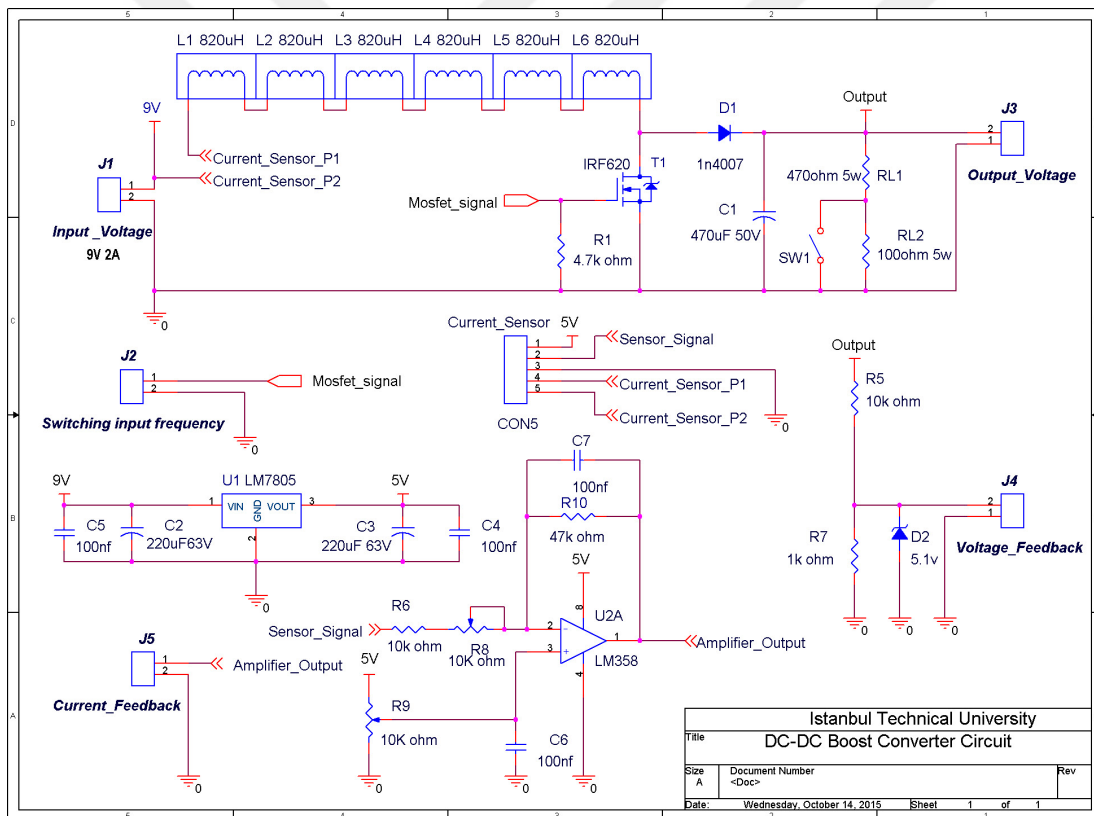


Figure 5.11 : Schematic diagram of DC-DC boost converter circuit.

In this work, the proposed EKF-based inverse optimal controller is implemented on an ARDUINO MEGA 2560 starter kit. One output pin is connected to the gate of the Mosfet to control the duty cycle by the mean of a PWM technique. The switching frequency is selected to be 20 kHz. Two analog input pins were used to read the current

Table 5.3 : Parameters values of the DC-DC boost converter.

Element	Value
Diode	1n4007
Power Mosfet	IRF 620
Inductor	4.9 mH
Capacitor	470 uF
Load resistor	470 Ω \rightarrow 570 Ω
Input voltage	9V

flow in the inductor and the output voltage level across the capacitor. The ARDUINO kit and the DC-DC boost converter are shown in Figure 5.12.

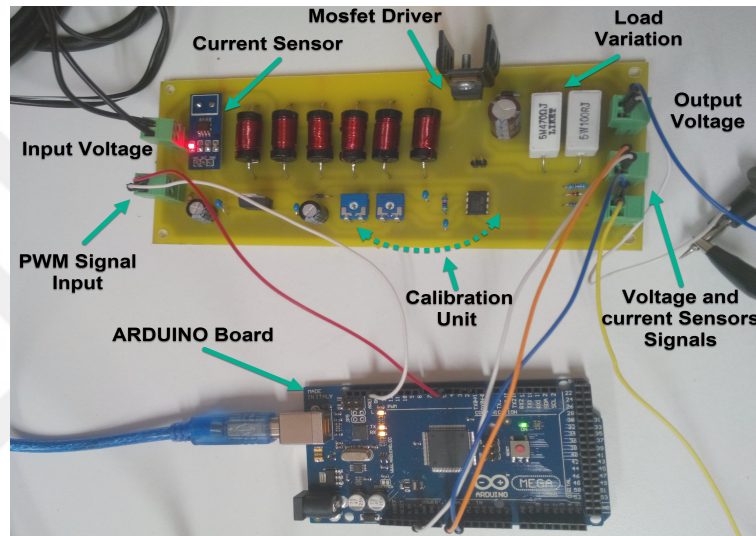


Figure 5.12 : DC-DC converter board and ARDUINO Mega 2560 controller kit.

In order to test the effectiveness of the proposed method on stabilizing the DC-DC boost converter, a comparative study has been done between the proposed EKF-based inverse optimal controls, advanced LQR state feedback controller based on BB-BC algorithm presented in Chapter (2) and the classical Ziegler-Nichols controllers. The advanced control technique given in Chapter (2) proposes a new way of selecting the weighing matrices Q and R of the linear quadratic regulator (LQR) using the global Big Bang-Big Crunch (BB-BC) optimization algorithm so as to optimize a special time domain fitness function. In this manner, the repeated adjustment process of LQR parameters has been avoided. On the other hand, the Proportional Integral Derivative - PID controller is a generic control loop feedback mechanism which has become the ‘industry standard’ in the control systems due to its simplicity and good performance. In fact, the PID controllers are still widely used for commercialized switching power supplies. The best way for PID parameters determination is indeed

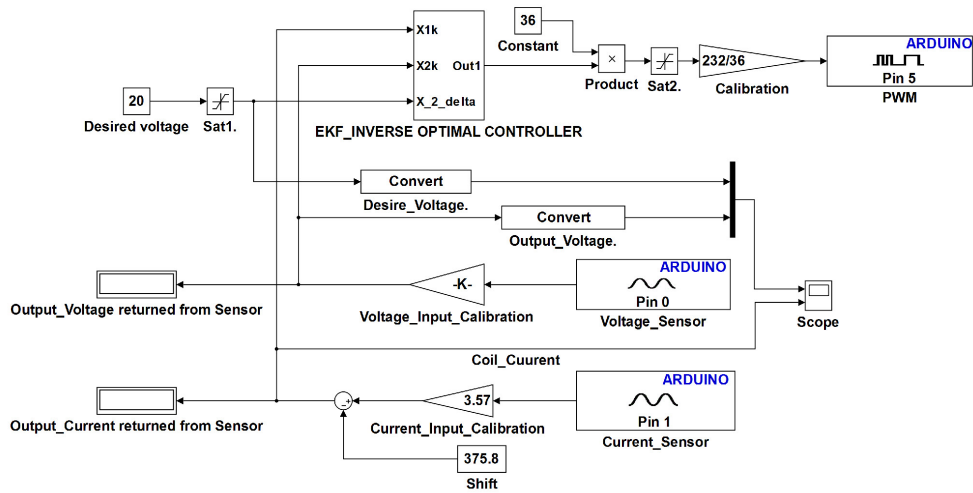
to use the mathematical model to get the desired response. However, the mathematical description of the system is often missing or inadequate and the experimental tuning of the PID parameters has to be performed in such cases. Therefore, in this research, the well-known heuristic Ziegler-Nichols is used to determine the parameters of PID controllers [63, 64]. The results of above mentioned two methods are compared with the results of the proposed method on the same test kit.

In order to implement the LQR and PID controllers, a linearized model of the DC-DC boost converter is required. The states x_1 and x_2 are selected as the current of inductor L and the voltage of capacitor C , respectively. The commutated model for the DC-DC boost converter is then presented as in Equations (2.33, 2.34). If the switching frequency is significantly higher than the converter's natural frequencies, this discontinuous model can be approximated around an appropriate equilibrium point and reformed in a continuous averaged model as illustrated in Chapter (2). Since we consider the control of the boost converter around the equilibrium point, we can neglect the nonlinear term of the converter average model and obtain a linearized model. Hence, the state space model of the boost converter is obtained as in Equations (2.36, 2.37).

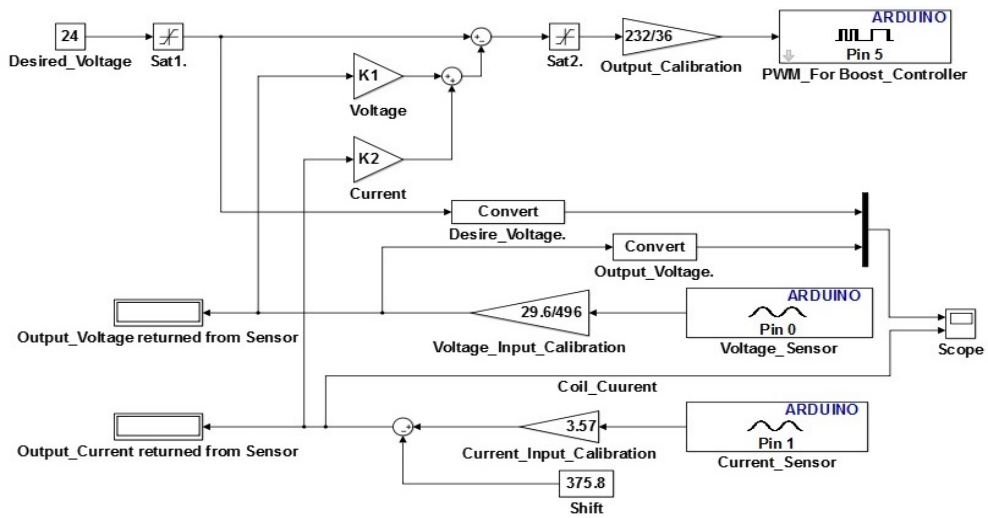
Figures 5.13(a), 5.13(b) and 5.13(c) illustrate the Simulink block diagrams of the EKF-based inverse optimal controller, optimized LQR state feedback controller and Ziegler-Nichols PID controller, respectively. These blocks are directly programmed on the ARDUINO kit from Simulink interface.

The feed forward gain scaling factor N_{bar} is selected as 6.44 in the case of the optimized LQR state feedback controller. The optimal weight matrices are obtained as: $Q = diag[403.159 \quad 749.712]$, $r = [732.293]$ after the application of BB-BC optimization algorithm. Then, the feedback gain matrix is computed as $K = [1.1016 \quad 0.9751]$. The Ziegler-Nichols PID controller parameters are obtained as $K_p = 0.12$; $K_i = 14$; $K_d = 0.02$.

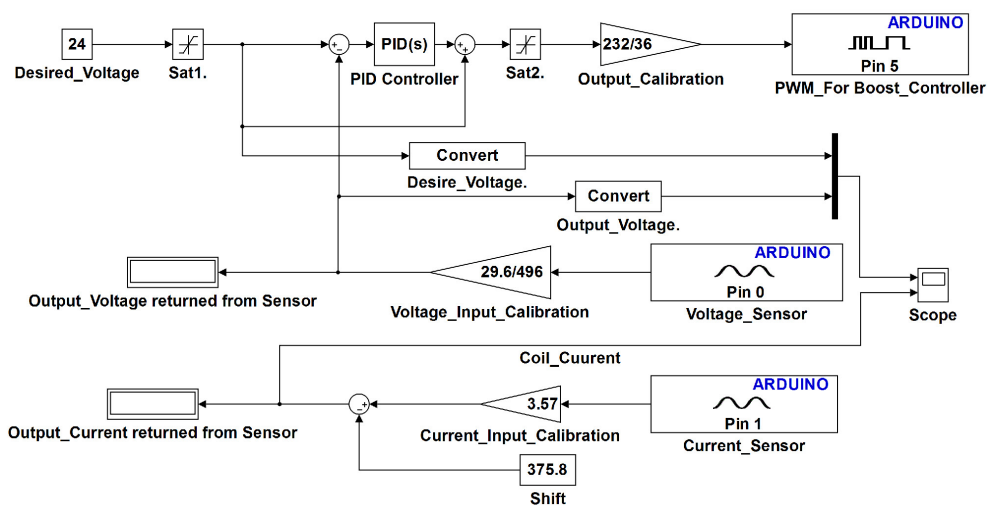
The internal construction of the EKF-based inverse optimal controller for DC-DC boost converter is shown in Figure 5.14. In the proposed controller case, the constants of the EKF algorithm are selected as $q_0 = 10$; $r_0 = 0.1$; $s_0 = 0.001$ and E constant is selected as 0.5 in the cost functional equation.



(a) EKF-based controller



(b) LQR state feedback controller



(c) Ziegler-Nichols PID controller

Figure 5.13 : Simulink interface for EKF-based inverse optimal controller, LQR state feedback controller and Ziegler-Nichols PID controller to be installed on ARDUINO board.

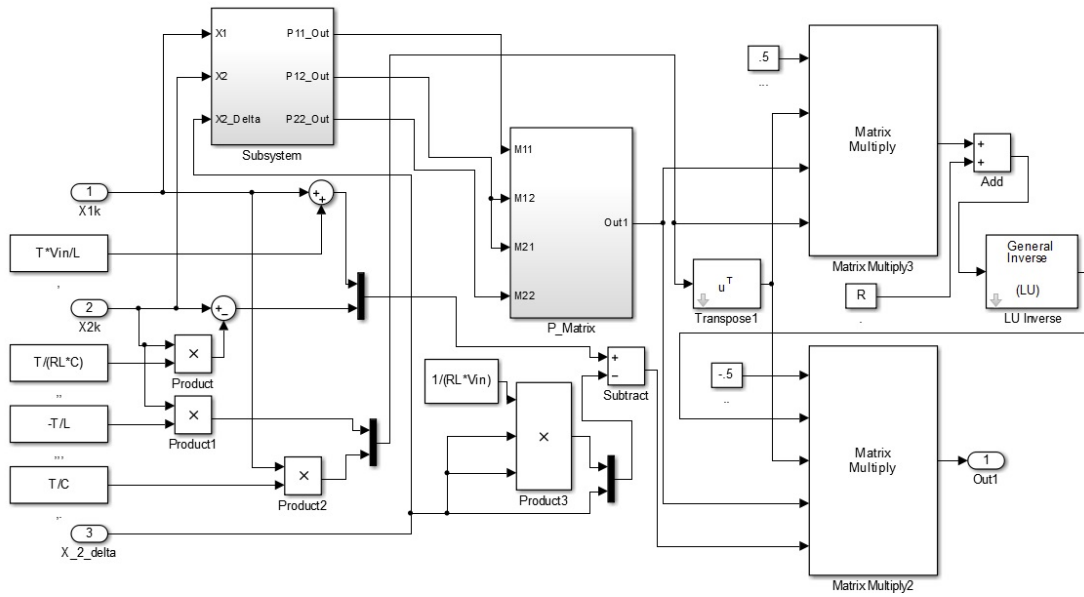
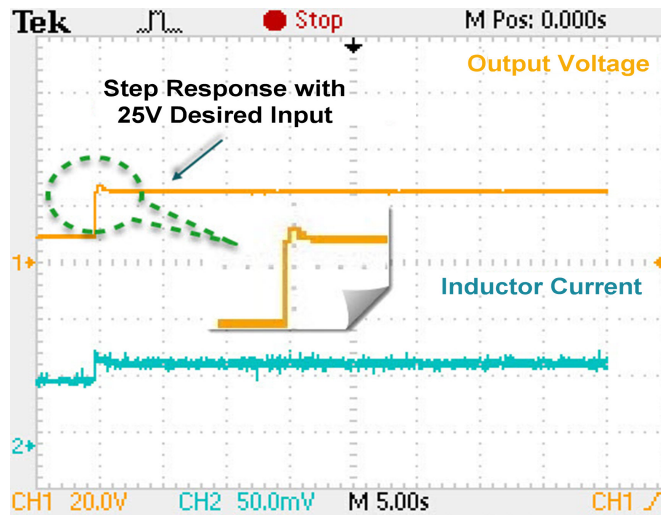
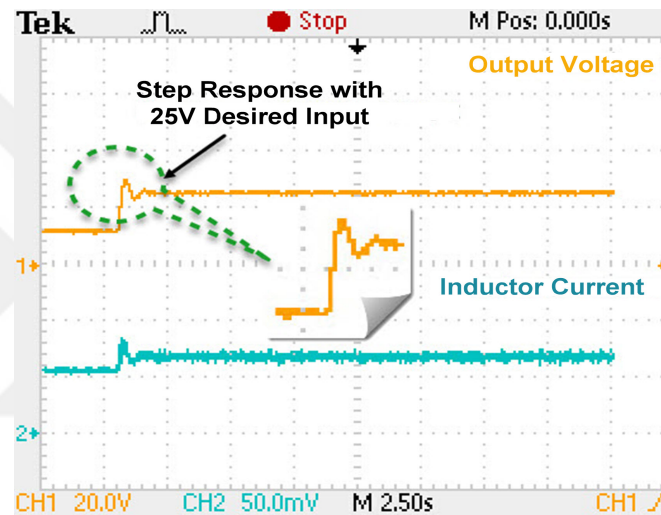


Figure 5.14 : Internal blocks of the EKF-based inverse optimal controller for boost converter.

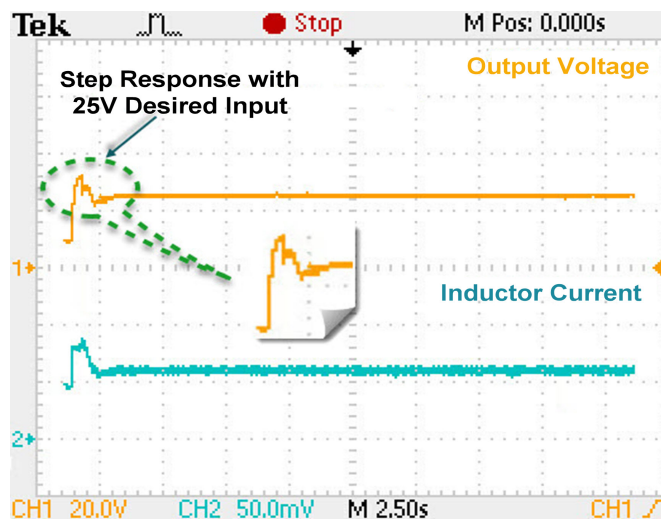
Figure 5.15 demonstrates the step responses of all three controllers under a sudden change in reference voltage from 9 V to 25 V. The overshoot and the settling time were significantly reduced in the case of an EKF-based inverse optimal control controller as shown in Table 5.4; whereas, there was no noticeable change on the rise time and steady-state-error (SSE) values.



(a) EKF-based controller



(b) LQR state feedback controller



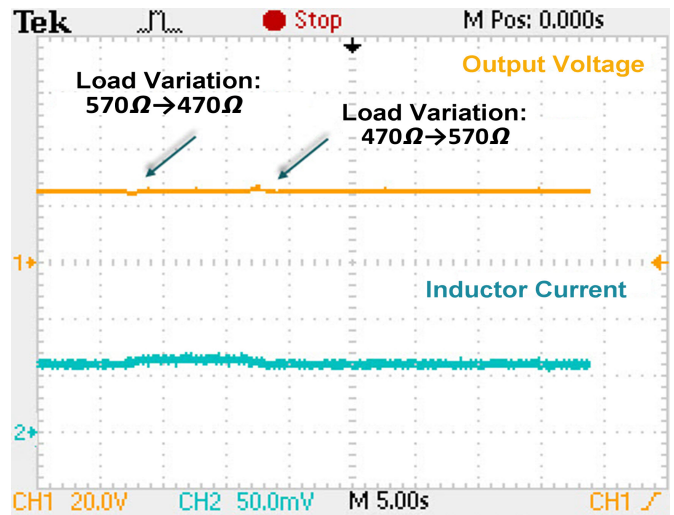
(c) Ziegler-Nichols PID controller

Figure 5.15 : Step response analysis of the DC-DC boost converter for EKF-based controller, LQR state feedback controller and Ziegler-Nichols PID controller.

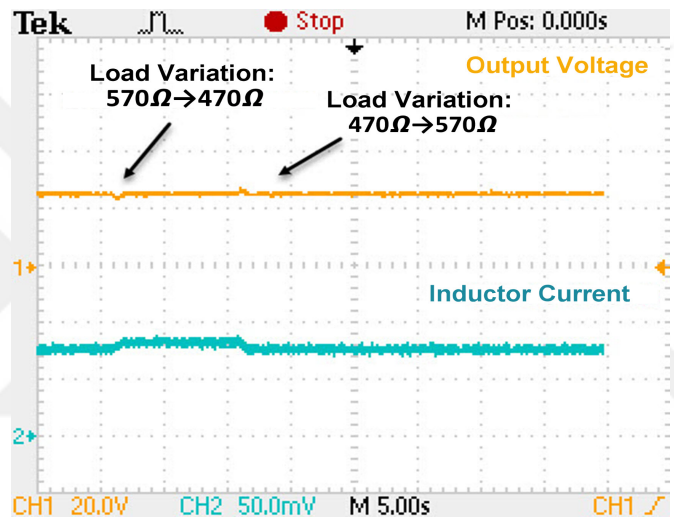
Table 5.4 : Step response analysis of the DC-DC boost converter for EKF-based controller, LQR state feedback controller and Ziegler-Nichols PID controller.

Parameters	EKF-based inverse optimal controller	LQR state feedback controller	Z-N PID controller
Peak amplitude	26.5	29	34
Over shoot (%)	6	15.1	27
Rise time(s)	0.1	0.25	0.21
Settling time(s)	0.5	1.7	2.1
SSE	0.09	0.2	0.15

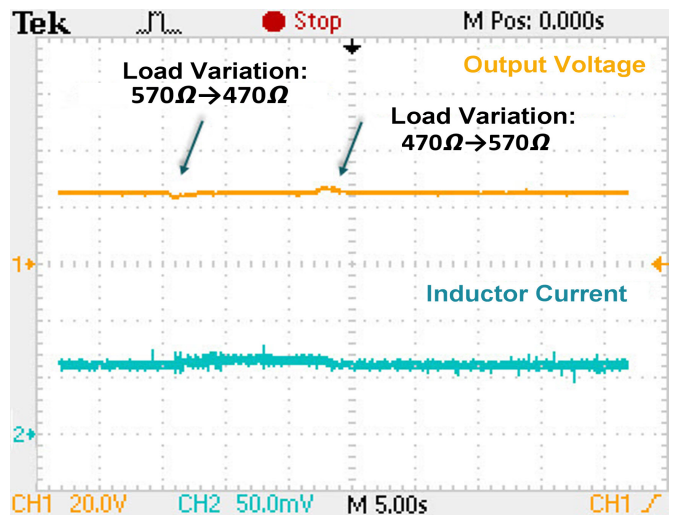
In order to check the dynamic performance and robustness of the proposed controller, the load disturbance is suddenly changed from 570Ω to 470Ω and then from 470Ω to 570Ω . The performance of the controllers under these load variations is shown in Figure 5.16. It is obvious that the proposed EKF-based inverse optimal controller reacts a lot faster than the others in recovering the reference voltage. Moreover, Figure 5.17 illustrates the dynamic responses of the controllers under input voltage variations. These responses also clearly show that the proposed EKF-based inverse optimal controller is more robust than the other controllers. Finally, Figure 5.18 illustrates that the proposed controller has a significant amelioration in the performance over the other controllers in maintaining the output voltage of the boost converter according to the desired voltage.



(a) EKF-based controller

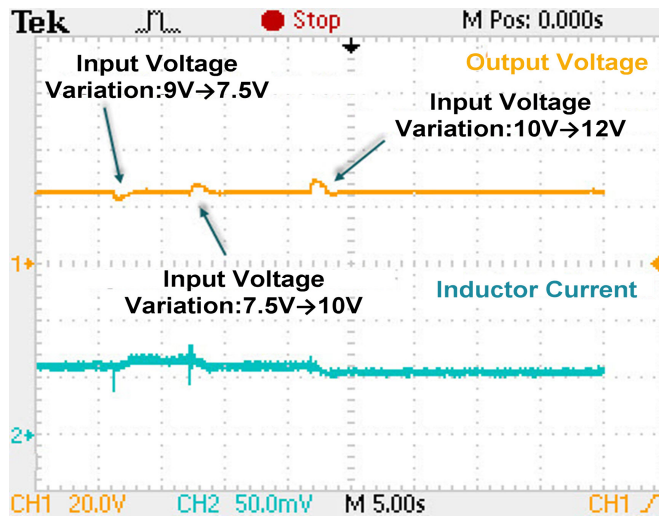


(b) LQR state feedback controller

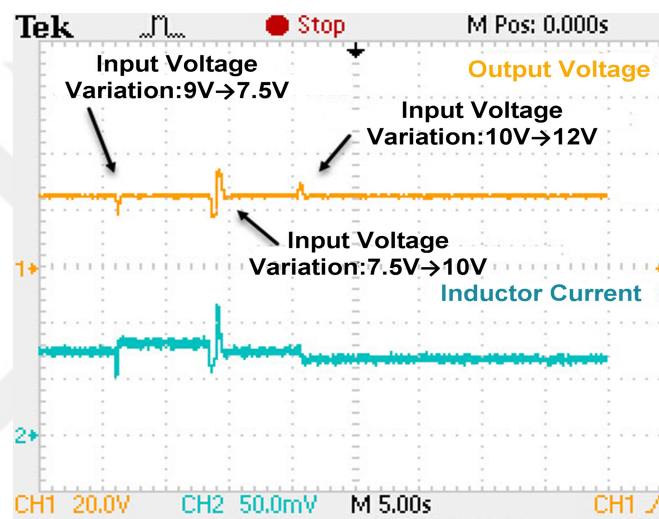


(c) Ziegler-Nichols PID controller

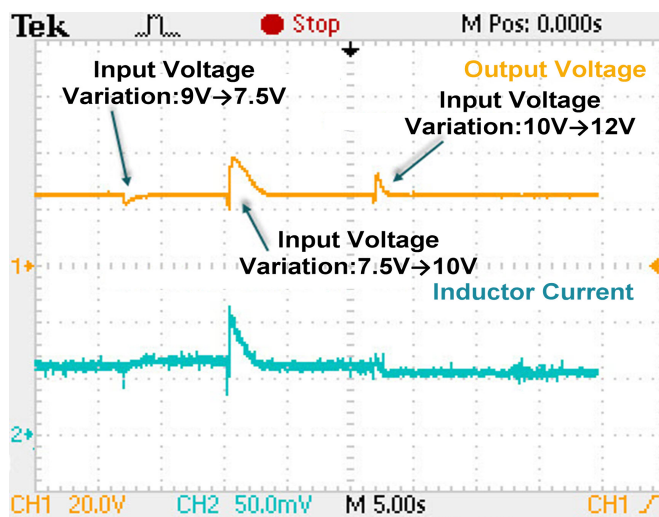
Figure 5.16 : Output response for EKF-based inverse optimal controller, LQR state feedback controller and Ziegler-Nichols PID controller with load variation.



(a) EKF-based controller

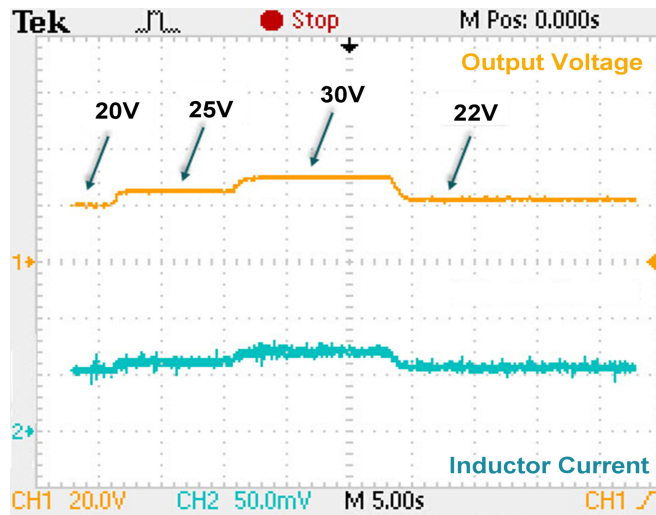


(b) LQR state feedback controller

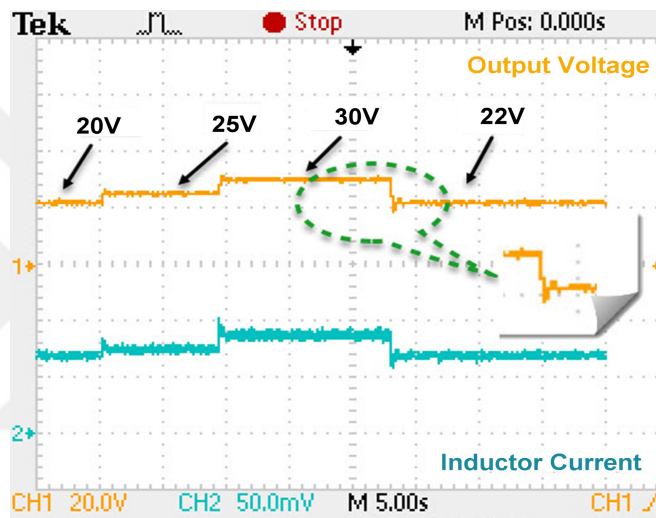


(c) Ziegler-Nichols PID controller

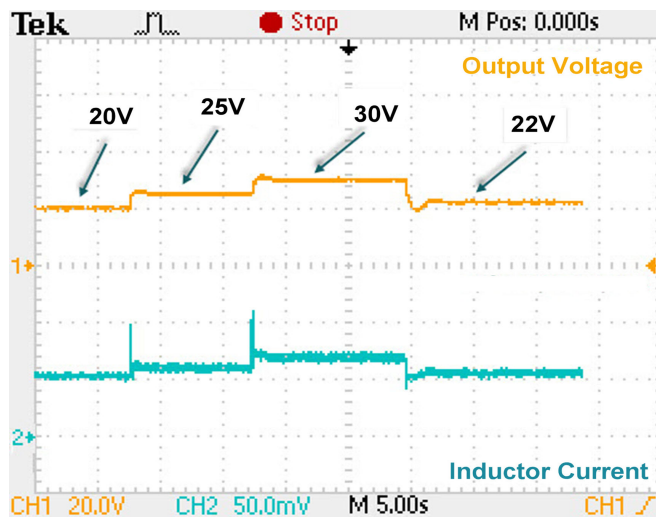
Figure 5.17 : Output response for EKF-based inverse optimal controller, LQR state feedback controller and Ziegler-Nichols PID controller with input voltage variation.



(a) EKF-based controller



(b) LQR state feedback controller



(c) Ziegler-Nichols PID controller

Figure 5.18 : Output response for EKF-based inverse optimal controller, LQR state feedback controller and Ziegler-Nichols PID controller with reference voltage variation.

From the previous comparison, it is obvious that the proposed controller has significantly much better performance compared to the LQR based on BB-BC and to the conventional PID controller under various disturbances of input voltage and load changes.



6. CONCLUSIONS AND RECOMMENDATIONS

The inverse optimal control technique has been firstly introduced to solve the nonlinear optimal control problem as an alternative to the traditional solution path of utilizing the Hamilton- Jacobi-Bellman (HJB) equation.

In this research, novel discrete-time inverse optimal control approaches based on quadratic control Lyapunov function (CLF) are proposed where the parameters of this CLF are estimated in both off-line and on-line manners. For off-line approach, two different algorithms are used to optimize the matrix of the quadratic CLF: a) particle swarm optimization (PSO) algorithm, b) Big Bang-Big Crunch (BB-BC) algorithm. The simulation results for BB-BC algorithm enlighten the designer in making a choice between the single objective inverse optimal control solution and the multi-objective function case where the root-mean-square-error (RMSE) of system states with respect to a reference trajectory and the sum-of-squares of control effort are utilized as the multi-objective optimization criterion. By means of MATLAB simulations, the proposed off-line approaches are successfully applied to a nonlinear example from the literature and to an inverted pendulum on cart nonlinear dynamics.

For the on-line manner, the parameters of CLF function are estimated using extended Kalman filter (EKF) algorithm in a recursive way. The simulation results attained on two different nonlinear systems demonstrate the effectiveness and superiority of the proposed controller. Next, in order to test the applicability of the proposed method in real-world scenarios, a set of experiments on a DC-DC boost converter prototype have been accomplished in the lab so as to assess the performance of the proposed controller. Experimental results illustrate the reliability of the proposed EKF-based inverse optimal controller in stabilizing the DC-DC boost converter where the system time constant is very low so the system responses are very fast. Moreover, a comparative study has been done between the proposed EKF-based inverse optimal controls, advanced LQR state feedback controller based on BB-BC algorithm and the classical Ziegler-Nichols controllers. In fact, the proposed controller has significantly much better performance compared to the optimized LQR based state feedback

controller and to the conventional ZN based PID controller under various disturbances of input voltage and load changes which applied to the DC-DC boost converter prototype.

In order to compare the results of the proposed EKF-based inverse optimal control approach with classical linearization based technique, this thesis proposes an effective solution to the HJB equation for linear system. In this method, the BB-BC algorithm is integrated in the design process of LQR controller by finding the optimum parameter values of the Q and R matrices for LQR design problem. The BB-BC algorithm optimizes a special time domain performance function which is selected to be inversely proportional to the step response parameters of the dynamic system (i.e. overshoot, settling time, rising time and steady state error). In order to test the effectiveness of the proposed LQR controller, the MATLAB simulation is used to analysis the performance response of the inverted pendulum on cart that demonstrated the superiority of the proposed controller in comparison to the experiential-LQR results from the literature. Furthermore, the proposed method has been successfully applied to a DC-DC boost converter prototype where the correctness of our approach is verified in presence of step changes of load and line voltage.

Possible future work for this thesis includes integration the proposed algorithms of inverse optimal control with the robustness to uncertainties. Applying the inverse optimal control to non-affine in input systems, and optimizing the initial values of the covariance at the EKF equations are another possible future works.

REFERENCES

- [1] **Naidu, D.S. and Naidu, S.** (2002). *Optimal Control Systems*, CRC Press, Inc., Boca Raton, FL, USA.
- [2] **Kirk, D.** (2004). *Optimal Control Theory: An Introduction*, Dover Books on Electrical Engineering Series, Dover Publications.
- [3] **Sanchez, E.N. and Ornelas-Tellez, F.** (2013). *Discrete-Time Inverse Optimal Control for Nonlinear Systems*, CRC Press, Inc., Boca Raton, FL, USA.
- [4] **Sepulchre, R., Jankovic, M. and Kokotovic, P.** (1997). *Constructive Nonlinear Control*, Springer-Verlag.
- [5] **Kalman, R.E.** (1964). When Is a Linear Control System Optimal?, *Journal of Fluids Engineering*, 86(1), 51–60.
- [6] **Freeman, R.A. and Kokotovic, P.V.** (1996). Inverse Optimality in Robust Stabilization, *SIAM Journal on Control and Optimization*, 34(4), 1365–1391.
- [7] **Willems, J. and Voorde, H.V.D.** (1977). Inverse optimal control problem for linear discrete-time systems, *Electronics Letters*, 13(17), 493.
- [8] **Krstic, M. and Tsiotras, P.** (1999). Inverse optimal stabilization of a rigid spacecraft, *Automatic Control, IEEE Transactions on*, 44(5), 1042–1049.
- [9] **Liao, F., Ji, H. and Xie, Y.** (2016). A nearly optimal control for spacecraft rendezvous with constrained controls, *Transactions of the Institute of Measurement and Control*, 38(7), 832–845.
- [10] **Li, W., Todorov, E. and Liu, D.** (2011). Inverse Optimality Design for Biological Movement Systems, *{IFAC} Proceedings Volumes*, 44(1), 9662 – 9667.
- [11] **Deng, H. and Krstic, M.** (1997). Stochastic Nonlinear Stabilization - Part II: Inverse Optimality, *Systems and Control Letters*, 32, 151 – 159.
- [12] **Freeman, R.A. and Kokotovic, P.V.** (2008). *Robust Nonlinear Control Design: State-Space and Lyapunov Techniques*, Modern Birkhäuser Classics, Birkhäuser Boston, Boston, MA.
- [13] **Krstic, M., Kokotovic, P.V. and Kanellakopoulos, I.** (1995). *Nonlinear and Adaptive Control Design*, John Wiley & Sons, Inc., New York, NY, USA, 1st edition.

- [14] **Freeman, R. and Primbs, J.A.** (1996). Control Lyapunov functions: new ideas from an old source, *Decision and Control, 1996., Proceedings of the 35th IEEE Conference on*, volume 4, pp.3926–3931 vol.4.
- [15] **Sepulchre, R., Jankovic, M. and Kokotovic, P.** (1997). Integrator Forwarding: A New Recursive Nonlinear Robust Design, *Automatica*, 33(5), 979–984.
- [16] **Teimoori, H., Pota, H., Garratt, M. and Samal, M.** (2012). Helicopter flight control using inverse optimal control and backstepping, *Control Automation Robotics Vision (ICARCV), 2012 12th International Conference on*, pp.978–983.
- [17] **Ornelas, F., Sanchez, E.N. and Loukianov, A.G.** (2011). Discrete-time nonlinear systems inverse optimal control: A control Lyapunov function approach, *Control Applications (CCA), 2011 IEEE International Conference on*, pp.1431–1436.
- [18] **Ornelas-Tellez, F., Sanchez, E.N., Loukianov, A. and Navarro-Lopez, E.** (2011). Speed-gradient inverse optimal control for discrete-time nonlinear systems, *Decision and Control and European Control Conference (CDC-ECC), 2011 50th IEEE Conference on*, pp.290–295.
- [19] **Ornelas-Tellez, F., Sanchez, E.N. and Loukianov, A.G.** (2014). Inverse optimal control for discrete-time nonlinear systems via passivation, *Optimal Control Applications and Methods*, 35(1), 110–126.
- [20] **Erol, O.K. and Eksin, I.** (2006). A New Optimization Method: Big Bang-Big Crunch, *Adv. Eng. Softw.*, 37(2), 106–111.
- [21] **Kumbasar, T., Eksin, I., Güzelkaya, M. and Yesil, E.** (2011). Adaptive fuzzy model based inverse controller design using BB-BC optimization algorithm., *Expert Syst. Appl.*, 38(10), 12356–12364.
- [22] **Dincel, E. and Gene, V.** (2012). A power system stabilizer design by big bang-big crunch algorithm, *Control System, Computing and Engineering (ICCSC), 2012 IEEE International Conference on*, pp.307–312.
- [23] **Basseur, M., Seynhaeve, F. and Talbi, E.G.,** (2004). Real-world multi-objective system engineering, chapter A cooperative metaheuristic applied to multiobjective flow-Shop problem, Nova Science Publishers, USA.
- [24] **Murata, T. and Ishibuchi, H.** (1995). MOGA: multi-objective genetic algorithms, *Proceedings of 1995 IEEE International Conference on Evolutionary Computation*, volume 1, pp.289–.
- [25] **Singh, R. and Verma, H.** (2011). Big bang–big crunch optimization algorithm for linear phase FIR digital filter design, *Int. J. Electron. Commun. Comput. Eng.(IJECC),* 3(1), 74–78.
- [26] **Sedighzadeh, M., Ahmadi, S. and Sarvi, M.** (2013). An Efficient Hybrid Big Bang–Big Crunch Algorithm for Multi-objective Reconfiguration of Balanced and Unbalanced Distribution Systems in Fuzzy Framework, *Electric Power Components and Systems*, 41(1), 75–99.

- [27] **Deris, S., Omatu, S. and Kitagawa, K.** (1995). Stabilization of inverted pendulum by the genetic algorithm, *Systems, Man and Cybernetics, 1995. Intelligent Systems for the 21st Century., IEEE International Conference on*, volume 5, pp.4372–4377 vol.5.
- [28] **Tripathi, S., Panday, H. and Gaur, P.** (2013). Robust control of Inverted pendulum using fuzzy logic controller, *Engineering and Systems (SCES), 2013 Students Conference on*, pp.1–6.
- [29] **Rani, M., Selamat, H., Zamzuri, H. and Ahmad, F.** (2011). PID controller optimization for a rotational inverted pendulum using genetic algorithm, *Modeling, Simulation and Applied Optimization (ICMSAO), 2011 4th International Conference on*, pp.1–6.
- [30] **Korkmaz, D., Bal, C. and Gokbulut, M.** (2015). Modeling of inverted pendulum on a cart by using Artificial Neural Networks, *Signal Processing and Communications Applications Conference (SIU), 2015 23th*, pp.2642–2645.
- [31] **Simon, D.** (2002). Training fuzzy systems with the extended Kalman filter, *Fuzzy Sets and Systems*, 132(2), 189 – 199.
- [32] **Hardan, F., Zhang, L. and Shepherd, W.** (1996). Application of an extended Kalman filter for high-performance current regulation of a vector-controlled induction machine drive, *Transactions of the Institute of Measurement and Control*, 18(2), 69–76.
- [33] **Almobaied, M., Eksin, I. and Guzelkaya, M.** (2015). A New Inverse Optimal Control Method for Discrete-time Systems, *Proceedings of the 12th International Conference on Informatics in Control, Automation and Robotics*, pp.275–280.
- [34] **Mitra, L. and Swain, N.** (2014). Closed loop control of solar powered boost converter with PID controller, *Power Electronics, Drives and Energy Systems (PEDES), 2014 IEEE International Conference on*, pp.1–5.
- [35] **Olalla, C., Leyva, R., El Aroudi, A. and Queinnec, I.** (2009). Robust LQR Control for PWM Converters: An LMI Approach, *Industrial Electronics, IEEE Transactions on*, 56(7), 2548–2558.
- [36] **Jawhar S, J., Marimuthu, N. and Singh N, A.** (2006). An Neuro-Fuzzy Controller for a Non Linear Power Electronic Boost Converter, *Information and Automation, ICIA 2006. International Conference on*, pp.394–397.
- [37] **Almobaied, M., Eksin, I. and Guzelkaya, M.** (16 April, 2017). Inverse Optimal Controller Based on Extended Kalman Filter for Discrete-Time Nonlinear Systems, *Optim Control Appl Meth.* 2017;0:1–16. <https://doi.org/10.1002/oca.2331>.
- [38] **Büchi, R.** (2012). *State Space Control, LQR and Observer: step by step introduction, with Matlab examples*, Books on Demand.

- [39] **Douglas, J. and Athans, M.** (1994). Robust linear quadratic designs with real parameter uncertainty, *IEEE Transactions on Automatic Control*, 39(1), 107–111.
- [40] **Chugh, V. and Ohri, J.** (2014). GA tuned LQR and PID controller for aircraft pitch control, *Power Electronics (IICPE), 2014 IEEE 6th India International Conference on*, pp.1–6.
- [41] **Almobaied, M., Eksin, I. and Guzelkaya, M.** (2016). Design of LQR controller with big bang-big crunch optimization algorithm based on time domain criteria, *2016 24th Mediterranean Conference on Control and Automation (MED)*, pp.1192–1197.
- [42] **Al-Tamimi, A.A.** (2007). Discrete-time Control Algorithms and Adaptive Intelligent Systems Designs, *Ph.D. thesis*, Arlington, TX, USA, aAI3284668.
- [43] **Al-Tamimi, A., Lewis, F.L. and Abu-Khalaf, M.** (2008). Discrete-Time Nonlinear HJB Solution Using Approximate Dynamic Programming: Convergence Proof, *IEEE Transactions on Systems, Man, and Cybernetics, Part B (Cybernetics)*, 38(4), 943–949.
- [44] **Ohsawa, T., Bloch, A.M. and Leok, M.** (2010). Discrete Hamilton-Jacobi theory and discrete optimal control, *49th IEEE Conference on Decision and Control (CDC)*, pp.5438–5443.
- [45] **Lewis, F., Vrabie, D. and Syrmos, V.** (2012). *Optimal Control*, EngineeringPro collection, Wiley.
- [46] **Tedrake, R.**, (2016), Underactuated Robotics: Algorithms for Walking, Running, Swimming, Flying, and Manipulation (Course Notes for MIT 6.832).
- [47] **Büchi, R.** (2012). *State Space Control, LQR and Observer: step by step introduction, with Matlab examples*, Books on Demand, <https://books.google.com.tr/books?id=JrofAgAAQBAJ>.
- [48] **Mellon, C.** (Accessed: 02-02-2016). Inverted Pendulum: State-Space Methods for Controller Design, *University of Michigan*, www.engin.umich.edu/group/ctm/examples.
- [49] **Nasir, A.N.K., Ahmad, M.A. and Rahmat, M.F.** (2008). PERFORMANCE COMPARISON BETWEEN LQR AND PID CONTROLLERS FOR AN INVERTED PENDULUM SYSTEM, *AIP Conference Proceedings*, 1052(1), 124–128.
- [50] **Khalil, H.K.** (1996). *Nonlinear Systems*, Prentice-Hall, Englewood Cliffs, NJ, 2nd edition.
- [51] **Vidyasagar, M.** (1992). *Nonlinear Systems Analysis (2Nd Ed.)*, Prentice-Hall, Inc., Upper Saddle River, NJ, USA.
- [52] **LaSalle, J.P.** (1986). *The Stability and Control of Discrete Processes*, Springer-Verlag New York, Inc., New York, NY, USA.

- [53] **Amicucci, G.L., Monaco, S. and Normand-Cyrot, D.** (1997). Control Lyapunov stabilization of affine discrete-time systems, *Proceedings of the 36th IEEE Conference on Decision and Control*, volume 1, pp.923–924 vol.1.
- [54] **Kellett, C.M. and Teel, A.R.** (2003). Results on discrete-time control-Lyapunov functions, *42nd IEEE International Conference on Decision and Control (IEEE Cat. No.03CH37475)*, volume 6, pp.5961–5966 Vol.6.
- [55] **Kennedy, J. and Eberhart, R.** (1995). Particle swarm optimization, *Neural Networks, 1995. Proceedings., IEEE International Conference on*, volume 4, pp.1942–1948 vol.4.
- [56] **Eberhart and Shi, Y.** (2001). Particle swarm optimization: developments, applications and resources, *Proceedings of the 2001 Congress on Evolutionary Computation (IEEE Cat. No.01TH8546)*, volume 1, pp.81–86 vol. 1.
- [57] **Coello, C. and Lamont, G.** (2004). *Applications of Multi-objective Evolutionary Algorithms*, Advances in natural computation, World Scientific.
- [58] **Marino, R.** (1995). *Nonlinear Control Design: Geometric, Adaptive, and Robust*, Prentice-Hall information and system sciences series, Prentice Hall.
- [59] **Welch, G. and Bishop, G.** (1995). An Introduction to the Kalman Filter, **Technical Report**, Chapel Hill, NC, USA.
- [60] **c. Janapati, R., Balaswamy, C. and Soundararajan, K.** (2015). Enhanced mechanism for localization in Wireless Sensor Networks using PSO assisted Extended Kalman Filter Algorithm (PSO-EKF), *Communication, Information Computing Technology (ICCICT), 2015 International Conference on*, pp.1–6.
- [61] **Thrun, S., Burgard, W. and Fox, D.** (2005). *Probabilistic Robotics (Intelligent Robotics and Autonomous Agents)*, The MIT Press.
- [62] **Raol, J., Girija, G., Singh, J. and of Electrical Engineers, I.** (2004). *Modelling and Parameter Estimation of Dynamic Systems*, IEE control engineering series, Institution of Engineering and Technology.
- [63] **Hwu, K.I. and Yau, Y.T.** (2010). Performance Enhancement of Boost Converter Based on PID Controller Plus Linear-to-Nonlinear Translator, *IEEE Transactions on Power Electronics*, 25(5), 1351–1361.
- [64] **Siva Subramanian, P. and Kayalvizhi, R.** An Optimum Setting of PID Controller for Boost Converter Using Bacterial Foraging Optimization Technique", bookTitle="Systems Thinking Approach for Social Problems: Proceedings of 37th National Systems Conference, December 2013", year="2015, Springer India, New Delhi, pp.13–23.



APPENDICES

APPENDIX A.1 : Theorem Proof





APPENDIX A.1

This thesis used the following theorem for inverse optimal control based on CLF, which proposed in [3], as the basis of the proposed approaches. Hence, I attached the proof of this theorem as an appendix.

Considering the affine-in-input discrete-time nonlinear system of the form:

$$x_{k+1} = f(x_k) + g(x_k)u_k \quad (\text{A.1})$$

where $x \in \mathbb{R}^n$ is the state of the system, $u \in \mathbb{R}^m$ is the control input. $f(x_k) : \mathbb{R}^n \rightarrow \mathbb{R}^n$ and $g(x_k) : \mathbb{R}^n \rightarrow \mathbb{R}^{n \times m}$ are smooth matrices. Without loss of generality, it can be assumed that the origin ($x = 0$) is the equilibrium point of the system in Equation (A.1), $f(0) = 0$ and $g(x_k) \neq 0$ for all $x_k \neq 0$. System in Equation (A.1) is assumed to be stabilizable on a predefined compact set $\Omega \in \mathbb{R}^n$.

For a nonlinear optimal control problem, it is desirable to determine a control law u_k , which minimizes the following cost functional:

$$V(x_k) = \sum_{k=0}^{\infty} (L(x_k) + u_k^T E u_k) \quad (\text{A.2})$$

where $V : \mathbb{R}^n \rightarrow \mathbb{R}^+$ is the cost functional, $L : \mathbb{R}^n \rightarrow \mathbb{R}^+$ is positive semi-definite function to weight the performance of the state vector x_k , and $E : \mathbb{R}^n \rightarrow \mathbb{R}^{m \times m}$ is a real symmetric positive definite weighting matrix to weight the control effort and could be a function of the system state in order to vary the control efforts according to the state value.

Definition 1: The control law u_k^* at Equation (A.1) can be assumed to be inverse optimal control if:

a) It achieves a global exponential stability of the equilibrium point $x_k = 0$ for the system in Equation (A.1).

b) It minimizes the cost functional in Equation (A.2), for which $L(x_k) := -\bar{V}$, with

$$\bar{V} := V(x_{k+1}) - V(x_k) + u_k^{*T} E u_k^* \leq 0 \quad (\text{A.3})$$

where $V(x_k)$ is radially unbounded positive definite function.

Theorem 1:

Consider the affine discrete-time nonlinear system A.1. If there exists a matrix $P = P^T > 0$ such that the following inequality holds

$$V_f(x_k) - \frac{1}{4} P_1^T(x_k) (E + P_2(x_k))^{-1} P_1(x_k) \leq -\zeta_Q \|x_k\|^2 \quad (\text{A.4})$$

where:

$$V_f(x_k) = V(f(x_k)) - V(x_k), \text{ with } V(f(x_k)) = \frac{1}{2} f^T(x_k) P f(x_k) ; \zeta_Q > 0$$

$$P_1(x_k) = g^T(x_k) P f(x_k) ; \quad P_2(x_k) = \frac{1}{2} g^T(x_k) P g(x_k)$$

then the equilibrium point ($x_k = 0$) of the system in Equation (A.1) is globally exponential stabilized by the following control law:

$$u_k^* = -\frac{1}{2}(E + \frac{1}{2}g^T(x_k)Pg(x_k))^{-1}g(x_k)^T Pf(x_k). \quad (\text{A.5})$$

with $V(x_k) = \frac{1}{2}x_k^T Px_k$ as a CLF. Moreover, this control law will minimize the cost functional in Equation (A.2):

with
$$L(x_k) := -\bar{V}|_{u_k^*}$$

and the optimal value function
$$V^*(x_0) = V(x_0). \quad \blacksquare$$

PROOF

First, we analyze stability. Global stability for the equilibrium point $x_k = 0$ of system A.1 with A.5 as input is achieved if Equation (A.5) is satisfied. Thus, \bar{V} results in

$$\begin{aligned} \bar{V} &= V(x_{k+1}) - V(x_k) + u_k^{*T} E u_k^* \\ &= \frac{f^T(x_k)Pf(x_k) + 2f^T(x_k)Pg(x_k)u_k^*}{2} \\ &\quad + \frac{u_k^{*T}g^T(x_k)Pg(x_k)u_k - x_k^{*T}Px_k}{2} + u_k^{*T} E u_k \\ &= V_f(x_k) - \frac{1}{2}P_1^T(x_k)(E + P_2(x_k))^{-1}P_1(x_k) \\ &\quad + \frac{1}{4}P_1^T(x_k)(E + P_2(x_k))^{-1}P_1(x_k) \\ &= V_f(x_k) - \frac{1}{4}P_1^T(x_k)(E + P_2(x_k))^{-1}P_1(x_k) \end{aligned} \quad (\text{A.6})$$

Selecting P such that $\bar{V} \leq 0$, the stability of $x_k = 0$ is guaranteed. Furthermore, by means of P , we can achieve a desired negativity amount for th closed-loop function \bar{V} in Equation (A.6). This negativity amount can be bounded using a positive definite matrix Q as follows:

$$\begin{aligned} \bar{V} &= V_f(x_k) - \frac{1}{4}P_1^T(x_k)(E + P_2(x_k))^{-1}P_1(x_k) \\ &\leq -x_k^T Px_k \\ &\leq -\lambda_{\min}(Q)\|x_k\|^2 \\ &= -\zeta_Q\|x_k\|^2, \quad \zeta_Q = \lambda_{\min}(Q) \end{aligned} \quad (\text{A.7})$$

where $\|\cdot\|$ stands for the Euclidean norm and $\zeta_Q > 0$ denotes the minimum eigenvalue of matrix $Q(\lambda_{\min}(Q))$. Thus, Equation (A.7) follows condition (A.4).

Considering (A.6),(A.7)

$$\bar{V} = V(x_{k+1}) - V(x_k) + u_k^{*T} E u_k \leq -\zeta_Q \|x_k\|^2 \implies \Delta V = V(x_k + 1) - V(x_k) \leq -\zeta_Q \|x_k\|^2.$$

Moreover, as $V(x_k)$ is a radially unbounded function. then the solution $x_k = 0$ of the closed-loop system (A.1) with A.5 as input is globally exponentially stable according to Theorem 1. When function $-l(x_k)$ is set to be the (A.7) right-hand side, that is,

$$l(x_k) := -V_f(x_k) + \frac{1}{4} P_1^T(x_k) (E + P_2(x_k))^{-1} P_1(x_k) \quad (\text{A.8})$$

then $V(x_k) = \frac{1}{2} x_k^T P x_k$ is a solution of the Discrete Time HJB equation:

$$V^*(x_k) = L(x_k) + V^*(x_{k+1}) + \frac{1}{4} \frac{\partial V^{*T}(x_{k+1})}{\partial x_{k+1}} g(x_k) E^{-1} g^T(x_k) \frac{\partial V(x_{k+1})}{\partial x_{k+1}} \quad (\text{A.9})$$

In order to obtain the optimal value for the cost functional (A.2), we substitute $l(x_k)$ given in (A.8) into (A.2); then

$$\begin{aligned} V(x_k) &= \sum_{k=0}^{\infty} (L(x_k) + u_k^T E u_k) \\ &= \sum_{k=0}^{\infty} (-\bar{V} + u_k^T E u_k) \\ &= -\sum_{k=0}^{\infty} \left[V_f(x_k) - \frac{1}{4} P_1^T(x_k) (E + P_2(x_k))^{-1} P_1(x_k) \right] + \sum_{k=0}^{\infty} u_k^T E u_k \end{aligned} \quad (\text{A.10})$$

Factorizing Equation (A.10), and then adding the identity matrix

$$I_m = (E + P_2(x_k))(E + P_2(x_k))^{-1}$$

with $I_m \in \mathbb{R}^{m \times m}$, we obtain

$$\begin{aligned} V(x_k) &= -\sum_{k=0}^{\infty} \left[V_f(x_k) - \frac{1}{2} P_1^T(x_k) (E + P_2(x_k))^{-1} P_1(x_k) \right. \\ &\quad + \frac{1}{4} P_1^T(x_k) (E + P_2(x_k))^{-1} P_2(x_k) (E + P_2(x_k))^{-1} P_1(x_k) \\ &\quad + \frac{1}{4} P_1^T(x_k) (E + P_2(x_k))^{-1} E \\ &\quad \left. \times (E + P_2(x_k))^{-1} P_1^T(x_k) \right] + \sum_{k=0}^{\infty} u_k^T E u_k. \end{aligned} \quad (\text{A.11})$$

Being $u_k^* = -\frac{1}{2} (E + P_2(x_k))^{-1} P_1^T(x_k)$, then Equation (A.11) becomes

$$\begin{aligned} V(x_k) &= -\sum_{k=0}^{\infty} \left[V_f(x_k) + P_1^T(x_k) u_k^* + u_k^{*T} P_2(x_k) u_k^* \right] + \sum_{k=0}^{\infty} \left[u_k^T E u_k - u_k^{*T} E u_k^* \right] \\ &= -\sum_{k=0}^{\infty} \left[V(x_{k+1}) - V(x_k) \right] + \sum_{k=0}^{\infty} \left[u_k^T E u_k - u_k^{*T} E u_k^* \right] \end{aligned} \quad (\text{A.12})$$

which can be written as

$$\begin{aligned}
V(x_k) &= -\sum_{k=1}^{\infty} \left[V(x_{k+1}) - V(x_k) \right] - V(x_1) + V(x_0) + \sum_{k=0}^{\infty} \left[u_k^T E u_k - u_k^{T*} E u_k^* \right] \\
&= -\sum_{k=2}^{\infty} \left[V(x_{k+1}) - V(x_k) \right] - V(x_2) + V(x_1) \\
&\quad - V(x_1) + V(x_0) + \sum_{k=0}^{\infty} \left[u_k^T E u_k - u_k^{T*} E u_k^* \right] \tag{A.13}
\end{aligned}$$

For notation convenience in Equation (A.13), the upper limit ∞ will be treated as $N \rightarrow \infty$, and thus

$$\begin{aligned}
V(x_k) &= -V(x_N) + V(x_{N-1}) - V(x_{N-1}) + V(x_0) \\
&\quad + \lim_{N \rightarrow \infty} \sum_{k=0}^N \left[u_k^T E u_k - u_k^{T*} E u_k^* \right] \\
&= -V(x_N) + V(x_0) + \lim_{N \rightarrow \infty} \sum_{k=0}^N \left[u_k^T E u_k - u_k^{T*} E u_k^* \right] \tag{A.14}
\end{aligned}$$

Letting $N \rightarrow \infty$ and noting that $V(x_N) \rightarrow 0$ for all x_0 , then

$$V(x_k) = V(x_0) + \sum_{k=0}^N \left[u_k^T E u_k - u_k^{T*} E u_k^* \right] \tag{A.15}$$

Thus, the minimum value of Equation (A.15) is reached with $u_k = u_k^*$. Hence, the control law in Equation (A.5) minimizes the cost functional (A.2). The optimal value function of (A.2) is $V^*(x_0) = V(x_0)$ for all x_0 .

Additionally, with $l(x_k)$ as defined in Equation (A.8), $V(x_k)$ solves the following Hamilton-Jacobi-Bellman equation:

$$V^*(x_k) = L(x_k) + V^*(x_{k+1}) + \frac{1}{4} \frac{\partial V^{*T}(x_{k+1})}{\partial x_{k+1}} g(x_k) E^{-1} g^T(x_k) \frac{\partial V(x_{k+1})}{\partial x_{k+1}} \tag{A.16}$$

■

CURRICULUM VITAE



Name Surname: Moayed Almobaied

Place and Date of Birth: Algeria 01/01/1978

Address: Gaza-Palestine \ Istanbul-Turkey

E-Mail: Malmobaied@gmail.com, Malmobaied@itu.edu.tr

B.Sc.: Islamic University of Gaza-Palestine, 2001

M.Sc.: Islamic University of Gaza-Palestine, 2008

Professional Experience and Rewards:

R&D Specialist (Full time, Since 2015): Isbak-Istanbul IT and Smart City Technologies Inc., Istanbul-Turkey.

Instructor (Full time, 2008 – 2011): Electrical Engineering Department, Faculty of Engineering, Islamic University of Gaza, Gaza-Palestine.

Technical Engineer (Full time, 2005 – 2008): Electrical Engineering Department, Faculty of Engineering, Islamic University of Gaza, Gaza-Palestine.

Teaching Assistant(Full time, 2001 – 2005): Electrical Engineering Department, Faculty of Engineering, Islamic University of Gaza, Gaza-Palestine.

Manager (2003-2011): Ashraf Engineering Office, Gaza-Palestine.

List of Publications and Patents:

- **Almobaied M.**, Eksin I., Guzelkaya M. Inverse optimal controller based on extended Kalman filter for discrete-time nonlinear systems. *Optim Control Appl Meth.* 2017;0:1–16. <https://doi.org/10.1002/oca.2331>.
- **Almobaied M.**, Eksin I., Guzelkaya M., 2015: A new inverse optimal control method for discrete-time systems. *International Conference on Informatics in Control, Automation and Robotics (ICINCO)*, vol. 01, pp. 275–280, 2015 Paris, France.
- **Almobaied M.**, Eksin I., Guzelkaya M., 2015: Design of LQR Controller with Big Bang-Big Crunch Optimization Algorithm Based on Time Domain Criteria. *24th Mediterranean Conference on Control and Automation, IEEE*, 2016 Athena, Greece.
- Arghavani N., **Almobaied M.**, Guzelkaya M., Eksin I., 2017: On-Line Rule Weighting For PID-Type Fuzzy Logic Controllers Using Extended Kalman Filter. *20th World Congress of the International Federation of Automatic Control, IFAC*, 2017 Toulouse, France.

- Dursun Y., **Almobaied M.**, Buyukkinaci B., 2016: A Status of Energy Efficient LED Based Traffic Lamps in Istanbul. *International Conference on Smart Cities, Smart Cities LNCS 9704 proceedings, Springer*, 2016 Malaga, Spain.
- Hamed B., **Almobaied M.**, 2010: Fuzzy Logic Speed Controllers Using FPGA Technique for Three-Phase Induction Motor Drives. *Engineering Sciences, Dirasat Inc.*, Volume 37, No. 2, 2010 Jordan.
- Hamed B., **Almobaied M.**, 2011: Fuzzy PID Controllers Using FPGA Technique for Real Time DC Motor Speed Control. *Intelligent Control and Automation*, 2 (3), 233-24.2011.

Books:

- **Almobaied M.**, 2011: Fuzzy Logic Speed Controllers Using FPGA Technique for Three-Phase Induction Motor Drives. *M.Sc thesis, LAP LAMBERT Academic Publishing.*, 7, April 2011, Germany.

